A genetic and molecular investigation into the pathomechanism of pterygium

Eleonora Maurizi

Faculty of Life and Health Sciences, Ulster University

A thesis submitted for the degree of

Doctor of Philosophy

October 2016

I confirm that the word count of this thesis is less than 100,000 words

DEDICATION

To Davide Schiroli,

for his advice, patience and love

Grazie.

Table of Contents

Acknowledgments

Firstly I would like to thank my parents: my mum Marina, my dad Maurizio and my brother Alessandro for their endless support they gave me from far away through a computer screen and for coming here more than once. I missed you a lot.

Thank you to all my relatives and friends for their support from Italy but also to who directly came here for a visit like my cousin Francesco, Maria Rosa, Tiziano, Luca, Marella, Lea and my friends Ciccio, Flavia, Tino, Robby, Chiara, Beghi and Luca.

A huge thank you to my international friends here in NI for the precious time spent together; without you guys those years wouldn't have been the same: Serena, Alex, Eduardo, Denise, Gary, Kevin, Katherine, Magda, Tony, Sabina, Jared, little Ayla, Ana and the beautiful Alena, Joe and his friends, Laura, Antonio, Anna Lisa, Elena, Carlos, and Gaetano. What we created here together is special and we will always be friends, in any part of the world we will be!

Thank you to my theatre mates: Sarah, Catherine, Zoe, George, Brandon, Emma, Gemma, Michael, Pat and all the others. In particular I want to thank Christine and Mik together with Sonya and Marc, you have been my family and my reference point here, always ready to help and to give me encouragement and suggestions.

I would like to greatly acknowledge Prof. Tara Moore for giving me the opportunity to undertake a PhD and together with Dr. Andrew Nesbit and Dr. Sarah Atkinson thank you very much for your constant supervision. Thank you to Tara for involving me in exciting projects, Andrew for sharing with me a bit of your knowledge in genetics and Sarah for your prompt availability and precise advice. Thanks to Prof. Johnny Moore for the numerous samples collection and to Sheena and the others in Belfast for helping me in the sample collection organization. Thanks to David for the help at the beginning together with Avinash, Rachelle and Michael but thanks in particular to Katie and Laura for the best birthday trio ever! I would also like to thank everyone else in the lab for your help and support during my three years of PhD: Michelle, Seodhna, Heather, Niall, Karla, Paul, Sarah Jane, Bob, Jaggan, DSB, Sagar, Rhonda, Bernie, Keith, Denny and all the others at Ulster University.

Dulcis in fundo, thank you so much Davide Schiroli, your presence here beside me was extremely important for the completion of this PhD and for our next future.

This thesis would not have been possible without the contribution of any of you.

Abbreviations

Acronym	*Definition*
ACE	Angiotensin Converting Enzyme
ACOP	Ambilateral CircumOcular Pigmentation
AMD	Age-related Macular Degeneration
APES	3-Aminopropyl triethoxysilane
BCC	Basal Cell Carcinoma
Bcl-2	B-cell lymphoma 2
BMP	Bone Morphogenetic Proteins
BOSCC	Bovine ocular squamous cell carcinoma
CDK	Climatic droplet keratopathy
CFH	Complement Factor H
CMT	Charcot-Marie-Tooth
CMV	Cytomegalovirus
COX2	Cycloxygenase-2
CPD	Cyclobutane pyrimidine dimer
CRIM1	Cysteine Rich Motoneuron protein1
CRBP1	Cellular retinol binding protein1
CREB	c-AMP Responsive Binding Protein
CRR	Cysteine Rich Repeat
CTGF	Connective tissue growth factor
DMEM	Dulbecco's Modified Eagle Medium
DMSO	Dimethyl sulfoxide
DUSPs	Dual-specificity phosphatases
ECM	ExtraCellular Matrix

215	**EMT**	Epithelial mesenchymal transition
216	**ERK (I)**	Extracellular signal–regulated kinases (Inhibitor)
217	**EST**	Expressed Sequence Tag
218	**FBN2**	Fibrillin2
219	**F(E)CD**	Fuchs' corneal (endothelial) dystrophy
220	**FHS**	Floating-Harbor syndrome
221	**FISH**	fluorescent in situ hybridization
222	**FGF**	Fibroblast growth factor
223	**GAPDH**	Glyceraldehyde 3-phosphate dehydrogenase
224	**GCD**	Granular corneal dystrophy
225	**GFP**	Green Fluorescent Protein
226	**GPx**	Glutathione Peroxidase
227	**GSTM1**	Glutathione S-transferase M1
228	**GWAS**	Genome Wide Association Studies
229	**HB-EGF**	Heparin-Binding epidermal growth factor-like growth factor
230	**HCE-S**	Human Corneal Epithelial cells
231	**HNMT**	Histamine N-methyltransferase
232	**hOGG1**	human 8-oxoguanine DNA N-glycosylase 1
233	**HPRT**	Hypoxanthine phosphoribosyltransferase
234	**HPV**	Human Papilloma Virus
235	**HRP**	Horseradish proxidase
236	**HSV**	Herpes Simplex Virus
237	**HUVEC**	Human Umbilical Vein Endothelial Cell
238	**IBD**	Inflammatory Bowel Disease
239	**IC**	Impression Citology

240	**IGFBP**	Insulin-like Growth Factor-binding Protein
241	**IGV**	Integrative Genomic Viewer
242	**IHC**	ImmunoHistoChemistry
243	**INDEL**	INsertion/DELetions
244	**IL**	Interleukins
245	**IOBA-NHC**	spontaneously immortalized-normal human conjunctiva
246	**JNK**	c-Jun N-terminal kinases
247	**KIF21B**	Kinesin family member 21B
248	**LCD**	Lattice corneal dystrophy
249	**LE**	Lens Epithelial
250	**LESC (D)**	Limbal Epithelial Stem Cells (Deficiency)
251	**LFS**	Li-Fraumeni syndrome
252	**LOD**	Logarithm of the odds
253	**LOH**	Loss Of Heterozygosity
254	**MACOM**	Colobomatous macrophthalmia with microcornea syndrome
255	**MAF**	Minor allele frequency
256	**MAPK**	Mitogen-activated protein kinases
257	**MDA**	Malone dialdehyde
258	**MEN1**	Multiple endocrine neoplasia type 1
259	**MET**	Mesenchymal epithelial transition
260	**MI**	Microsatellite Instability
261	**MMC**	MitoMycinC
262	**MMP**	Metalloproteinase
263	**MTT**	3-(4,5-dimethylthiazol-2-yl)-2,5-diphenyltetrazolium bromide
264	**MUC1**	Mucin1

265	**NHEJ**	Non Homologous End Joining
266	**NGS**	Next Generation sequencing
267	**NI**	Northern Irish
268	**NO**	Nitric oxide
269	**NOS**	Nitric oxide synthase
270	**OSSN**	Ocular Surface Squamous Neoplasia
271	**PAM**	Primary Acquired Melanosis
272	**PBS**	Phosphate Buffered Saline
273	**PCR**	Polymerase Chain Reaction
274	**PDGF**	Platelet-derived growth factor
275	**PKA**	Protein Kinase A
276	**POAG**	Primary Open Angle Glaucoma
277	**PolyPhen**	Polymorphism Phenotyping
278	**qRT-PCR**	quantitative Real Time-PCR
279	**QTL**	Quantitative Trait Loci
280	**RBCD**	Reis-Bücklers corneal dystrophy
281	**RFLP**	Restriction Fragment Length Polymorphism
282	**ROS**	Reactive Oxygen Species
283	**RT**	Room Temperature
284	**SCC**	Squamous Cell Carcinoma
285	**SEM**	Standard Error of the Mean
286	**SIFT**	Sorting Intolerant From Tolerant
287	**siRNA**	short interfering RNA
288	**SMA**	Smooth Muscle Actin
289	**SMAD**	Small Mother Against Decapentaplegic

290	**SNP**	Single Nucleotide Polimorphism
291	**SNV**	Single Nucleotide Variant
292	**SOD**	SuperOxide Dismutase
293	**SRCAP**	Snf2-related CREBBP activator protein
294	**TBCD**	Thiel-Behnke corneal dystrophy
295	**TCF4**	Transcription Factor 4
296	**THBS-1**	Thrombospondin-1
297	**TiGER**	Tissue-specific Gene Expression and Regulation
298	**TGF-β(I)**	Transforming Growth Factor- β (Induced)
299	**TGM-2 (orTG2)**	TransGlutaMinase-2
300	**TNF-α**	Tumor Necrosis Factor-α
301	**TUNEL**	Terminal deoxynucleotidyl transferase dUTP nick end labelling
302	**uPA**	Urokinase-type plasminogen activator
303	**UV**	Ultra Violet
304	**VEGFA**	Vascular Endothelial Growth FactorA
305	**VW(F) C**	Von Willebrand (Factor) C
306	**WDR12**	WD repeat domain 12
307	**WES**	Whole Exome Sequencing
308	**WGS**	Whole Genome Sequencing
309	**WHO**	World Health Organization
310	**WT**	wild type
311	**XP**	Xeroderma pigmentosum
312	**ZO-1**	ZonulaOccludens1
313	**4-HHE**	4-hydroxyhexenal
314	**4-HNE**	4-hydroxynenal

5-FU 5-fluoracil

8-OHdG 8-Hydroxydeoxyguanosine

Declaration

Note on access to contents

I hereby declare that for 2 years with effect from the date on which the thesis is deposited in Research Student Administration of Ulster University, the thesis shall remain confidential with access or copying prohibited. Following expiry of this period I permit:

1. The Librarian of the University to allow the thesis to be copied in whole or in part without reference to me on the understanding that such authority applies to the provision of single copies made for study purposes or for inclusion within the stock of another library.

2. The thesis to be made available through the Ulster Institutional Repository and/or EThOS under the terms of the Ulster eTheses Deposit Agreement which I have signed.

ABSTRACT

Pterygium is a pathological condition of the ocular surface of the eye, characterized by a highly vascularized and fibrovascular tissue formation arising from the limbus and invading the central cornea. Despite the controversy about pterygium patho-mechanism, UV exposure represents the main trigger for this uncontrolled overgrowth, mainly due to the high incidence of the disease around the equatorial areas. However, in certain families a much higher susceptibility to developing pterygium has been observed, suggesting a genetic etiologic component.

In this study, a Northern Irish family affected in three generations by pterygium and yet rarely exposed to direct UV light was identified. Whole Exome Sequencing and subsequent bioinformatic analysis, literature review and expression analysis prioritised a novel missense variant (p.H412P) in *CRIM1* gene, encoding for a type I transmembrane protein, which co-segregates with the disease within the family.

A higher CRIM1 expression was shown in pterygium tissues with respect to the conjunctival controls in the North European (low UV-exposure) population and another missense mutation in *CRIM1*, R745C, was identified in an individual pterygium patient from Bolivia.

In vitro functional analysis showed an antiproliferative and proapoptotic role for CRIM1 overexpression, which is able to modulate the extracellular signal–regulated kinases (ERK) phosphorylation induced by UV light.

For the first time CRIM1 expression revealed an pivotal role in UV mediated intracellular ERK pathway and apoptosis; pathway which was already documented in pterygium and which resulted in an impaired function when introducing H412P mutation in CRIM1, reinforcing the significance of this mutation identified in the Northern Irish pterygium family.

CHAPTER 1

Literature review

Contribution

Eleonora Maurizi carried out all research unless otherwise stated.

1.1 The eye

Eyes are the organs of vision, responsible for the perception of light stimuli coming from the external world.

1.1.1 Eye evolution and anatomy

The eye has developed in many different ways to allow the various organisms to adapt to the surrounding environment and in particular to detect and respond to the sunlight. It has been estimated that the eye evolved independently around 50-100 times (Land and Nilsson, 2002).

The simplest photoreceptive organelle, found even in unicellular organisms, is formed by photoreceptor transmembrane proteins (opsins) containing a chromophore (retinal) which is able to catch light photons and distinguish them from the darkness. This light sensitivity is important for direction during movement and the circadian rhythm, but is not strong enough to distinguish one object from another (Land and Fernald, 1992).

More advanced eye structures have evolved for 96% of the animal species and in particular during the Cambrian explosion, an extraordinary evolution event began around 500million years ago.

Humans possess an almost spherical eye, where the light enters from the anterior cornea (responsible for two thirds of the refractive power) and crosses the aqueous humour, a transparent viscous fluid-like substance with a low protein concentration (Cole, 1977).

The light amount entering through the pupil is regulated by the iris, a diaphragm which determines people’s eye colour, and is further refracted by crystalline lens.

Passing through the jelly vitreous humour, the light finally reaches the photoreceptors (cones and rods) located in the posterior retina from where is transmitted to the brain via the optic nerve (Figure 1.1).

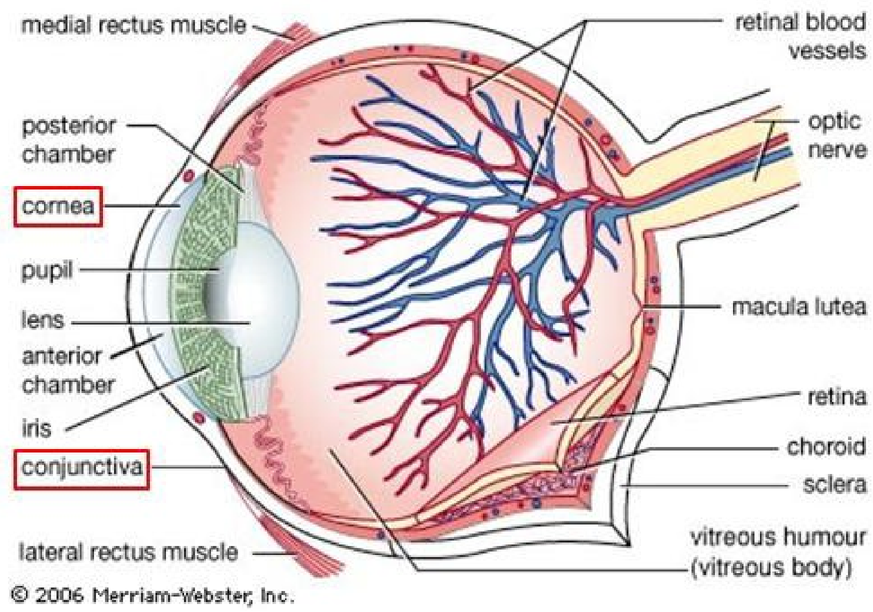

Figure 1.1 Structure of the human eye

The picture represents a longitudinal cross section of the human eye, showing its multiple functional components. The red squares highlight the cornea and the conjunctiva, which are the subject of this thesis work.

1.1.2 The anterior eye

The cornea is the avascular lens located in the anterior part of the eye and represents our window towards the external world. It is composed of five overlapping layers; the corneal endothelium, Descemet’s membrane, stroma, Bowman’s membrane and corneal epithelium, the latter covered by the tear film.

Maintaining corneal transparency is fundamental in eliciting optimal vision. This is obtained by the correct functioning of all the layers composing the cornea: from the homeostasis of the inner endothelial pump, passing through the well organised collagen fibrils into the stroma to the external barrier of corneal epithelial cells.

The inner endothelium is a monostratified layer of flat epithelial cells, which are polygonal in shape and non-proliferating, they are important to regulate the relative dehydration of the cornea (deturgescence) through the action of its active fluid pumps (Joyce, 2012).

A thin acellular layer called Descemet’s membrane, composed of collagen IV and VIII, laminin and fibronectin, divides the endothelium from the stroma.

Separating the Descemet’s membrane with endothelial cells from the rest of the cornea, a novel acellular layer mostly composed of collagen I has been recently described: the Dua’s layer (Dua et al., 2013).

The stroma, representing 90% of the entire corneal thickness, is composed of fibroblastic cells (keratocytes) interspersed in an extracellular matrix (ECM) of collagen fibrils (type I and V), which are responsible for corneal transparency due to their organised parallel disposition.

In continuity with the stroma, collagen I and III and proteoglycans constitute the Bowman’s layer, another acellular layer produced by the overlying corneal epithelium.

The corneal epithelium is the outermost part of the cornea acting as a barrier to protect the eye from the external environment together with the overlying tear film. Lying on a basement membrane of collagen IV and laminin, the corneal epithelium is a stratified squamous epithelium, non-keratinised layer, composed of 4-6 cell layers, from the internal portion: basal, wing and squamous cells (DelMonte and Kim, 2011).

Deriving its name from the Latin “cornu” which means horn for its stiffness, the cornea is important for maintaining the structure of the eye bulb and continues to the posterior part of the eye with the sclera. The sclera, which is distinct from the cornea, appears white in colour because of the light, which is scattered by the randomly arranged collagen fibrils and the vessels, these make up the superior portion named the episclera.

The anterior sclera together with the eyelids are covered by the **conjunctiva**, a stratified columnar epithelial layer interspersed by goblet cells secreting mucins into the tear film which overlies a vascularised connective tissue rich in elastin fibres (Copeland et al., 2013).

There are six different types of conjunctiva based on their localization: marginal, tarsal, orbital, forniceal, bulbar and limbal, the latter in continuity with the corneal epithelium.

It is exactly at the junction between cornea, conjunctiva and sclera, at the basal epithelial cell level, that the niche of corneal epithelial stem cells has been identified: the limbus (Figure 1.2).

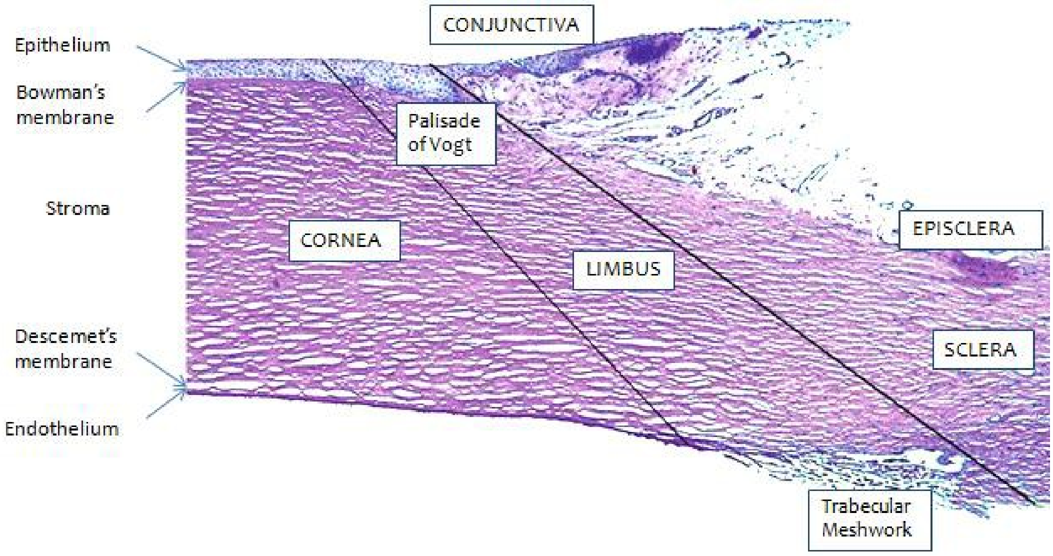

Figure 1.2 Structure of the anterior eye

The five overlapping corneal layers are listed in the left part of the image, from the external to the internal side: Epithelium, Bowman's membrane, Stroma, Descemet's membrane and Endothelium.

The transition area between the cornea and the conjunctiva (top part of the image) is delimited by the limbus, located in the Palisade of Vogt

Source of the image: (Dawson et al., 2009)

1.2 Diseases affecting the anterior eye

Diseases affecting the anterior part of the eye are numerous. We can distinguish between them in the following ways: infectious diseases affecting the cornea and the conjunctiva (bacterial, viral or fungal keratitis and conjunctivitis respectively), immunologic diseases where the eye is a target of allergic reactions (seasonal conjunctivitis, the most common), metabolic disorders including diabetes mellitus, trauma (physical and chemical), corneal dystrophies and other ocular surface diseases.

Corneal dystrophies represent a group of bilateral rare genetic disorders causing the degeneration of corneal tissue.

They can affect all the layers of the cornea and have been recently classified into four major groups: epithelial and subepithelial dystrophies, epithelial-stromal TGFBI dystrophies, stromal dystrophies and endothelial dystrophies (Weiss et al., 2015).

Other ocular surface diseases include dry eye syndrome caused by decreased tear production or increased evaporation, blepharitis caused by meibomian gland dysfunction, Keratoconus in which the cornea acquires a conical shape as well as several malignant neoplasia and pterygium.

Pterygium, together with eyelid malignancies (basal cell carcinoma (BCC) and squamous cell carcinoma (SCC)) photokeratitis, climatic droplet keratopathy (CDK), and cortical cataract are strongly associated with UV damage to the eye surface.

Limited evidence associates UV exposure with other eye diseases like pinguecula, nuclear and posterior subcapsular cataract, ocular surface squamous neoplasia (OSSN) and ocular melanoma (Yam and Kwok, 2014).

1.2.1 What is Pterygium?

Pterygium is a common eye surface disease, deriving its name from the Greek *pterygos*, wing, pathognomonic with its characteristic triangular shaped conjunctival tissue overgrowth invading the central cornea.

The first description of pterygium dates back to the Egyptian papyri in 1600-1300 B.C. (Chen et al., 2013) and to Susruta (India) who, before 1000 B.C., described in detail how to surgically remove pterygium in his Samhita (Rosenthal, 1953).

Lengthwise pterygium can be distinguished in three parts: a cap, flat fibroblastic tissue invading the cornea through Bowman's membrane disruption, a highly vascularised head, firmly attached to the cornea and a tail, covering the bulbar conjunctiva (Torres et al., 2011) (Figure 1.3A).

When analysing the morphology of pterygium tissue, two different types of tissue can be distinguished. Externally it is composed of a squamous metaplastic epithelia interspaced with hyperplastic goblet cells, glandular epithelial cells secreting mucins and internally presents an extracellular matrix interspersed with fibroblastic cells, vessels, collagen I and IV and fragmented elastin fibres (Detorakis and Spandidos, 2009b).

Although sometimes bilateral, pterygium is normally asymmetric with one eye more severely affected than the other and normally arises from the nasal or more rarely from the temporal conjunctiva (Detorakis and Spandidos, 2009b).

The development of this fibrovascular eye lesion has been associated with several etiologic and pathogenic factors, later described in more detail. However, the information collected to date on this condition has not been exhaustive enough to explain the complex mechanism behind the formation of pterygium.

1.2.2 What is Pinguecula?

Pinguecula, deriving its name from the latin "pinguiculus" which means fatty, is histologically similar to pterygium, presenting as a collagenic degradation with abnormal elastin deposition in the inflamed and vascularised stroma beneath a dysplasic epithelial layer (Lemercier et al., 1978).

Furthemore, similarly to pterygium, pinguecula prefers the nasal side of the limbus (Jakobiec et al., 2014) and there is a strong correlation in terms of age, sex and habits between the two diseases (Hill and Maske, 1989).

The aetiology of pinguecula has been associated with ageing (97% of the population over 50 years presents with pinguecula), sun exposure, dust and wind (Kaji et al., 2006).

However, pinguecula differs from pterygium because it is visible as a smaller yellowish deposit emanating from the conjunctiva beside the limbus and it does not show a proliferative potential (Figure 1.3B).

Despite several associations between the two pathologies, is still not clear if pinguecula is a pterygium precursor.

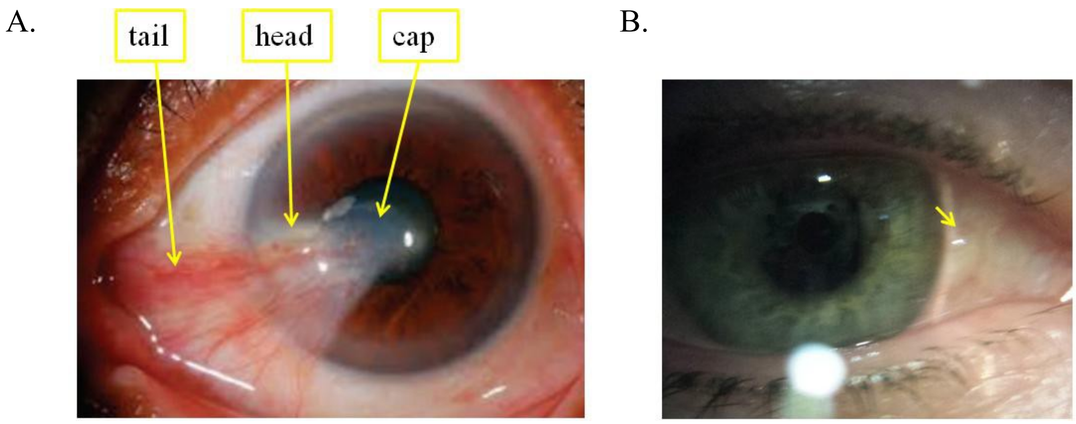

Figure 1.3 Pterygium and pinguecula

Panel A. Pterygium invading the central cornea. From the left we can distinguish the vascularised tail, the advancing head attached to the cornea and the cap which reaches the pupil (Najafi et al., 2016)

Panel B. Pinguecula visible at the limbus area (yellow arrow), between the cornea and conjunctiva of the III.5 member of the Northern Irish family affected by pterygium studied in this thesis (genealogic tree described in Chapter 2)

The image was obtained courtesy of Prof. Johnny Moore.

1.3 Pterygium symptoms

While pinguecula is asymptomatic and normally doesn't require any surgical intervention, initial presentation of pterygium is asymptomatic, but, as the disease progresses, it has been associated with different symptoms like tearing, itching and burning similar to dry eye. More severe cases present with chronic inflammation and blurred vision inducing astigmatism as the lesion increases in size and interferes with the visual axis (Cardenas-Cantu et al., 2015).

The progression of the pathology is variable between individuals. A slower growth potential has been observed upon iron accumulation in the basal layer of the corneal epithelium close to the head of the pterygium (Stocker's line) (Detorakis and Spandidos, 2009b).

Iron is fundamental for many cellular activities like oxygen transport and the tricarboxylic acid cycle even if its accumulation leads to oxidative stress thus damaging the tissue (Ortak et al., 2012).

Four iron lines have been described in the cornea: Stocker's Line, Hudson-Stahli Line, Fleischer's Ring and Ferry's Line. Several theories were formulated to explain iron lines formation including the tear-pooling hypothesis in which the iron present in tears is deposited in the closure lid epithelium (Gass, 1964) or a slower migration of the basal epithelial cells at the interpalpebral fissure where the oldest and most pigmented cells accumulates (Rose and Lavin, 1987).

Another theory proposes that the iron accumulates in regions with a higher tear instability due to excessive tear evaporation or in cells with a slower turnover (Assil et al., 1993). Loh et al. propose instead that stress of epithelial basal cells causes an increase in transferrin or lactoferrin receptor expression which bind iron and result in its uptake (Loh et al., 2009). However, the reason for iron accumulation in Stocker's line in pterygium is still unknown and possibly due to the excessive physical stress on the tissue.

1.4 Pterygium treatment options

The only effective treatment of an advanced pterygium obstructing the visual axis is the surgical excision of all the overgrown collagenous tissue followed by multiple adjuvant therapies.

1.4.1 Surgical techniques

The surgical treatment for pterygium consists in excision of the overgrown tissue with different additional strategies to prevent pterygium recurrence.

The bare sclera technique consists of the surgical removal of the whole pterygium and suturing the remaining conjunctiva to the bare sclera, which will re-epithelialize the excised area. Because of a high recurrence rate (up to 70%), this procedure incorporates a graft replacing the excised pterygium tissue.

Two kinds of graft are normally used: a conjunctival autograft or amniotic membrane graft, reducing the recurrence rate to 10% in some cases (Chen et al., 2013).

The conjunctival autograft consists of the transposition of a conjunctival flap, normally obtained from the superotemporal bulbar conjunctiva, into the area where the pterygium has been excised. To stabilize the graft sutures, which are more uncomfortable and prone to chronic inflammation, a more expensive fibrin glue can be used (Cardenas-Cantu et al., 2015). A simple sutureless and glue free technique of conjunctival autograft revealed to be particularly efficient with no complications registered pre- and post-surgical intervention in any of the 15 eyes in which pterygium was excised (de Wit et al., 2010).

An alternative technique is the application of amniotic membrane, which helps the re-epithelialization of the conjunctiva, possessing anti-inflammatory and anti-fibrotic properties. It is positioned over the bare sclera that comes in contact with the stroma of the amniotic membrane while the basement membrane is facing up. Fibrin glue is generally used to help graft adhesion and accelerate

cor
neal
rest
orat
ion
(De
tora
kis
and
Spa
ndi
dos,
200
9b).

1.4.2 Adjuvant therapies

Adjuvant therapies are used after pterygium surgical removal to prevent recurrence, which can be even more aggressive than the primary pterygium.

Mitomycin C (MMC) is an antibiotic and antitumor agent able to alkylate DNA double helix and used to block keratocyte and fibroblast proliferation in the case of pterygium. MMC is normally applied intraoperatively direct to the sclera bed but also postoperatively at different intervals. Patients treated with MMC are normally carefully selected because it can cause severe complications such as corneal perforation and scleral calcification (Cardenas-Cantu et al., 2015).

Beta-irradiation has the purpose of focally reducing fibroblast cell population. This treatment, however, can be responsible for serious side effects, including sclera necrosis and endopthalmitis (Detorakis and Spandidos, 2009b).

5-fluoracil (5-FU) is a chemotherapeutic pyrimidine analogue which, inhibits the thymidylate synthetase, blocks DNA synthesis and causes cell death in proliferating cells (Chui et al., 2008).

Anti-VEGF (Vascular Endothelial Growth Factor) monoclonal antibodies like bevacizumab inhibit angiogenesis but only temporarily and are associated with several side effects including cardiovascular toxicity (Detorakis and Spandidos, 2009b).

Doxycycline, a wide spectrum antibiotic, it is used to treat different mechanisms observed in pterygium for example inflammation, angiogenesis and apoptosis (Rúa et al., 2012).

Ethanol treatment, which destabilizes epithelial cell junctions, is normally performed directly during the operation.

Other less common adjuvant methods are all targeted against pterygium fibroblast proliferation like thioepa, an alkylating agent, Tropomyosin receptor kinase A (TrkA) inhibitor, curcumin and tetrandrine, an alkaloid (Cardenas-Cantu et al., 2015).

Despite the surgical outcome improvement given by adjuvant therapies, pterygium still presents a 10% recurrence rate (Ono et al., 2016). The lack of both a complete successful treatment and a clear pterygium pathogenic mechanism, drives researchers to investigate the molecular bases of pterygium development in order to find a more specific and effective therapeutic approach.

1.5 Development of pterygium

1.5.1 Limbal origin of epithelial pterygium

The outermost corneal epithelium is maintained functional and completely renewed every 9-12 months (Wagoner, 1997) by limbal epithelial stem cells (LESC) residing at the limbal Palisade of Vogt, located all around the border between the cornea and the conjunctiva (Das et al., 2015).

Altered limbal stem cells with abnormal gray dots (Cardenas-Cantu et al., 2015) have been observed in proximity to where the pterygium initially arises, before they stretch centripetally towards the cornea. Conjunctival epithelial cells and stromal fibroblasts follow the limbal cells centripetal movement towards the cornea progressively acquiring the characteristic triangular shape (Chui et al., 2008, Cardenas-Cantu et al., 2015, Das et al., 2015).

The limbal origin of pterygium formation has long been debated but seems to find confirmation in the latest works. An alteration of the limbal epithelial stem cells microenvironment was described in the initial phases of pterygium development (Das et al., 2015). Moreover, a similar expression of VEGF and VEGFR was observed in limbal as well as in pterygium samples, but those levels of expression were lower in normal conjunctival samples (Gebhardt et al., 2005). Finally, an invasion of vimentin-positive limbal stem cells was identified in pterygium (Dushku and Reid, 1994), together with a cluster of small p63α-positive cells in the basal epithelial cells of pterygium (Chui et al., 2011).

This cluster of cells was firstly identified in 1892 by Ernest Fuchs as flecks at the advancing head of the pterygia (Fuchs, 1892), thus resulting in them being defined as "Fuchs flecks" and commonly visualised nowadays under slit-lamp examinations as diagnostic sign of pterygium.

Moreover, based on its limbal origin elucidated above, but also on histopathological studies and clinical observations, pterygium has been described as a localised limbal stem cell deficiency (LSCD) (Anguria et al., 2014, Das et al., 2015). LSCD is a serious corneal epithelial condition in which the occurrence of damage in limbal stem cells results in a loss in their capacity to regenerate the epithelium, thus leading to a complete conjunctivalization of the cornea, neovascularisation and chronic inflammation finally eliciting blindness (Pellegrini et al., 2014).

Pterygium formation resembles the scarring and conjunctivalization seen in LSCD even if it is localised in a small portion of the corneal-conjunctival barrier, probably due to focused damage to a small portion of limbal stem cells.

1.5.2 Pterygium fibroblasts

Surrounded by conjunctival epithelium, the internal fibroblasts forming pterygium are thought to be responsible for the accumulation of elastoid material beneath the bulbar conjunctiva, resulting in degenerated type I and type IV collagen, abnormal elastin fibres and eosinophil-granular material (Detorakis and Spandidos, 2009b, Austin et al., 1983, Hill and Maske, 1989).

Even the origin of pterygium fibroblasts is still unclear: different hypotheses suggest they can originate from resident stromal cells, myofibroblasts coming from periorbital fibroadipose tissue, bone-marrow derived progenitor cells or limbal epithelial cells undergoing epithelial mesenchymal transition (EMT) (Chui et al., 2008, Kim et al., 2016).

1.5.3 Epithelial mesenchymal transition (EMT)

EMT is a common process observed during cell development, wound healing or carcinogenesis in which epithelial cells lose their morphology and expression markers to acquire the mesenchymal cells features (Kalluri and Weinberg, 2009, Lamouille et al., 2014).

During the EMT process cells acquire new structural features like cytoskeleton reorganization, cell polarity and functional properties including an increased motility and invasiveness, higher resistance to apoptosis and secretion of extracellular matrix components (Kalluri and Weinberg, 2009).

Gene expression reprogramming which occurs during EMT is initiated and controlled mainly by TGFβ family signalling; including among others three TGFβs, two activins and several Bone Morphogenetic Proteins (BMPs). TGFβ promotes EMT through activation of SMAD but also ERK, c-Jun N-terminal kinases (JNK) and p38 Mitogen Activated Protein Kinases (MAPK) intracellular pathways. (Lamouille et al., 2014).

Given the epithelial tissue plasticity, EMT results in a reversible process, and this was revealed by the occurrence of mesenchymal epithelial transition (MET), the opposing process in which the mesenchymal cells acquire epithelial characteristics.

Many molecular markers are used to identify this process: E-cadherin switches into N-cadherin, cells loose markers like ZO-1, mucin1 (MUC1) and miR200 and acquire typical mesenchymal markers like α-SMA, vimentin and β-cadherin (Zeisberg and Neilson, 2009).

Typical features of EMT were observed in pterygium: actively proliferating fibroblast-like cells were dissociating to basal epithelial cells expressing lower levels of E-chaderin, increased levels of α-SMA and vimentin and accumulating β-catenin intranuclearly (Kato et al., 2007).

Downregulation of microRNA (miR-200 family) in pterygium tissue compared to normal conjunctiva represents another proof of TGF-β induced EMT involvement in pterygium pathogenesis (Engelsvold et al., 2013); given the importance of miR-200 downregulation in TGF-β mediated EMT (Gregory et al., 2008).

Moreover, TGF-βR1 was found to be highly expressed alongside the epithelial surface of pterygium (Das et al., 2015), suggesting again an important role for TGF-β signalling in EMT and pterygium development.

1.5.4 Cell proliferation

Initially described as degenerative and hyperplastic degeneration, recent evidence suggests pterygium more as a proliferating process in response to external injuries. Pterygium is considered to be a proliferating condition of the eye because it begins with limbal epithelial cells overgrowing centripetally towards the cornea and continues with a continuous proliferation of conjunctival epithelial cells and inner fibroblasts (Dushku et al., 2001).

Cell proliferation is supported by a vast array of growth factors like heparin-binding epidermal growth factor (HB-EGF), basic fibroblast growth factor (bFGF), platelet derived growth factor (PDGF), transforming growth factor-b (TGFb) and insulin like growth factor binding protein-2 (IGFBP-2), all found to be overexpressed in pterygium (Bradley et al., 2010, Cardenas-Cantu et al., 2015).

An increased pterygium fibroblast proliferation has also been associated with an altered cholesterol metabolism, with increased levels of hydroxyl-methylglutaryl-coenzyme A reductase and low density lipoprotein receptor if compared to pingueculae and normal conjunctiva (Peiretti et al., 2004).

In order to facilitate the passage of the cells in active proliferation process, metalloproteinases (MMPs) are necessary to degrade the proteins to disperse them into the extracellular matrix. MMP-1 (collagenase), MMP-2 (gelatinase-A), MMP-3 (stromelysin 1), MMP-7 (matrilysin) and MMP-9 (gelatinase-B) have been found elevated in the advancing head of pterygium; with MMP-8 (neutrophil collagenase), MMP-13 (collagenase), MMP-14 and MMP-15 (membrane MMPs) reported in the overgrowing pterygium tissue (Bradley et al., 2010).

A successive study contradicts this observation, showing inhibition of MMPs mediated by TGFβ activation in pterygium, responsible for a reduced collagenolysis and thus an accumulation of collagen typical of pterygium morphology (Anguria et al., 2014).

Actively overproliferating fibroblasts are in fact immersed in an abnormal collagenic extracellular matrix that they itself produce, determining an excessive and deregulated connective tissue deposition which interferes with the normal eye function. This mechanism resembles the fibrosis scarring repair normally due to severe and deep damage to the epithelium but also to the inner stroma (Anguria et al., 2014, Kato et al., 2007).

1.5.5 Inflammation and angiogenesis

Besides cell overproliferation, both inflammatory and angiogenic processes take place, similarly to what happens during injury repair by fibrosis scarring.

Fibrosis is the process occurring during damage repair as an alternative to the regeneration of the native cells, in which the defect is filled with newly synthetized connective tissue. Closely associated with this repair process, the inflammation and angiogenetic processes aim to neutralise the injurious agent allowing the repair to be completed (Kumar et al., 2014).

In pterygium, the angiogenic mechanism occurs together with fibrosis to promote a chronic inflammation mediated pathogenetic process (Anguria et al., 2014, Hill and Maske, 1989, Coroneo et al., 1999a). Chronic inflammation occurs whenever the injury is persistent or there is prolonged exposure to a damaging agent which determines a continuous inflammatory response, substantial tissue remodelling and permanent scar formation, leading in some cases to complete organ failure (Wynn, 2007).

During pterygium development, many pro-inflammatory mediators were shown to be overexpressed including different interleukins (IL-1, IL-6, IL-8), tumor necrosis factor-α (TNF-α), able to activate cycloxygenase-2, which was also found to be up-regulated in pterygium, and which, in turn, is able to promote prostaglandin synthesis in the inflammatory cascade (Bradley et al., 2010).

The inflammatory response in pterygium is in fact mediated by a tissue infiltration of inflammatory cells like T lymphocytes, mast, plasma and dendritic cells (Beden et al., 2003) and by phospholipase-D up-regulation (Tong et al., 2008).

Infiltration and proliferation of inflammatory cells are supported by angiogenesis, the physiological process of new blood vessel formation from pre-existing ones, ensuring all the necessary nutrients are supplied.

VEGF, the most potent and specific angiogenic factor, and substance P were found to be elevated in pterygium (Bianchi et al., 2012, Bradley et al., 2010) while thrombospondin-1 (THBS-1), an antiangiogenetic adhesive glycoprotein was downregualted in pterygium (Aspiotis et al., 2007). Angiogenic factors induce vascular endothelial cells to activate nitric oxide synthase (NOS), which synthesise and release nitric oxide (NO), both found to be increased in pterygium (Lee et al., 2001). NO has an important role in promoting vasodilatation and endothelial cell proliferation, migration and interaction with extracellular matrix.

Interestingly, if the cornea is subjected to a small focal lesion, blood vessels start growing from the limbal area nearest to the injury and assume a triangular form resembling pterygium and reinforcing the hypothesis of pterygium as a focused LSCD (Campbell and Michaelson, 1949).

An active process of fibroblast proliferation, chronic inflammatory cellular infiltration and angiogenesis play therefore a central role in the inner connective tissue remodelling and pterygium progression.

But which is the agent responsible to trigger all those events in the eye surface when pterygium occurs?

1.6 Pathogenesis

Pterygium is often considered as an ophthalmic enigma (Coster, 1995) because, despite numerous studies trying to delineate its nature, the pathogenesis still remains unclear.

1.6.1 UV

The main cause of pterygium, as previously mentioned, has long been attributed to UV radiation (Moran and Hollows, 1984, Taylor et al., 1989, McCarty et al., 2000).

This hypothesis has been supported by multiple etiologic studies registering a 22% average prevalence in areas within 40° from the equator, compared to 2% outside this area (Detorakis and Spandidos, 2009b). Pterygium in fact is also known as surfer's eye because it affects many Australian surfers and generally those people spending a lot of time outdoors.

The morphology of the human eye is unique and can be distinguished by the one of the other species by a characteristic wide exposed white sclera elongated horizontally (Kobayashi and Kohshima, 1997). Although this guarantees humans a larger visual field, it lacks protection from UV light, especially on the nasal and temporal sides, exactly where pterygium generally arises, with a predilection for the nasal limbus.

The human nasal limbus in fact, compared to the temporal limbus, receives higher incidental light coming from the inner corneal surface following the alternative transcameral route (Coroneo, 1993). Moreover, possibly because of their peculiar eye anatomy, pterygium only affects humans and has not been documented in any other animal (Chui et al., 2008).

In early reports elucidating pterygium pathogenesis, UV light exposure was often associated to repeat exposure to dust and sand, triggering chronic inflammation as well as to wind and eye surface desiccation, which would explain the tear abnormalities seen in pterygium (Coroneo, 1993). The tear film is crucial for corneal surface homeostasis and its role in protecting the epithelial cells from environmental agents and supplying them with oxygen and nutrients. Moreover, a decreased and unstable tear production correlates pterygium with dry eye syndrome; with the two ocular conditions often documented in concomitance with each other (Ishioka et al., 2001, Das et al., 2015).

1.6.1.1 In vitro studies associating UV and pterygium

In vitro studies attempt to correlate both UVA and UVB with pterygium on the basis of altered cellular mechanisms.

An increase in IL-6, IL-8 and TNF-α in UVB treated pterygium cells represented a proof of the UV mediated immune response (Di Girolamo et al., 2002). A successive work of the same group showed that the UVB mediated IL-6 and IL-8 increase was reduced when the ERK1/2 intracellular pathway was inhibited (Di Girolamo et al., 2006b). The same pathway was found to be altered when cells were treated with UVA radiation, together with increased levels of Urokinase-type plasminogen activator (uPA); a serine protease promoting cell migration and tissue remodelling (Chao et al., 2013).

The study of cellular response to UV light helped to identify internal pathways involved in the pterygium activated response to solar radiation.

1.6.1.2 UV and oxidative stress

Oxidative stress is a cellular process observed when there is an imbalance between formation of reactive oxygen species (ROS) and cellular mechanisms designated to remove them, including antioxidant enzymes. This imbalance in favour of ROS causes DNA, protein and lipid damage together with disruption of the extracellular matrix, alteration in collagen and elastin synthesis; normally related to skin ageing (Martindale and Holbrook, 2002).

Oxidative stress has been reported in different diseases including cancer and chronic inflammation and more specifically in ocular disease like glaucoma, macular degeneration, age-related cataract and keratoconus (Chui et al., 2008).

In particular oxidative stress caused by UV mediated ROS production has been described in the ocular surface and pterygium (Kau et al., 2006).

In pterygium in fact has been reported a decrease in antioxidant enzymes like superoxide dismutase (SOD), catalase and glutathione peroxidase (GPx) possibly responsible for ROS accumulation (Balci et al., 2011a). A decrease in SOD was further reported by another study together with reduced NO; in accordance with the ability of ROS to reduce bioactive NO (Ozdemir et al., 2005). However, this is in contrast to the previously reported work demonstrating an increase in NO and NOS in pterygium (Lee et al., 2001).

Other oxidative stress markers have been reported to be up-regulated in pterygium like 8-Hydroxydeoxyguanosine (8-OHdG), a major product of DNA oxidative damage due to ROS activity (Kau et al., 2006) and its metabolising enzyme human 8-oxoguanine DNA N-glycosylase 1 (hOGG1) (Tsai et al., 2005b).

Ser326Cys homozygous substitution in hOGG1 gene was found more frequently in pterygium affected individuals, as following discussed (Kau et al., 2004).

Accumulation of a sufficient amount of ROS is also responsible for activation of the lipid peroxidation process, which might have a role in pterygium given the increased expression of Malone dialdehyde (MDA) and reactive aldehydes 4-hydroxyhexenal (4-HHE) and 4-hydroxynenal (4-HNE) in pterygium (Cardenas-Cantu et al., 2015). Also up-regulation of bFGF and VEGF is due to ROS accumulation (Anguria et al., 2014), enabling fibroblast growth and the capillary formation described above.

1.6.1.3 Pterygium: a premalignant condition?

Although always diagnosed as a benign lesion, pterygium can be considered a premalignant condition because of its association with different malignant pathologies.

Bilateral pterygium was found in 40% of individuals affected by Xeroderma pigmentosum (XP), a rare autosomal recessive genetic disorder resulting in a defective nuclear excision repair (NER) mechanism, which determines hypersensitivity to UV light radiation mediated DNA impairment. XP represents a precancerous condition because it is associated with 60% of malignant skin neoplasm (Goyal et al., 1994). Other studies have associated manifestation of pterygium with the presence of XP (El-Hefnawi and Mortada, 1965, Ramkumar et al., 2011).

Moreover, pterygium has often been diagnosed in concomitance with OSSN, which includes a variety of pathologic conditions from epithelial dysplasia to carcinoma *in situ* and invasive squamous cell carcinoma (Chui et al., 2011). Similarly to pterygium, sunlight exposure is a known etiologic factor for OSSN, with its prevalence higher in the equatorial area, together with dust and dry environment causing corneal surface irritation. Infection with human papilloma virus (HPV) and human immunodeficiency virus have been also shown to be essential in OSSN development (Mittal et al., 2013).

The prevalence rate of coexistent OSSN and pterygium is reported to be 9.8% of all pterygium specimens analysed in an Australian study (Hirst et al., 2009), 1.7% of pterygium samples in Florida (Oellers et al., 2013) and 5% of pterygium in another study from Australia (Chui et al., 2011).

Furthermore Chui et al. identified 2% of the participants with nevi (one with a history of skin melanoma and the other with epidermolysis bullosa) and 6% of the cases with primary acquired melanosis (PAM), both entailing atypical melanocytic lesions potentially leading to invasive melanoma (Chui et al., 2011). These results are similar to a previous study on the Ecuadorian population, which identified 8.75% of cases with PAM and 2.5% of cases with nevi, examining a total of 80 patients with pterygium (Perra et al., 2006).

Another study describes how a progressive degeneration of solar keratosis and pterygium is responsible for squamous cellular carcinoma (SCC) in the tropics, where it presents with a higher incidence in comparison to temperate areas (Clear et al., 1979).

Finally, proteins belonging to the S100 family, dimeric calcium-binding proteins, which modulate different biological processes, are normally used as markers to identify melanoma (Nonaka et al., 2008, Blessing et al., 1998) and other tumors as well as inflammatory diseases. S100 proteins have been shown to be overexpressed (S100A6, S100A8, S100A9, S100A11) in pterygium in comparison with normal conjunctiva (Riau et al., 2009). Upregulation of S100A8 and S100A9 has been identified in the tear film of pterygium patients (Zhou et al., 2009) and using microarrays comparing pterygium and healthy conjunctiva from the same patient (Hou et al., 2014) confirms the previous data and associates once more pterygium to abnormal epithelial differentiation, melanoma and chronic inflammation.

The importance of the role of solar radiation in pterygium is unquestionable as it is considered the most common ophthalmoheliosis (sun-related eye disease), however, UV damage is not sufficient to explain all occurrences of the pathology. In fact, several cases of pterygium are registered outside the equatorial zone, where UV exposure is not elevated; therefore suggesting other factors might be involved.

1.6.2 Viral Infection

Different oncogenic viruses have been found in pterygium cases including human papilloma virus (HPV), cytomegalovirus (CMV) and herpes simplex virus (HSV) (Cardenas-Cantu et al., 2015).

Viral infection rate however demonstrates geographical variability, with the highest prevalence registered in Italy where all the samples were positive for HPV (Piras et al., 2003), 50% was documented in English patients and the lowest in the Turkish and Japanese populations where HPV infection reached 10% (Otlu et al., 2009) and 4.8% (Takamura et al., 2008) of pterygium cases respectively.

The reasons for this divergence in prevalence is not clear, it has been attributed to ethnical variability or different techniques used in the different laboratories

(Cardenas-Cantu et al., 2015).

1.6.3 Genetic predisposition and inheritance mechanism

A higher susceptibility to developing pterygium has been observed in multigenerational families in comparison with the general population (Coroneo et al., 1999b).

An autosomal dominant mechanism of inheritance with incomplete penetrance has been suggested by several studies (Detorakis and Spandidos, 2009b, Hill and Maske, 1989, Hilgers, 1960), not excluding, however, the possibility of multifactorial, polygenic or recessive genetic models (Anguria et al., 2014).

Studies in families affected by pterygium include an interesting report analysing eleven cases in a rural three generation family in China in which all the offspring of an affected individual were affected (Zhang, 1987b). A recent work examined a Caucasian family from the UK with four affected members in two generations: three out of four offspring were affected (Romano et al., 2016) and an aggressive and recurrent pterygia with early onset (early 20s, 6, and 4 years of age) was studied in Saudi Arabia (Islam and Wagoner, 2001a). Even a rare congenital form of pterygium has been described in six members of a three generation family (Jacklin, 1964); in this case environmental factors were not influential in the disease development, therefore giving more importance to the genetic aetiopathogenesis.

Moreover, reported cases of monozygous twins with pterygium reinforced the importance of the hereditable mutations influencing predisposition in development of pterygium.

Monozygous twins affected by pterygium were found for example in a three generation family from Florida, USA with seven bilateral and one unilateral pterygia (Hecht and Shoptaugh, 1990), in another family from Turin, Italy, both carrying a bilateral pterygium (Contrucci Faraldi and Gracis, 1976) and in one from New York, USA, with a particularly early onset (Bloom et al., 2005).

Date	Authors	Affected family members
1914	Armaignac	8 bilateral in 22 members
1937	Strebel	4 affected in 3 generations
1951	Enroth	6 affected in 7 members
1962	Forsius and Eriksson	19 affected in 2 generations
1964	Jacklin	6 affected in 3 generations
1966	Murken and Dannheim	Monozygous twin
1977	Faraldi and Gracis	Two monozygotic twins
1983	Gutierrez- Ponce	5 males in 3 generations
1990	Hect and Shoptaugh	7 bilateral and 4 unilateral in 2 generations
2001	Islam Wagoner	3 early onset in 2 generations
2005	Bloom	Young twins
2016	Romano	4 affected in 5 members of 2 generations

Table 1.1 Familial genetic studies on pterygium

1.6.3.1 Genes involved in pterygium

Despite several families affected by pterygium, few studies have associated pterygium affected individuals to a single gene variation.

An increased predisposition to developing pterygium has been observed in individuals carrying polymorphisms in genes related to carcinogenesis. **p53** is a tumour suppressor gene better defined as the "guardian of the genome" because of its ability to detect the occurrence of DNA damage, induce cell cycle arrest and repair the DNA or promote apoptosis if the DNA cannot be repaired. Mutations in the *p53* gene have been detected in over 50% of all tumours (Levine et al., 1991). While changes in expression of p53 in pterygia specimens is still controversial because different immunohistochemical studies have shown conflicting results for the presence or absence of p53 in pterygia (Chui et al., 2008), however *p53* mutations have been detected in pterygium.

Using fluorescent *in situ* hybridization (FISH), a monoallelic deletion in p53 has been detected in four out of nine pterygium specimens. A subsequent analysis both at mRNA and protein level showed reduced expression of p53 to non-detectable levels, suggesting a possible loss of heterozygosity for the remaining wild type allele (Reisman et al., 2004).

DNA sequencing has been used to find mutations in the *p53* gene by analysing 51 patients affected by pterygium. Eight patients (15.7%) were reported with point mutations: six substitutions and two deletions. p53 protein expression was detected in the six cases with substitutions and was not found in the two deletion cases (Tsai et al., 2005a).

Another gene of interest in the pathogenesis of pterygium is the ***Ku70*** gene, which was analysed because of its importance in Non Homologous End Joining (NHEJ) repair upon UV radiation. A significant correlation between the T991C mutation in the Ku70 promoter and pterygium susceptibility was observed (Tsai et al., 2007).

Additionally, proto-oncogenes (POD) like the *ras* gene were studied because of their susceptibility to UV rays and are often mutated in skin tumours. RFLP analysis was performed in codons 12 and 13 of ***Ki-ras***, *H-ras*, and *N-ras* revealing a Gly-Val transition at codon 12 of *Ki-ras* in 10% of pterygia analysed (Detorakis et al., 2005b).

The *Human-8-oxoguanine glycosilase1 (hOGG1)* gene, previously reported as important for UV related cell oxidative stress, has also been analysed and a Ser326Cys polymorphism was found to be more abundant in pterygium samples than unaffected controls, the same polymorphism was found to be altered in many different kinds of cancer (Kau et al., 2004).

The *Glutathione S-transferase M1 (GSTM1)* null genotype, associated with cutaneous UV sensitivity for its ability to block GST antioxidant enzymatic activity, was found to be highly frequent in only young patients affected by pterygium (Tsai et al., 2004b).

Together with *GSTM1*, the previously described mutations in *Ki-ras* and *hOGG1* genes were found to be prevalent in young participants, implying a particular importance of genetic alteration in pterygium in early development.

A recent study showed an increased risk of developing pterygium if carrying a deletion (DD genotype) in the *Angiotensin Converting Enzyme (ACE)* gene, a zinc metalloproteinase able to convert angiotensin I to angiotensin II, a potent vasoconstrictor (Demurtas et al., 2014).

Finally, the *VEGFA* 936 C>T variant (rs3025039) was associated with pterygium onset because of a higher percentage of the T/T homozygous genotype in pterygium (16.7%) compared to unaffected controls (2.5%) (Peng et al., 2014).

Based on the association of pterygia with neoplastic alteration, in which inactivation of tumour suppression genes plays a central role, several primary pterygia were analysed for loss of heterozygosity (LOH) and microsatellite instability (MI). The first study analysing 15 pterygia with 7 selected highly polymorphic microsatellite markers showed 8 specimens (53%) presenting with LOH and 2 (13%) with MI (Spandidos et al., 1997). In a later study, the same group increased the number of pterygia to 50 and described LOH for chromosome 9p in 24 samples (48%) and for chromosome 17q in 21 samples (42%). Only 3 samples presented with MI (Detorakis et al., 1998).

gene	function	samples	mutation	rate	reference
p53	Tumor suppressor gene, genome stability	DNA from pterygium epithelial cells	4 deletions	tot mutations in p53: 44.4% of pterygium patients	Reisman et al. 2004
		DNA from pterygium epithelial cells	6 substitutions 2 deletions	tot mutations p53: 15.7% of pterygium patients	Tsai et al.2005
Ku70	NHEJ, telomere	Genomic DNA from blood	T991C promoter	T/C or C/C genotype in 25% of pterygium vs 10% of control cases	Tsai et al. 2007
Ki-ras	oncogene	DNA from pterygium tissue	Codon 12 Gly>Val	10% of pterygia, correlated with young age	Detorakis et al. 2005
h-OGG1	Antioxidant	Genomic DNA from blood	1247 C>G, codon 326 Ser>Cys	Cys/Cys in 40% pterygium vs 23.3% control cases, prevalent in young age	Kau et al. 2004
GSTM1	Antioxidant	Genomic DNA from blood	Null genotype	80.6% of pterygium vs 50% of control patients under 60 years of age	Tsai et al. 2004
ACE	angiotensinI>II, vasoconstrictor	Genomic DNA from blood	287bp Alu repeat, Ins/Del	D/D in 48% pterygium vs 15% control cases	Demurtas et al. 2014
VEGF	Angiogenetic factor	DNA from pterygium tissue	936 C>T	T/T in 16.7% pterygium vs 2.5% control cases	Peng et al. 2013

Table 1.2 List of genetic mutations found in pterygium specimens

1.6.3.2 Epigenetics and pterygium

Epigenetics, as the prefix epi- (Greek: επί-outside) suggests, distinguishes from conventional genetics because it focuses, not on DNA sequence changes, but on DNA alteration mechanisms like DNA methylation or histone modifications due to random or external influences which determine a stable alteration of the genome (Jaenisch and Bird, 2003).

Based on the similarity of pterygium with cancerous progression previously described, epigenetic modifications, as critical in the development of many different cancer types as genetic modifications, were studied in pterygium (Cardenas-Cantu et al., 2015).

Pterygium samples, compared to normal conjunctiva from the same patient, demonstrated a decreased methylation in *MMP-2*, a gene important for matrix remodelling, and *CD24*, a cell adhesion molecule, together with an increased methylation of transglutaminase 2 (*TGM-2*), important for ECM stability, wound healing, cell proliferation and motility, all processes characterizing pterygium formation (Riau et al., 2011).

Hypermethylation in the promoter of *p16*, an important regulator of the cell cycle progression from G1 to S phase, was observed in 16.3% of 129 pterygia analysed. Among the 21 pterygial samples with p16 promoter hypermethylation, almost all (90.5%) were negative for p16 expression (Chen et al., 2006). Another study however reported an increase in p16 expression, which was thus not silenced, in all the 70 pterygium samples (primary and recurrent) analysed in comparison with conjunctival controls (Ramalho et al., 2006).

Another hypermethylation status was observed in the *E-cadherin* gene promoter, in 32 (26.7%) of the 120 pterygia studied, with 79 *E-cadherin* protein expressing pterygia and 41 negative specimens. Hypermethylation and silencing of the *E-cadherin* gene is a key step during EMT process, when the expression of E-cadherin switches off and N-cadherin expression switches on (Young et al., 2010).

1.6.4 Other causes

Many *in vitro* and *ex vivo* (pterygium tissue) studies correlated pterygium to several possible causative pathogenic mechanisms: increased growth factors and metalloproteinases (Dushku et al., 2001, Bianchi et al., 2012, Di Girolamo et al., 2004), EMT (Kato et al., 2007, Engelsvold et al., 2013), impaired immunologic response (Beden et al., 2003), abnormal tumor p53 expression (Weinstein et al., 2002, Tan et al., 1997), altered lipid metabolism (Peiretti et al., 2006) and apoptosis (Tan et al., 2000). However, all these pathways might represent only a consequence of the pathologic process of pterygium rather than a causative mechanism.

In general, the data collected to date does not suggest a single cause which determines pterygium formation, but rather a multistep process, possibly following the two hit hypothesis or Knudson's theory (Detorakis and Spandidos, 2009b). A genetic variation in this case would become a first hereditable predisposition factor which determines pterygium occurrence only in cases of a secondary trigger like excessive sunlight exposure or viral infection (Anguria et al., 2014).

A general scheme of pterygium pathogenesis is shown in Figure 1.4.

However, further studies on pterygium or *in vitro* models associated with UV radiation become fundamental in order to shed light on the causative mechanism determining pterygium development.

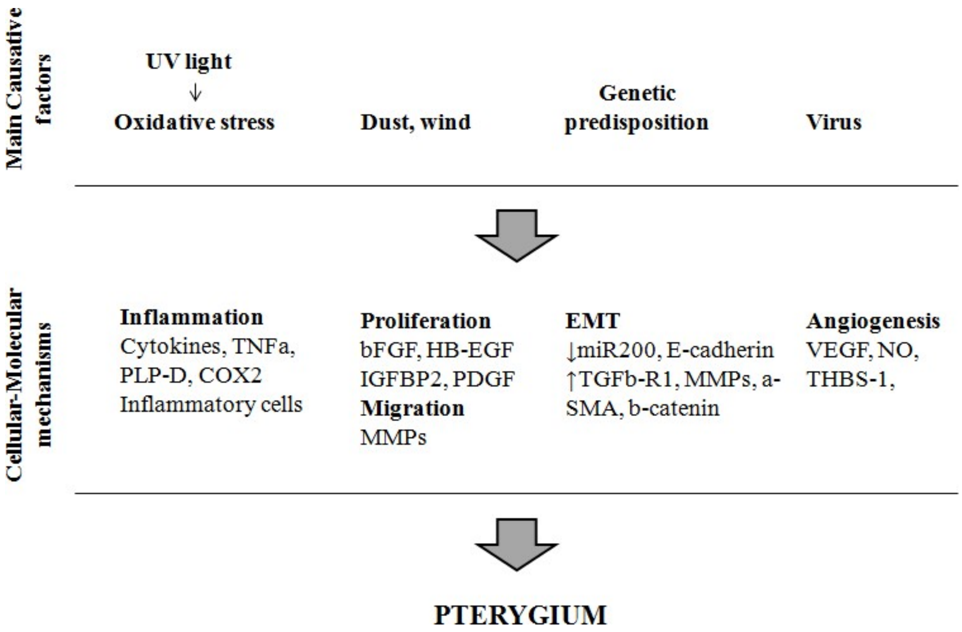

Figure 1.4 Proposed scheme of pterygium pathogenesis

Pterygium is a multifactorial disease: UV light is considered the main pathogenetic factor but a genetic predisposition documented in several affected families as well as viral infection or dusty and windy environments have been shown to concur to its development.

During pterygium formation several molecular mechanisms have been described through relative markers: inflammation, cellular proliferation and migration, EMT and angiogenesis.

1.7 Aim of the project

In this study, a large Northern Irish family with a documented low exposure to sunlight but showing pterygium at a multigenerational level is assessed. In the case of this family, a strong genetic predisposition plays a key role in the development of the disease, which is then passed on through three successive generations.

The general aim of this project is to identify a causative mutation for pterygium development within the Northern Irish family. A Whole Exome Sequencing (WES) approach and downstream Ingenuity analysis, *in silico* study, Sanger sequencing and expression analysis were used to initially screen and determine the most plausible causative variant. A subsequent functional analysis, based on pterygium known pathogenetic mechanisms like proliferation and UV irradiation as well as pterygium associated intracellular pathways like ERK activation and apoptosis, was performed. The series of functional experiments allowed a deeper understanding of the pathomechanism of pterygium, in which the selected candidate gene was found to play a pivotal role. This not only strengthened the possibility of the selected variant as the responsible for pterygium development in the Northern Irish family but is fundamental for future improvements in pterygium diagnosis and treatment.

CHAPTER 2

Finding a novel mutation: the Pterygium family and WES

Contribution

Eleonora Maurizi carried out all research unless otherwise stated

Dr Sarah Atkinson – DNA extraction, supervised research, proofread manuscript

Prof Johnny Moore – clinical instruction, sample collection from Northern Ireland

Prof Tara Moore – supervised research, proofread manuscript

Dr Andrew Nesbit – WES genetic screening, supervised research and proofread manuscript

Dr Davide Schiroli – helped with figures design

2.1 INTRODUCTION

The occurrence of variations in the DNA sequence of biological organisms, resulting from genetic mutations, DNA rearrangements or chromosome recombination, is what makes each individual unique and allows species evolution.

Human DNA has been estimated to have an average mutation rate of 1.3 x 10^{-8} bp^{-1} $generation^{-1}$ using Next Generation Sequencing (NGS) techniques, (Scally and Durbin, 2012). Considering the human genome size is 3.2 x 10^{9} bp, this estimation results in around 40 new base substitution mutations each generation per gamete which, added to other events like duplication, insertions and deletion would result in an average of 50-100 new mutations in a diploid newborn (Lynch, 2010). This number is in accordance with another study which estimates 74 novel Single Nucleotide Variants (SNVs) per diploid genome per generation (Veltman and Brunner, 2012). However, only a small fraction of those mutations, numbering 0.9 to 4.5 per diploid genome per generation (Lynch, 2010), is deleterious with the ability to cause the development of a genetic disease which is transmitted to the next generation.

Another common and naturally occurring way to promote diversity between individuals and create new phenotypes is genetic material recombination. Recombination frequency in gametes averages 10^{-5} crossover events kb^{-1} $meiosis^{-1}$ (Lynch, 2010) which corresponds to around 30 crossovers per meiosis. Our chromosomes are therefore inherited as a patch of genetic material from either of the two homologous chromosomes and whether two genes which are located the farthest apart from each other are inherited together or not depends on an even or odd number of recombination events, respectively. The farther apart two genes are located on a chromosome, the higher the probability that they will be separated by a crossing over and in this way the recombination frequency becomes a measure of the distance between two loci and the base of linkage analysis and genetic mapping.

2.1.1 Linkage analysis and GWAS

An important tool in studying the inheritance of genetic disease in humans is the analysis of a family pedigree, a pictorial representation of the transmission of a particular trait through the generations.

Genetic mapping is based on pedigree analysis of the recombination fraction between pairs of loci as mentioned above. To map a certain human trait, the disease character under examination needs another informative genetic marker co-segregating with it to evaluate the recombinant fraction within a family pedigree.

Once it is determined that the disease and the marker are co-segregating is still not always obvious to understand if this is due to chance or because of a linkage between the two, especially if the case studied is not a large multigenerational family. The probability that there is linkage between two loci is given by the LOD (logarithm of the odds) score, symbolised as a Z and calculated as $\log_{10}$ of the ratio between the probability of a newborn sequence with a certain linkage value and the one without any linkage (Strachan and Andrew, 1999).

The first studies able to connect the Mendelian trait of a disease to a variation in the DNA were carried on in 1980 through the linkage analysis of familial inheritance using Restriction Fragment Length Polymorphism (RFLP) as a genetic marker (Botstein et al., 1980).

RFLP distinguishes variations in the DNA sequence that can be detected by a restriction digest. RFLP analysis consists of screening all the fragments produced by a certain restriction enzyme and comparing the fragment pattern obtained. The restriction enzyme is chosen for its ability to discriminate between the altered sequence and the normal one. In this way is possible to modify the fragment pattern resulting from the enzyme digestion, which is visualised through agarose gel fragments resolution and radiolabeled or fluorescent probes hybridization.

A subsequent positional cloning is then necessary to narrow down the minimal critical region for the disease and obtain a more accurate disease locus map. This can be determined by following haplotypes through generations and looking for recombination events that limit the boundary of the critical region. The last step is to sequence the genes in the critical interval in order to finally identify the mutation which causes the disease (Collins, 1992). The main limitation of this approach is the fact that the resolution depends on the number of meiosis and the progeny generated in humans are normally quite small. In addition to this, several pathologies are not fully penetrant therefore the genotype does not always correspond to the observed phenotype. In the past this was limited further by the lack of the whole human genome sequence to even know which genes lay within the critical interval.

Linkage analysis using RFLP and subsequent positional cloning were successful in finding disorders caused by a single gene, the first of many was the linkage of CFTR with cystic fibrosis (Riordan et al., 1989).

In pterygium, several studies involving Polymerase Chain Reaction (PCR) and subsequent RFLP analysis were able to associate pterygium with genetic alterations in genes like *Ku70* (Tsai et al., 2007), *K-ras* (Detorakis et al., 2005b) and *hOGG1* (Kau et al., 2004).

Each RFLP can be distinguished by only two alleles: one containing the restriction site and the other without it. Simple sequence length polymorphisms (SSLPs) are much more informative then RFLPs because they consist of repeat sequence arrays with variable length and are therefore multiallelic. SSLPS can be distinguished in minisatellites or variable number of tandem repeats (VNTRs) and microsatellites or single tandem repeats (STRs). While minisatellites are composed of repeated DNA motifs of 10-50bp in length, microsatellites are characterized by 2-5bp repeats (Brown, 2006).

Genetic analysis of seven highly polymorphic microsatellite markers in pterygium DNA allowed the identification of a region in chromosome 17q with a high frequency of LOH and a considerable incidence of MI (Spandidos et al., 1997). A common LOH event in recurrent pterygium was described subsequently also at chromosome 9q, correlated with young age and high altitude residence (Detorakis et al., 1998). However, disease characterized by complex traits cannot be studied by linkage analysis.

2.1.2 The human genome era

The completion of the human genome sequence in 2001 allowed annotation of millions of common Single Nucleotide Polymorphisms (SNPs), single base pair variations between individuals, occurring on average every 1000-2000 bases (Sachidanandam et al., 2001).

All the common SNPs, those present in at least the 1% of the population, were catalogued by an international collaboration which began in 2002, the HapMap project.

The HapMap consortium had the scope to characterize the variants, describe where they occur in the DNA and determine their frequency in populations coming from different parts of the world: European, African, Asian and American. DNA variants includes SNPs and mutations and are respectively defined as present in >1% or <1% of the population (Karki et al., 2015).

The HapMap project and the availability of commercial SNP platforms determined the development of another type of approach to genetic diseases: the Genome Wide Association Study (GWAS). GWAS allowed comparison of millions of common SNPs between two populations: affected and unaffected and then associate the differential variants to the disease phenotype.

The description of haplotype blocks, or human genomic regions conserved in different populations alongside historical evidence of recombination in which are present only a few haplotypes, facilitated the association studies (Gabriel et al., 2002). This allowed selection of a single tag SNP between all the SNPs located within a haplotype block, reducing economic and time costs to genotype areas associated with the disease.

One of the first successful GWAS, published in 2005, was performed on an eye-related disease: age-related macular degeneration (AMD). Two polymorphisms in an intron of the complement factor H (CFH) gene were found to be strongly associated with AMD. Since the two SNPs were found in an intron, they are non coding and not responsible for any sequence alteration; however, they were found located in a region with high linkage disequilibrium, within a haplotype block of

41kb entirely contained in CFH gene. A subsequent resequencing of the exonic DNA including the intron-exon boundaries in the 96 cases of AMD participating to the previous GWAS revealed a Tyrosine to Histidine variation at amino acid 402 of CFH (Klein et al., 2005).

Several GWAS followed and multiple other ocular conditions were examined, including the elucidation of nitric oxide synthase and TGFb pathway in primary open angle glaucoma (POAG) pathogenesis and numerous SNPs in Transcription Factor 4 (TCF4) were found to be independently associated with Fuchs' corneal endothelial dystrophy (Chandra et al., 2014). However, the GWAS approach requires careful population selection and can only be performed for common diseases because it requires a large number of individuals carrying the trait of interest. The genotyping coverage of 70-90% requires extensive data quality control and can be statistically challenging when distinguishing the true from the false associations.

Moreover, despite the advantages of using haplotype block information which allows analysing not all the SNPs located in the same region but only a representative SNP tag, it is possible to lose the private SNP, or the SNP responsible for the disease development.

2.1.3 Next generation sequencing era

A revolutionary new era of genomic analysis started in 2005 when Next Generation sequencing (NGS) technologies became widely available because the cost of sequencing decreased over four orders of magnitude compared to Sanger sequencing (Bamshad et al., 2011).

From the first human genome published in 2001 which required US$3billion and 13 years of work between 23 laboratories (Sastre, 2014) it is now possible to sequence a human genome for approximately US$1000. The human genome is composed of over 3 x 10^9 base pairs of which only 3 x 10^7 (1%) are coding sequences, the exome.

NGS technologies can be applied to the entire genome (Whole Genome Sequencing, WGS) or limited to its coding portion (Whole Exome Sequencing, WES). WES represents a powerful approach in identifying novel mutations in genetic diseases and has advantages in over the use of WGS: firstly, less than 10% of the human genome sequence is well characterized and the majority (85%) of disease-causing mutations occur in the exonic portion of the genome (Rabbani et al., 2014). Moreover, exonic variants that alter protein-coding sequences have a direct functional impact on the proteins, while for mutations in the intronic region the phenotypic effect is more difficult to demonstrate. Secondly, given the remarkable size difference between the genome and the exome, WES guarantees a more affordable price and a lighter sub-sequential computational analysis. Finally, a terabase (Tb) of data, more than five human genomes, are normally captured by NGS techniques in a single sequencing run, allowing a greater depth of coverage with WES than with WGS.

Beside the advantages, which make WES a powerful tool for the discovery of gene association with a disease, there are some disadvantages in using WES approach like the fact that some variations in non protein-coding regions (eg. regulatory sequences or 5’ or 3’ UTR site) are not detected. Another technical limitation is the fact that during the purification process 5-10% of exons are poorly covered or missed (Bamshad et al., 2011).

2.1.4 Aims of Chapter 2

The research outlined in this chapter investigated the appearance of pterygium in a large Northern Irish family, an important clinical case to study the genetics behind pterygium formation.

Although pterygium was identified in three subsequent generations within this family, it resulted in too small a sample size to perform linkage analysis. Similar sized families have been used by WES to find the causative gene, for instance fibrillin2 (FBN2) in autosomal dominant macular degeneration (Ratnapriya et al., 2014) and STAT-1 in chronic mucocutaneous candidiasis (Dhalla et al., 2016).

Moreover, according to our questionnaire, no history of particular sun exposure for each member of this family was registered, revealing an even more interesting case for a possible genetic cause in the development of the pathology, minimally influenced by what is considered the major cause of pterygium: UV light.

It is hypothesised therefore that genetic predisposition plays a fundamental role in the etiologic process of pterygium development in the family presenting in Northern Ireland.

For all those reasons and for the fact that 85% of the mutations occur in the exome (Rabbani et al., 2014) and that WES guarantees a more affordable price other than a greater depth of coverage than WGS, the WES approach was chosen in an attempt to identify the causative variant within this family. Because the inheritance mechanism in this pedigree is most easily explained as autosomal dominant, as reported for previous pterygium family cases (Detorakis and Spandidos, 2009b), the variant was expected to be a rare heterozygous mutation differing between affected and unaffected individuals within the family.

The large amount of variants obtained by WES was rationalized using analytical software like Ingenuity Variant Analysis, helping to prioritize a smaller number of candidate genes through a cascade of filters.

The candidate genes obtained were further analyzed for their tissue specific expression pattern (TiGER), the impact that the variation would have in the structure and function of the protein (Polyphen, SIFT), the conservation of the amino acid residue between species, the heterozygosity within family members (IGV) and the diseases previously associated with that gene.

Only one gene that fulfilled all these criteria was finally selected for a complete functional analysis to assess if the gene was associated to the pterygium pathomechanism.

2.2 METHODS

2.2.1 Patient clinic examination and genealogical family analysis

Clinical examinations of a Caucasian Northern Irish family affected by pterygium were performed at the Cathedral Eye Clinic, Belfast, UK. A total of 24 patients from three subsequent generations (6 affected and 18 unaffected) were investigated: three with pterygium, two with pinguecula and one unaffected family member participated to the WES study.

Following informed consent, collection of blood and a completed questionnaire was obtained from each participating family member under ethical approval from ORECNI Northern Ireland, UK.

The questionnaire given to the participating patients provided the following information: date of birth, sex, date of pterygium first diagnosis, therapies time spent abroad and in sunny climates and whether eye protection is worn.

2.2.2 Whole Exome Sequencing

Genomic DNA from five affected family members and one unaffected sibling was extracted from venous blood leukocytes using QIAamp DNA Blood mini kit (QIAGEN, Manchester, UK). The high sensitivity Qubit system (Thermo Fisher Scientific, Loughborough, UK) was used to quantify genomic DNA and integrity of the DNA was confirmed by running samples on a 1% agarose gel in 1xTBE (UltraPure Agarose, Thermo Fisher Scientific, Loughborough, UK).

The SureSelect Human All Exon v2 kit was used for Whole Exome capture according to the manufacturer's instructions (Agilent Technologies UK, Wokingham, Berkshire, UK). Briefly, DNA libraries were prepared: 3 μg of genomic DNA was fragmented using the Covaris S2 ultrasonication system, extended adding an “A” base at the 3’ end, ligated with adaptor primers and PCR amplified (four cycles).

Libraries of exome enriched sequences were selected by hybridization with biotinylated RNA probes (~120bp) and captured by streptavidin coated magnetic beads. After washing the beads and digesting the RNA probes, a final library of exonic DNA was further amplified (11 cycles).

Sure Select n.2100 Bioanalyser (Agilent Technologies) allowed an assessment of the quality of the library and quantitative PCR was used for quantitative analysis.

Massive parallel sequencing was then performed by Illumina GAIIx using 150bp-paired-end reads. Generated reads were aligned to the Human 37 reference genome with a short read mapper (Stampy) generating data in BAM format.

Coverage of the target region was verified to be in excess of 70% (greater than 10 reads). Platypus, an in-house variant caller able to detect SNVs and short (<50bp) insertion/deletions (INDEL), was used to detect variant sites and alleles. Once the false positive rate was reduced, the resulting variants were stored as Variant Call Format (VCF) files.

2.2.3 Ingenuity Variant Analysis

Ingenuity Variant analysis was used to filter and select a smaller number of candidate genes; assuming autosomal dominant mechanism of inheritance. Further selections were made on the basis of cross-species conservation, known expression in tissues (Tissue-specific Gene Expression and Regulation database) and disease association through a literature review. Aligned reads were viewed with the Integrative Genomic Viewer (IGV) platform, a open source software enabling visualization and analysis of large data sets.

2.2.4 Sanger Sequencing

Sanger sequencing was performed on genomic DNA extracted from the blood leukocytes of pterygium family members; to confirm the presence of the mutation in each candidate gene.

Genomic primers specific for each gene were designed using Primer3:

SRCAP_F 5’GCGTACCCAATGTTTAGCTCC 3’,

SRCAP_R 5’CAGAAGCCCATCCCAGTACC 3’,

WDR12_F 5’CACACCCAGTCATCGTCATC 3’,

WDR12_R 5’ACCAGGGATTCAAACTGAGC 3’,

HNMT_F 5’ CTGCTGGTCTTATCCTGTCCC 3’,

HNMT_R 5’ GGTCTTTTAAAATGTATCAGAAGCCG 3’,

CRIM1_F 5’ CTTCTTTTGCATGCACCCCC 3’,

CRIM1_R 5’ TCACATGTGCAACCTTTCCTC 3’,

KIF21B_F 5’ TGATTTCCCCAGAGTGTGGC 3’,

KIF21B_R 5’ ACCCCTTTTGAGTGTCCCAC 3’

BigDye Terminator v3.1 Cycle Sequencing Kit (Life Technologies) and ABI 3730 automated capillary sequencer (Applied Biosystems) were used to determine DNA sequences of the PCR products.

To determine the polymorphism frequency of our selected variants compared to a Northern European population, the NHLBI – ESP (National Heart, Lung, and Blood Institute – Exome Sequencing Project) server was used.

2.2.5 HCE-S (Human Corneal Epithelial cells) culture

Human Corneal Epithelial cells (HCE-S), a spontaneously generated corneal cell line (Notara and Daniels, 2010) (a kind gift from Prof. Julie Daniels), were cultured (37°C, 5% CO_2) in Dulbecco's modified Eagle's medium (DMEM) containing 4 g/L glucose (Thermo Fisher Scientific, UK), and supplemented with 10% fetal bovine serum (Thermo Fisher Scientific, UK).

2.2.6 Semi-quantitative PCR

A semi quantitative PCR was performed in cDNA obtained from HCE-S cells at 20, 25, 30 and 35 cycles in order to determine the expression levels in cornea of the five genes selected by WES data analysis.

Exonic primers used for the semi quantitative PCR were:

SRCAP_ F 5' AAATTGCAGAACAGGCCAAG 3',

SRCAP_R 5' GATCACCATGCGCACCAC 3',

WDR12_F 5' TCCAAACACGCTTCTACACTG 3',

WDR12_R 5' TCCACGTATTCTATTTCCACAAC 3',

HNMT _F 5' TGCAGGAATTCATGGACAAG 3',

HNMT _R 5' CTCGAGGTTCGATGTCTTGG 3',

CRIM1_F 5'CTCCCTCACCGAGTACGAAG 3',

CRIM1_R 5' GGCCTTGGAGCAATCTGG 3',

KIF21B_F 5'TGCTTCGAGGGCTATAATGC 3',

KIF21B_R 5'GGTCAAGGATCTCCTCGTTG 3'

Products were run on a 1% agarose gel (UltraPure Agarose, Thermo Fisher Scientific) in 0.5x TBE buffer (Tris base, Acetic acid and EDTA) alongside the molecular size marker Hyperladder (Bioline, London, UK).

2.3 RESULTS

2.3.1 A multigenerational Northern Irish family pedigree analysis

A multigenerational Northern Irish family composed of twenty-four members was investigated (Figure 2.1). Six members of the family from two different generations were affected by pterygium or pinguecula while 18 were unaffected.

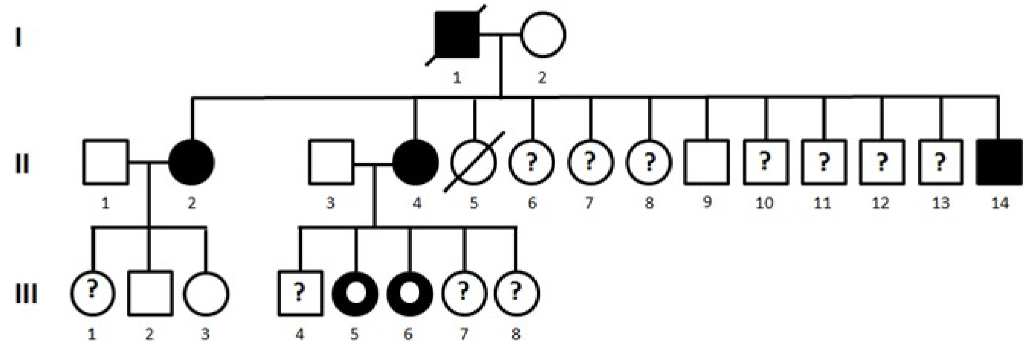

Figure 2.1 Northern Irish family affected by pterygium

Pedigree of a Northern Irish family affected with pterygium. Open symbols denote unaffected individuals; filled black symbols denote pterygium affected individuals and filled black symbols with open circles inside denote pinguecula affected individuals. Squares represent male and circles represent female individuals. Question marks are for individuals not participating in the study and slashed symbols denote deceased family members.

Pterygium affected both males and females and the onset age was on average 48 years old. From the questionnaire, there was no history of unusual sun exposure for all family members; only holidays in sunny climates for a couple of weeks every year with most using sunglasses (Table 2.1).

A familial predisposition for development of pterygium was apparent within the family.

Family member	Year of birth	Sex	Eye condition	Age onset	Lived abroad	Time in sunny climates	Wear sunglasses
II.2	1944	F	pterygium	40 years	No	1/year, 3 weeks	Sometimes
II.4	1946	F	pterygium	59 years	Canada 13 years	1/year, 2 weeks	No
II.9	1958	M	unaffected	-	No	1/year, 3 weeks	Yes
II.14	1951	M	pterygium	62 years	No	1/year, 1 week	Yes
III.2	1967	M	unaffected	-	No	1/year, 1 week	Yes
III.3	1982	F	unaffected	-	No	1/year, 1 week	Sometimes
III.5	1968	F	pinguecula	38 years	Canada 13 years	1/year, 2 weeks	Sometimes
III.6	1970	F	pinguecula	40 years	Canada 13 years	1/year, 2 weeks	Sometimes

Table 2.1 Northern Irish pterygium family questionnaire results

List of participant family members with relative information

2.3.2 Whole Exome Sequencing

In order to identify the gene responsible for pterygium onset in this family, Whole exome sequencing (WES) analysis was performed in DNA extracted from three family members with pterygium: II.2, II.4 and II.14 (72, 70 and 65 years old respectively) two with pinguecula: III.5 and III.6 (48 and 46 years old respectively) and one unaffected relative: II.9 (58 years old) (Figure 2.1 and Table 2.1).

WES resulted in the identification of 451,153 variants in 18,858 different genes.

2.3.3 Ingenuity Variant Analysis

Ingenuity Variant Analysis was used to prioritize some of these variants: the first filter, Confidence, allowed selection of 30,000 variants based on the call quality and read depth, therefore ensuring a higher quality of the subsequent analysis.

The previous number was further reduced to 25,000 using the second filter, Common Variants, able to exclude the variants more frequently observed in the population, setting a Minor Allele Frequency (MAF) < 0.005.

The third filter picked out 11,000 variants predicted to be deleterious through two algorithms based on the evolutionary conservation of an amino acid within a certain protein family: PolyPhen (Polymorphism Phenotyping) and SIFT (Sorting Intolerant From Tolerant).

Polyphen2 (Adzhubei et al., 2010) is a predictive software which aligns the sequence containing the mutation to multiple homologous sequences. The research is then refined by a series of algorithms implementing the quality and gathering together specific clusters of sequences.

Eight sequence-based and three structure-based features are used to classify the alignments including the probability of different amino-acids to occupy the affected position in the aligned sequences (PSIC score), how distant the mutation is from the normal allele and if it generates a hypermutable CpG nucleotide.

The reliability of the prediction is tested with two different datasets: HumDiv, consisting in all damaging variations causing human Mendelian diseases and HumVar detecting milder deleterious variants without any disease association (Knecht and Krawczak, 2014).

SIFT (Ng and Henikoff, 2001) is another prediction program using sequence homology to discriminate between neutral and damaging variants. Based on the assumption that amino-acids are conserved within protein families among different species, SIFT uses a multiple alignment of homologous sequences generated by SwissProt and then calculates the probability of any amino-acid substitutions in the affected position, taking onto consideration both the position and the type of amino acid. These results are then normalised by the most probable substitution and given a score ranging from 0 to 1, setting a threshold at 0.5: the variant will be damaging if SIFT score is ≤ 0.5 and tolerated if it will be ≥ 0.5.

A measure of confidence of the prediction in this case is given by the median value ranging from 0 when at that specific position all the 20 different amino acids are observed to 4.32 ($\log_2 20$) when only that amino-acid is observed and the position is conserved (Kumar et al., 2009).

A final genetic screening enabled selection of 67 relevant variants assuming a dominant inheritance pattern, thus heterozygous in the affected and homozygous wild type in the unaffected relative control.

Genes carrying mutations previously associated with pterygium like *Ku70*, *K-ras*, *hOGG1* (Tsai et al., 2007, Detorakis et al., 2005b, Kau et al., 2004) were not selected from the Ingenuity Variant filters.

Each of the variants obtained with Ingenuity was then manually analysed to discriminate the ones most relevant for an involvement in pterygium pathogenesis.

BLAST and Clustal Omega alignments were used to check the conservation of the mutated amino acid among the species. The possible impact of the mutation on the structure and function of the protein was studied, together with the diseases normally associated with that gene mutation and the tissue-specific gene expression pattern for each gene.

Considering and comparing all those more stringent criteria, we selected five candidate variants for a subsequent *in vitro* analysis (Table 2.2)

Filters	No. of variants
WES	451,153
Ingenuity Confidence	30,000
Ingenuity Common Variants	25,000
Predicted Deleterious	11,000
Genetic Screening	67
In silico, literature	5

Table 2.2 WES variant screening

2.3.4 Selection of five candidate genes

The five candidate variants selected were found in genes coding for proteins all expressed in the eye and the amino acidic residues in which they were located were all highly conserved through the species (Table 2.3).

Gene	Chr	Expressed in	Protein Variant	Associated Diseases	Function
KIF21B	1	Eye, Brain, Blood	p.T105M	multiple sclerosis, inflammatory bowel disease	Regulation of Notch signalling and protein-protein interactions
CRIM1	2	Placenta, Kidney, Eye	p.H412P	syndactyly, neuronitis, bovine ocular squamosus cell carcinoma	Transmembrane protein regulating BMP and VEGF signalling.
HNMT	2	Bladder, Kidney, Liver, Eye	3'UTR	asthma, eosinophilia-myalgia syndrome	Inactivation of Histamine by N-methylation
WDR12	2	Blood, small intestine, thymus, Eye	p.L169S	gigantism, neuronal ceroid lipofuscinosis	Intracellular transport of membranous organelles
SRCAP	16	Larynx, thymus, spleen, Eye	p.R968H	floating-harbor syndrome, Eosinophilic angiocentric fibrosis	transciptional regulation of genes activated by CREB, steroid receptor and Notch

Table 2.3 Five selected candidate genes

The candidate genes are described below in more detail.

2.3.4.1 CRIM1 (H412P)

CRIM1 (cysteine-rich motor neuron 1 protein) gene encodes for a single pass transmembrane protein (type I), oriented with the C-terminal into cell cytoplasm and the N-terminal facing the extracellular portion of the cell.

Although its molecular function has not yet been fully elucidated, CRIM1 has been revealed to be important for cell adhesion through interaction with N-cadherin and β-catenin (Ponferrada et al., 2012). Its role in mediating cell adhesion has been also confirmed by the accumulation of CRIM1 at cell-cell junctions upon stimulation of endothelial cells (Glienke et al., 2002).

As well as forming complexes with cell adhesion proteins, CRIM1 is able to bind growth factors including Bone Morphogenetic Proteins (BMPs) (Wilkinson et al.,

2003) and VEGFA (Wilkinson et al., 2007b) through its Von Willebrand factor domains where our H412P variant is located.

CRIM1 expression has been documented in different types of tissue, especially during their development, including the vertebrate CNS (Kolle et al., 2000a, Pennisi et al., 2007), vascular system (Glienke et al., 2002, Pennisi et al., 2007, Wilkinson et al., 2007b), urogenital tract (Georgas et al., 2000), kidney (Wilkinson et al., 2007b) and eyes (Lovicu et al., 2000, Beleggia et al., 2015) Regarding the eye, even if low expression levels were documented during the lens placode formation, CRIM1 has been shown to be upregulated during embryonic and foetal development. It is expressed in several ocular tissues like lens epithelium and lens fibres, conjunctival epithelium, corneal endothelium, retinal pigmented epithelium, ciliary and iridial retinae and ganglion cells. (Lovicu et al., 2000).

Confirmation of CRIM1 importance in the embryonic development comes from the generation of mice homozygous for a gene trap mutant allele (CRIM1$^{KST264/KST264}$) or germline mutants (CRIM1$^{\Delta flox/\Delta flox}$), which showed perinatal lethality and dysfunction in multiple organs including digit syndactyly, hemorrhagic necrosis, eye and kidney abnormalities (Wilkinson et al., 2007b, Chiu et al., 2012).

2.3.4.2 SRCAP (R968H)

SRCAP (Snf2-related CREBBP activator protein) gene encodes for a member of the SNF2 family of proteins participating in different kinds of transcriptional regulation, including chromatin remodelling, DNA repair and regulation of gene transcription (Monroy et al., 2001).

SRCAP was identified by its ATPase activity as transcription factor and its ability to interact with c-AMP Responsive Binding Protein (CREB)-binding protein (CBP), enhancing their transcriptional activation (Johnston et al., 1999)

By exploring the mechanism by which SRCAP regulates transcription it emerged that SRCAP is a coactivator of Protein Kinase A (PKA) activated factors including CREB (Monroy et al., 2001), steroid receptors (Monroy et al., 2003) and Notch mediated transcription (Eissenberg et al., 2005).

Using the WES approach, heterozygous truncating mutations were identified in *SRCAP* in five unrelated individuals affected by Floating-Harbor syndrome (FHS), a rare disease characterised by delayed speech development, short stature and distinctive facial abnormalities. Sanger sequencing allowed identifying mutations in eight more affected individuals confirming an important role for SRCAP in the disease (Hood et al., 2012). All the mutations were found in a small region of the final exon (codons 2435-2517), while R968H variant selected in this study doesn't lie in any defined functional domain.

2.3.4.3 KIF21B (T105M)

KIF21B (kinesin family member 21B) gene encodes for an ATP-dependent motor protein capable of movement along microtubules, thus responsible for intracellular transport of membranous organelles.

Alternative splicing transcript variants encode for four different isoforms of KIF21B: T105 residue is located within the kinesin motor domain which is conserved in all the splice variants and was predicted to be phosphorylated by NetPhos 2.0, an online server producing an artificial neural network predictions for phosphorylation sites in serine, threonine and tyrosine residues of eukaryotic proteins (Blom et al., 1999).

Kinesin motor domains have been found to be mutated in diseases affecting the neuromuscular system: autosomal recessive mutations in KIF1A (Erlich et al., 2011) and KIF1C (Dor et al., 2014) causes hereditary spastic paraparesis.

Autosomal dominant mutations in *KIF5A* are responsible for spastic paraplegia type10 and axonal Charcot-Marie-Tooth (CMT) type2 disease (Crimella et al., 2012) while autosomal dominant mutations in *KIF22* cause spondyloepimetaphyseal dysplasia with joint laxity (Boyden et al., 2011, Min et al., 2011).

Mutations in *KIF21B* gene have been documented in rheumatic diseases like inflammatory bowel disease (IBD), multiple sclerosis (Goris et al., 2010) and ankylosing spondylitis (Liu et al., 2013b).

2.3.4.4 WDR12 (L169S)

WDR12 (WD repeat domain 12) belongs to the WD-repeat protein family found prevalently in eukaryotic cells, characterised by a peculiar amino acid sequence motif (WD40 unit) present in several copies (4-16). Those WD40 units are organised into a "β-propeller-like" structures given by repetition of successive four-stranded antiparallel β sheet (Nal et al., 2002).

The peculiar WDR12 structure has been revealed to be important in regulating different protein-protein interactions, including the Notch signalling pathway (Nal et al., 2002), ribosome assembly and cell proliferation processes through the formation of the PeBoW complex (complex between Pes1, Bop1 and WDR12) (Holzel et al., 2005).

Moreover, WDR12 has been considered responsible for cardiac function deterioration since it is found to be up-regulated in heart failure (Moilanen et al., 2015).

Human WDR12 protein, like Wdr12 in mouse, is composed by 423 amino acids and seven WD units; L169 residue, where the pterygium associated variant was found, lies in the second WD unit, not associated with any post-translational modification (Nal et al., 2002).

2.3.4.5 HNMT (3'UTR miR-186 binding site)

HNMT (histamine N-methyltransferase) is a ubiquitously expressed enzyme able to N-methylate and inactivate histamine, an organic compound important in the inflammatory response increasing capillary permeability and as neurotransmitter.

Functionally active histamine and H1 histamine receptor expression have been described in pterygium (Maini et al., 2002).

Histamine is produced and eventually released by mast cells, granulocyte type cells that have been found increased in pterygium tissues compared to the control conjunctival tissues in several studies (Ratnakar et al., 1976, Butrus et al., 1995, Nakagami et al., 1999). In our case a sequence change in the 3'UTR of HNMT gene disrupted the miR-186 binding site. Disruption of a miRNA binding site implies the target gene overexpression: a HNMT overexpression in this case would determine a decrease in histamine concentration. Histamine plays a central role in the pathogenesis of allergic diseases like asthma, rhinitis or anaphylaxis (Garcia-Martin et al., 2007) and decreased histamine levels have been associated with schizophrenia (Nakai et al., 1991).

2.3.5 Five candidate genes analysis

Integrative genomic viewer (IGV) allowed confirmation of the coverage and the percentages of hetero/homozygosity in each family member for the five selected genes. The presence of heterozygosity in the affected members and homozygosity of the wild-type allele in the unaffected control confirmed that the allele was inherited in a dominant manner (Figure 2.2 A).

Sanger sequencing was then performed around the five mutated regions to confirm the presence of the variants identified by WES and eliminate any possible artefact coming from the NGS technique; all five mutations in the selected genes were confirmed by Sanger Sequencing (Figure 2.2 B).

Subsequently, the expression of the candidate genes in the cornea was evaluated. Three online available gene expression databases were interrogated: TiGER (Tissue-specific Gene Expression and Regulation), mainly relying on EST (Expressed Sequence Tag) information, Expression Atlas from EMBL including microarray and RNAseq data and Human Protein Atlas, based on the human proteome obtained through antibody and transcriptome analysis. All these databases showed expression of each of the genes limited to the whole eye, without distinguishing the specific parts within it: the cornea, conjunctiva and retina.

To corroborate expression data on the whole eye found in online available databases, a semi-quantitative RT-PCR was performed on RNA extracted from HCE-S corneal epithelial cells using newly designed intron-spanning primers. All five genes analyzed were expressed in HCE-S, but at different expression levels. The two most highly expressed genes, detectable even with 20 PCR cycles, were CRIM1 and SRCAP (Figure 2.2 C).

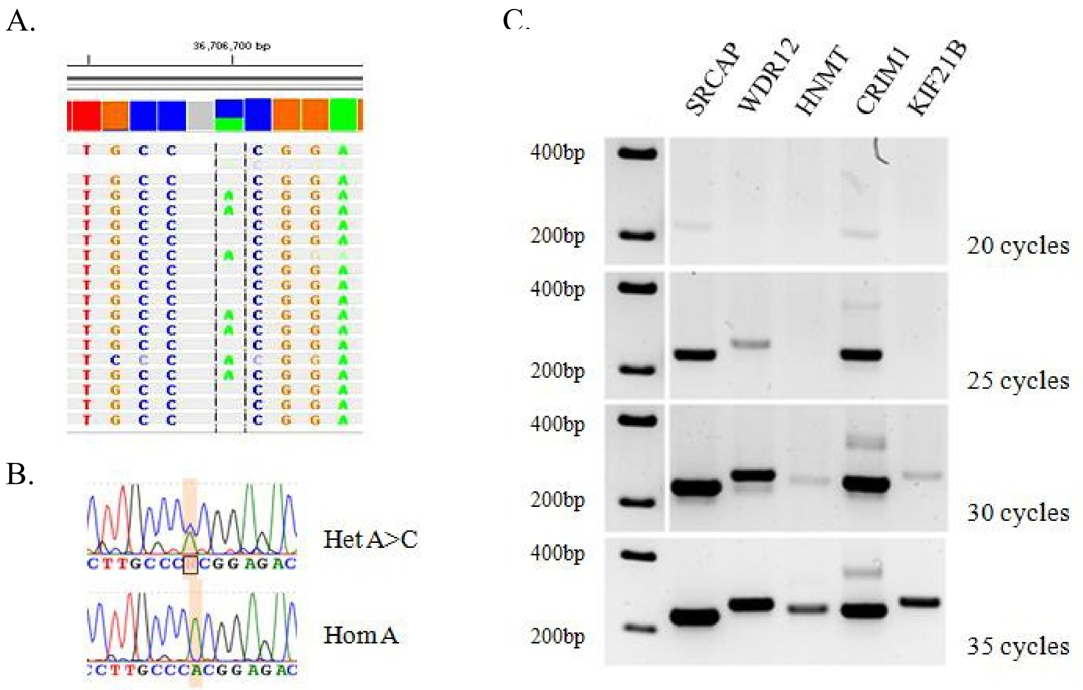

Figure 2.2 Candidate genes analysis

Panel A. Example of a pterygium family members sequence data from WES and visualised using IGV. The percentage of heterozygosity obtained is shown: A 42% and C 58%, with coverage of 19 counts

Panel B. Sanger sequencing performed in the family members confirmed the Adenine > Cytosine SNP is Heterozygosis in the affected individuals and is homozygous Adenine in the unaffected control.

Panel C. Semi-quantitative PCR at 20-25-30-35 cycles in HCE-S cells evaluating expression levels of the five candidate genes: *SRCAP, WDR12, HNMT, CRIM1 and KIF21B.*

Recent studies elucidated the importance of CRIM1 expression in eye development: CRIM1 was found to be upregulated in developing corneal and conjunctival epithelia (Lovicu et al., 2000) and a mouse CRIM1$^{KST264/KST264}$ line, producing a shortened isoform of CRIM1 protein, presenting with perinatal lethality, syndactyly as well as eye and kidney abnormalities (Pennisi et al., 2007). A whole exome sequencing approach identified a deletion in *CRIM1* in Colobomatous macrophthalmia with microcornea syndrome (MACOM), an autosomal dominant malformation of the eye (Beleggia et al., 2015) and experiments on mouse mutant Crim1 alleles showed a role for CRIM1 in regulating the levels of active β1 integrin in Lens Epithelial (LE) cells, phosphorylating FAK and ERK (Zhang et al., 2015).

Finally a GWA study demonstrated CRIM1 association with eye tumours in cattle: *CRIM1*, together with eleven other genes, was identified as a Quantitative Trait Loci (QTL) underlying ambilateral circumocular pigmentation (ACOP), a peculiar pigmentation surrounding the Fleckvieh cattle eyes which confer them with reduced susceptibility in development of bovine ocular squamous cell carcinoma (BOSCC) the most common eye cancer (Pausch et al., 2012).

Therefore, based on expression data and on the role of CRIM1 in the eye revealed by an extensive literature review, we decided to prioritise the analysis of CRIM1 as our top candidate gene.

2.3.6 CRIM1: domains, interactors and sequence analysis

CRIM1, the gene we selected for further analysis, is a large transmembrane protein (1002 amino acids, plus 34 amino acids of the signal peptide) in which, as previously described, there are 11 different protein domains annotated (Figure 2.3A): 6 Von Willebrand factor C, 4 antistasin-like and 1 Insulin-like Growth Factor-binding Protein (IGFBP) at the N-terminal, all of them are extra-cellular, while only two small C-terminal portions of the protein are predicted to be transmembrane (21 amino acids) and cytoplasmic (76 amino acids) (Kolle et al., 2000b). The mutation H412P is positioned in the second von Willebrand factor C (ref SNP: rs113372122). Analysing the alignments with various orthologues of CRIM1 we observed that the residue H412 is conserved through human (*Homo sapiens*), cattle (*Bos Taurus*), mouse (*Mus musculus*), rat (*Rattus norvegicus*), frog (*Xenopous laevis*), zebrafish (*Danio rerio*) (Figure 2.3B).

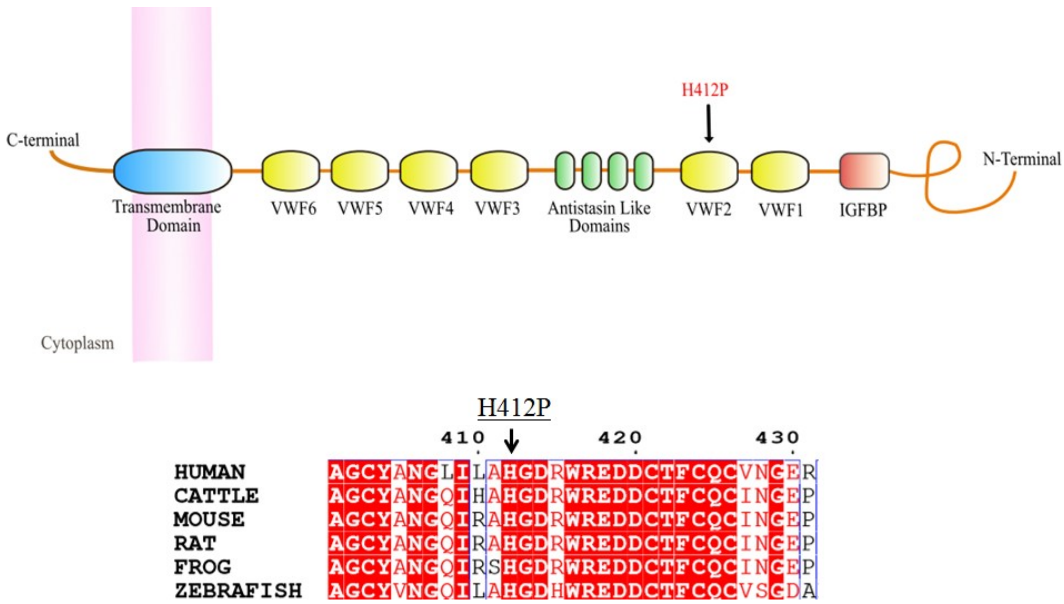

Figure 2.3 *CRIM1* (cysteine-rich motor neuron 1 protein)

Panel A. A schematic ideogram shows the Human CRIM1 transmembrane protein. In the CRIM1 plasmid used for *in vitro* experiments, at residue 412, the wild type Histidine was substituted with a Proline.

Panel B. Clustal X2.1 alignment of CRIM1 between Human, Cattle, Mouse, Rat, Zebrafish indicates that H412P missense mutation occur in a highly conserved residue. Alignment with the homologous Crm1 protein in C. elegans shows the presence of an Arg (R), an acidic residue similar to His (H). Results were visualized with EsPript 3.0. Legend: Red box, white character: strict identity; Red character: similarity in a group; Blue frame: Similarity across groups.

Von Willebrand factor type C (VWC) domains, known also as Cysteine-rich repeats (CRRs), are characterised by a conserved consensus sequence composed by ten cysteines ($CXnWX_4CX_2CXCX_6CX_4CX_{4–6}CX_{9–11}CCPXC$) for a total of 60-80 amino acids (Wilkinson et al., 2003).

The histidine residue (H412 in CRIM1) is also conserved in the Von Willebrand Factor C (VWFC)-2 of the human chordin and in VWFC-2 and 3 of human neuralin expressed in neural plate and axial skeleton (O'Leary et al., 2004a) as well as in the amnionless (Amn) transmembrane protein of the visceral endoderm (Abreu et al., 2002), all proteins playing a major role during embryo development.

Chordin and Neuralin in particular are secreted proteins which antagonize BMP signalling pathway by direct BMP binding and consequent receptor inhibition (Wilkinson et al., 2003). BMPs are members of the transforming growth factor- β (TGF-β) family and play a role in tissues and organs development as well as in patterning of mammalian embryo (O'Leary et al., 2004a).

BMPs 4 and 7 have been shown to interact with CRIM1 through the VWF domains (Wilkinson et al., 2003) (Kinna et al., 2006). However the VWF2 of chordin, similar to VWF2 of CRIM1 (% identity), was proved not to bind to BMP-7, which preferentially binds instead to VWF1 and 4 of chordin (Zhang et al., 2007).

CRIM1 has been also shown to interact with VEGFA, TGF-βs and PDGF through its VWF domains: if the latter are deleted, the interaction with the TGF-β superfamily members is disrupted (Wilkinson et al., 2007b). The role of the interaction with VEGFA has been further validated and found to be involved in the regulation of angiogenesis (Fan et al., 2014).

2.4 DISCUSSION

This project began with the identification of a multigenerational Northern Irish family affected by pterygium. This family presented as an interesting case because they were affected by a sun-related disease in three different generations, without high levels of sunlight exposure. The family members live in Northern Ireland, with some having spent thirteen years in Canada, but aside from this having only spent one or two weeks per year in sunny climates. It was proposed that within this family, genetic predisposition plays a fundamental role in the etiologic process of pterygium development.

Ingenuity and the subsequent *in silico* analysis allowed the screening of the variants found in common between the affected family members and to finally select five candidate genes: *SRCAP, KIF21B, WDR12, HNMT* and *CRIM1*.

In *KIF21B*, our T105M variant is located within the kinesin motor domain where other mutations were found associated with diseases affecting the neuromuscular system, including the extraocular muscles type I of the eye (Yamada et al., 2003) and neuronal transmission, including mammalian photoreceptors in retina (Marszalek et al., 2000).

Despite the above mentioned involvement of kinesin with eye function, there are no evident correlations between KIF21B and anterior cornea diseases.

WDR12, as previously reported, interacts with several proteins, including Notch. Notch, a key molecule in promoting myofibroblast differentiation during EMT, was found to be upregulated in pterygium (Engelsvold et al., 2013) and also retaining an important role in regulating migration in corneal epithelial wound healing through vitamin A and retinol binding protein1 (CRBP1) (Vauclair et al., 2007). Notch1 results in fact inhibited at the leading edge of the healing corneal epithelial cells promoting their migration (Movahedan et al., 2012), similarly to what could happen in pterygium cell overproliferation and migration through an altered interaction between the mutated WDR12 and Notch. No other relevant associations between WDR12 and eye diseases or sun-related effects have been reported.

HNMT, fundamental for histamine inactivation, if mutated could interfere with mast cell histamine release observed in pterygium. The disruption of a miRNA binding site normally causes an overexpression of the gene which is not properly silenced: in this case an overexpression of HNMT would cause an increased histamine inactivation and therefore downregulating the mast cells activity which is supposed instead to increase in pterygium. However, no *HNMT* mutations have been yet associated to any eye or UV related disease.

An expression analysis specific for the tissue under examination, the cornea in our case, helped at this point to understand how much the gene is expressed and therefore how much a missense mutation would interfere with its expression and function, affecting the tissue homeostasis.

From the *in vitro* analysis the two most expressed genes resulted to be *SRCAP* and *CRIM1*.

SRCAP, as previously mentioned in the results, plays a role in the regulation of CREB, steroids and Notch gene expression. Interestingly, CREB was found to be overexpressed in pterygium under UVB radiation (Nubile et al., 2013) and Notch, as we know from WDR12, is involved in EMT and regulation of cell migration in cornea. Therefore, mutations in *SRCAP* can alter those pathways involved in pterygium development.

However, in the identified variant R968H, a positively charged residue, Arginine (R) is substituted with another positively charged one, Histidine (H): even if the side chain differs for the imidazole in the H, the charge remains the same, thus not changing massively the residue properties.

Moreover no eye related diseases has yet been directly associated to SRCAP alteration.

CRIM1 presents as a credible candidate for playing a role in pterygium pathomechansim for several reasons.

Firstly, its association with UV associated eye tumors in cattle in a GWA study (Pausch et al., 2012). In this study *CRIM1* was identified as a quantitative trait locus (QTL) in the ambilateral circomocular pigmentation (ACOP) cattle when compared to normal Fleckvieh (FV) cattle. The ACOP cattle, a minority of the FV animals, present a peculiar pigmentation surrounding the eye which is associated to a reduced susceptibility in developing the common bovine ocular squamous cell carcinoma (BOSCC), normally caused by an elevated UV exposure.

Secondly, CRIM1 has recently been proven to be crucial in eye organogenesis (Beleggia et al., 2015) (Zhang et al., 2015). A germline mutation in *CRIM1* can cause an abnormal eye development, leading to a major vulnerability of the eye surface to other environmental factors like the UV radiation or viral infections.

Thirdly, an elegant experiment proved the interaction between CRIM1 and VEGFA through the von Willebrand factors domains, where the mutation we detected in this family is located (Wilkinson et al., 2007b). VEGFA, the most important angiogenic factor, has an important role in new vessels formation in pterygium (Bianchi et al., 2012, Detorakis et al., 2010) and in pterygium pathogenesis when mutated (Peng et al., 2014).

Fourthly, the substitution of a positively charged histidine (H) with an apolar proline (P), as found in this family, can strongly change the physico-chemical properties of the amino acid residue, thus interfering with the CRIM1 conformation and function.

All the family members affected by pterygium participated to the present study and were compared with an unaffected sibling during the WES analysis. Unfortunately, data from other family members were not available. Analysing the presence of the selected variants in additional family members would have helped during the selection process. However, given the reduced penetrance of pterygium (Islam and Wagoner, 2001b, Bradley et al., 2010), finding one variant in an unaffected family member would not necessary invalidate that candidate gene. On the contrary, not finding the selected variant in an affected member would have been more invalidating.

CHAPTER 3

Screening of mutations in CRIM1

Contribution

Eleonora Maurizi carried out all research unless otherwise stated

Dr Sarah Atkinson – Bolivian samples organization, supervised research, proofread

Dr David Courtney – sample collection from Belfast

Dr Vicky Mc Gilligan – sample collection from Belfast

Laura Mairs – sample collection from Belfast

Prof Johnny Moore – clinical instruction

Prof Tara Moore – Bolivian samples organization, ethical approval, recruitment and sample collection from Bolivia, supervised research, proofread

Dr Andrew Nesbit – supervised research, proofread

Dr Davide Schiroli – helped with PCR, qRT-PCR and statistical analysis

Jesus Vasquez – follow up sample collection in Santa Cruz, Bolivia

Daniel E. Illness Velarde – liaison for ethical approval in Bolivia

3.1 INTRODUCTION

CRIM1, as discussed in Chapter 2, is a type I transmembrane protein, characterised by an IGF-binding protein domain and six cysteine-rich repeats (Kolle et al., 2000a) which has been revealed to have an important role during eye development (Lovicu et al., 2000, Beleggia et al., 2015).

CRIM1 is able to stabilize cell-cell junctions through interaction with β-catenin, cadherins (Ponferrada et al., 2012) and β1 integrins, modulating cell adhesion, polarity and proliferation during murine lens formation (Zhang et al., 2016).

Another role attributed to CRIM1 is its involvement in blood vessel formation (Glienke et al., 2002, Kinna et al., 2006), enhancing the autocrine signalling of VEGFA in retinal vascular endothelial cells (VECs)(Fan et al., 2014). CRIM1 was also shown to be upregulated in the presence of VEGFA in HUVECs, with ERK signalling possibly involved in this process (Nakashima and Takahashi, 2014).

A direct interaction between CRIM1 and VEGFA has been proven using a series of CRIM1 deletion constructs in co-immunoprecipitation reactions with VEGFA: the presence of all CRIM1 cysteine-rich repeat (CRR) domains was revealed to be essential for VEGFA binding, since no binding was displayed if those domains were deleted (Wilkinson et al., 2007b).

CRR (otherwise known as VWC) domains have been identified in more than 200 extracellular matrix proteins including chordin, von Willebrand factor, thrombospondins, connective tissue growth factor, and procollagen type IIA (ColIIA), which act on binding and modulating members of the TGF-β superfamily and regulate growth factor signalling (O'Leary et al., 2004b).

BMPs, for example are secreted growth factors of the TGF-β superfamily playing an important role during embryonic development or tissue repair in adults. Chordin or VWFC containing proteins act as antagonists to BMP signalling and their inhibitory potential resides in the CRR domains (Garcia Abreu et al., 2002). In CRIM1, the six CRR domains are located in the extracellular portion and are able to bind BMP4 and BMP7 when they are co-expressed within the Golgi, leading to a reduction in the processing and secretion of the BMP (Wilkinson et al., 2003).

Mutations occurring in one of those domains (like the H412P in VWF2 detected in this study) could impair the interaction of CRIM1 with other proteins like VEGFA or BMPs. Alternatively, because these domains are rich in cysteine which are essential to form disulphide bonds and loops that stabilise the tertiary structure of the protein (Vitt et al., 2001), a mutation in this domain could cause protein misfolding and consequently its dysfunction.

Because of the direct involvement of VWFs in protein-protein interaction and signal transduction sequencing was performed for all the CRIM1 VWFs in individual patients with pterygium from Northern Ireland and Bolivia.

The rationale for this is that other ocular diseases can be caused by different mutations in the same gene: three different *COL8A2* mutations were identified in early onset Fuchs' endothelial dystrophy (Elhalis et al., 2010) and over 60 mutations in the *TGFBI* gene, in four different corneal dystrophies: Lattice corneal dystrophy (LCD), Granular corneal dystrophy (GCD), Reis-Bücklers corneal dystrophy (RBCD), Thiel-Behnke corneal dystrophy (TBCD) (Munier et al., 2002).

Screening for *TGFBI* mutations revealed the presence of two hotspots (Arginine at positions 124 and 555) where mutations with consequent amino acid substitutions occur more frequently in various populations. These mutations are the most representative of two extracellular fascilin domains (Fas1 and 4, respectively), where also almost all the other amino acid substitutions have been identified. (Kannabiran and Klintworth, 2006).

However, while mutations in Fas4 affected the overall stability of TGFBI, reducing the proteolytic degradation and leading to aggregate accumulation, mutations in Fas1 do not alter the TGFBI stability (Runager et al., 2011, Underhaug et al., 2013), implying that mutations in Fas1 act through a different pathogenic mechanism; possibly impairing the interaction with other proteins.

CRIM1, as well as TGFBI, is characterised by several extracellular repeated domains and therefore I wanted to investigate if, also in this case, it was possible to identify mutations in those structural domains.

UV light is now considered the primary cause of pterygium pathogenesis; this follows from several studies beginning in 1954, the first time pterygium was related to geographical distribution of the population (Anderson, 1954). This encouraged many researchers to collect data of pterygium prevalence and risk factors in affected populations of different ethnicities: Barbados (Luthra et al., 2001), Iran (Rezvan et al., 2012, Fotouhi et al., 2009), China (Liang et al., 2010), Spain (Viso et al., 2011) and India (Nangia et al., 2013).

A meta analysis study tried to pool together all the results obtained in twenty population studies (Liu et al., 2013a), calculating a pooled pterygium prevalence rate of 10.2% in the general population coming from 12 different countries. Low latitudes, outdoors activities and age were associated with the highest prevalence while the gender association remained uncertain.

In Western Australia a comparison between sun exposure and pterygium incidence confirmed the importance of ocular exposure to UV rays, positively correlated to the risk of developing pterygium (Threlfall and English, 1999).

However, a study comparing sawmill workers from Canada, Northern India, Thailand, and Taiwan showed that the environment inside the sawmills had a greater effect than ethnicity in determining a higher prevalence of pterygium. Working in the sawmills involves indoor work and this study underlines the fact that pterygium is not solely caused by UV radiation, but often other kinds of eye irritants such as the dust in sawmills (Detels and Dhir, 1967).

Surfing was also found to be significantly associated with pterygium prevalence within the Hawaiian population, possibly explained by the wind, the UV enhanced reflection by the sea and the difficulty of using protective eyewear while surfing (Lin et al., 2016).

3.1.1 Aims of Chapter 3

The aim of this chapter is finding more evidences that CRIM1 is involved in pterygium pathogenesis. To pursue this purpose, other possible causative variants within CRIM1 VWFs were investigated analysing the DNA coming from additional pterygium affected individual patients either from Northern Ireland (low UV exposure) and Bolivia (high UV exposure). Genomic primer design around each CRIM1 VWF and direct Sanger sequencing were chosen as reliable and affordable techniques for a limited number of samples. Finding another missense mutation within the same gene in a different individual patient affected by pterygium would strengthen the hypothesis of CRIM1 as an important factor in pterygium aetiopathogenesis.

CRIM1 expression levels were further determined by qRT-PCR (quantitative RealTime-PCR) performed on RNA obtained from Impression cytologies samples of Northern Irish and Bolivian affected and unaffected individuals. The two populations differ significantly in climate exposure, altitude and latitude, the main epidemiologic factor for pterygium development (Detorakis and Spandidos, 2009a) but also in culture and habits.

3.2 METHODS

3.2.1 Patient recruitment

Informed consent, completed questionnaires and a blood sample were obtained from each individual examined. Ethical approval for the study was obtained from ORECNI (Office for Research Ethics Committees Northern Ireland), UK and Comité de Bioética de la Facultad de Medicina, Santa Cruz, Bolivia.

Clinical examinations were performed at Cathedral Eye Clinic, Belfast, UK and in Facultad de Medicina, Santa Cruz, Bolivia.

Two additional unaffected family members of the Northern Irish family studied in Chapter 2 were recruited together with 12 Northern Irish and 9 Bolivian pterygium affected individuals for sequence analysis of *CRIM1*.

3.2.2 DNA extraction from Blood and CRIM1 VWF Sanger sequencing

Genomic DNA was extracted from blood leukocytes using QIAamp DNA Blood mini kit (QIAGEN, Manchester UK) and quantified using a Nanodrop 1000 spectrophotometer (Thermo Fisher Scientific).

VWFs of CRIM1 were amplified using PCR optimised conditions as following: initial denaturation at 95°C for 3 minutes, then 35 cycles of: denaturation at 95°C for 30 seconds, annealing at 56°C for 30 seconds, elongation at 72°C for 1 minute and final elongation at 72°C for 5 minutes.

Primer3 software was used to design the following genomic primers:

Exon6_F 5’ TTGAAAAACATCAAAGGACACAA 3’ (VWF1),

Exon6_R 5’ CCATGTATGCTCCTGTTAATCTG 3’ (VWF1),

Exon7_F 5’GATGACTAGAACCCAGGGAAAA 3’ (VWF2),

Exon7_R 5’ AGCAGACATTATGCCCAAGG 3’ (VWF2),
Exon11_F 5’ GCCTGTTTCTCCTGTGCAGT 3’ (VWF3),
Exon11_R 5’ TGCAAGGCAGAAGTCATTTG 3’ (VWF3),
Exon12_F 5’ CCAGGCTTTCAAGAGTTGGA 3’ (VWF4),
Exon12_R 5’ GGGTCCCACAGAATGACAAC 3’ (VWF4),
Exon13_F 5’ CTGGCCAACAGCATCTTCTT 3’ (VWF5),
Exon13_R 5’ GACATGTCAAGCAGGGAAAAA 3’ (VWF5),
Exon14_F 5’ AAGATCGTGTGCGTTGTCAC 3’ (VWF6)
Exon14_R 5’ GTCGAGCTCTGCTTCGATTT 3’ (VWF6)

Once the PCR products were verified in a 1% agarose gel (UltraPure Agarose, Thermo Fisher Scientific), they were sent to Department of Zoology at University of Oxford to be purified and Sanger sequenced.

Sequences were then aligned to the *CRIM1* consensus one and analysed using DNA Dynamo software.

3.2.3 Pterygium samples

Pterygium tissues samples were collected during the pterygium surgery and immediately submerged in RNA later (Qiagen) at room temperature.

3.2.4 Impression cytology samples

Conjunctival epithelial and pterygium cells from the superficial portion of the patients eyes were harvested using 4 x 4 mm strips of sterile LCR biopore membrane filter (pore size, 0.45 um; Millipore, Watford, UK) as previously described (Moore et al., 2011). Briefly, the membrane filter was placed over the conjunctival epithelium; a light pressure was applied and the filter was then removed so that epithelial cells remained attached to the filter which was then stored in RNAlater (Qiagen) at room temperature.

3.2.5 RNA extraction and reverse transcription

Impression cytology samples were vortexed at maximum speed for 2 minutes to promote conjunctival and pterygium cell detachment from the filter.

Pterygium tissue was disrupted by submerging the tissue in liquid nitrogen and then homogenising it with mortar and pestle until a white powder was obtained.

RNA was then extracted using the RNeasy Plus Mini Kit (Qiagen, Manchester, UK) following the manufacturer’s instructions. Briefly: tissue or cell lysates were spun through the first column (gDNA Eliminator spin column) to eliminate the genomic DNA and then a second column (RNeasy Mini spin columns) was used to purify total RNA.

Total RNA was subsequently quantified using Nanodrop 1000 (Thermo Fisher Scientific), run out on an agarose gel to assess quality and then 1 μg of total RNA was reverse transcribed into cDNA using the High Capacity cDNA Reverse Transcription Kit (Life Technologies, Paisley, UK) according to the manufacturer's protocol. Briefly: the reaction mix includes 1μg of total RNA, reverse transcriptase, random primers, mix of the four dNTPs (deoxynucleoside triphospate) and reaction buffer. Random primers have been proven to efficiently initiate cDNA synthesis with all RNA molecules present, including mRNA and rRNA. cDNA relative quantification is possible given that the reverse transcriptase reaction generates products which are directly proportional to the amount of initial RNA template

3.2.6 qRT-PCR

The qRT-PCR assays were performed using a Lightcycler 480 II (Roche, West Sussex UK) on cDNA obtained from the extracted RNA.

Real Time Ready Assays for CRIM1 (assay id. 112278), GAPDH (assay id. 141139) and hypoxanthine phosphoribosyltransferase (HPRT) (assay id. 102079) were purchased from Roche (Burgess Hill, West Sussex, UK). The qRT-PCR conditions used were: 45 cycles: 1) Denaturation at 95 °C for 10 seconds, 2) Annealing at 60 °C for 30 seconds and 3) Extension at 72 °C for 1 second.

Data were normalised using HPRT and GAPDH as housekeeping controls for ΔCt and ΔΔCt calculations (Schmittgen and Livak, 2008). HPRT and GAPDH were chosen as they have been shown to the most stable corneal housekeeping genes (Kulkarni et al., 2011). For each condition all complementary cDNA samples were run in duplicate in two independent experiments.

3.2.7 Statistical Analysis

All error bars represent the standard error of the mean (SEM) calculated between sample replicates of the same biological group. Significance was estimated using a Student's t-test from an Excel spreadsheet.

A Mann-Whitney U test was used in GraphPad Prism 5 software for comparison of CRIM1 expression between two different populations in Figure 3.3. Data were illustrated using Box plot (or Box-and-Whisker plot) in Excel, including $2^{-\Delta Ct}$ median values (central horizontal line), the first and third quartile (upper and lower box horizontal lines) and minimum and maximum values (whiskers).

p value ≤ 0.05 was deemed to be significant (*p value ≤ 0.05, **p value ≤ 0.01 and ***p value ≤ 0.001).

3.3 RESULTS

3.3.1 Screening of mutations in CRIM1

The CRIM1 H412P mutation was analysed using Sanger sequencing in genomic DNA from two family members, additional to those samples used for the WES (III.2 and III.3, see Figure 2.1 in Chapter 2), 12 Northern Irish pterygium affected individuals and 9 pterygium affected individuals from Bolivia.

The two additional family members (III.2, age 49 and III.3, age 34) were shown to have the same H412P CRIM1 mutation found in the other affected family members; despite having not developed any signs of pterygium yet (Figure 3.1).

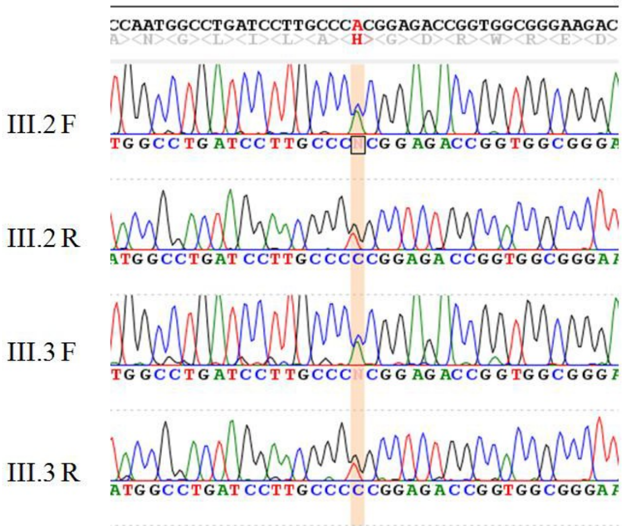

Figure 3.1 Pterygium unaffected III.2 and III.3 family members carry the H412P mutation

Sanger sequencing performed in exon7 of CRIM1 revealed the same H412P (A>C) mutation in two members of the pterygium family who are unaffected by pterygium (III.2 and III.3). Both Forward and Reverse primers confirmed the presence of the H412P mutation in CRIM1.

In the top part of the figure is the *CRIM1* nucleotide sequence with the corresponding amino acid sequence below in grey. The base changed is highlighted in red; sequencing results were visualized using DNA Dynamo DNA Sequence Analysis Software.

Table 3.1 includes information regarding pterygium affected individuals from Northern Ireland together with a pterygium affected member belonging to a British family: patient n.12, which corresponds to patient II.1 of a previous study (Romano et al., 2016).

Patient	Year of birth	Sex	Eye condition	Age onset (years)	Lived abroad	Time spent in sunny climates (every year)	Wear sunglasses
1	1942	M	pterygium		no	-	no
2	1950	M	minor pterygium	62	no	-	no
3	1931	M	pterygium	79	no	1 week	no
4	1954	M	pterygium				
5	1946	M	pterygium	59	no	10 weeks	sometimes
6	1975	M	pterygium				
7	1941	M	pterygium				
8	1958	F	pterygium	50	no	1 week	sometimes
9	1984	F	pterygium				
10	1934	M	pterygium				
11	1974	F	pterygium	42		3 weeks	
12*	1967	F	pterygium family	47	no	-	no

Table 3.1 Pterygium individual patients from UK

List of pterygium affected individuals collected in UK and the relative information obtained through the questionnaire.

Blank spaces indicate missing information and "–" indicates no time spent in sunny climates.

*Patient n.12 denotes the pterygium affected II.1 family member previously studied by Romano *et al.* 2016

Blood was collected from each individual patient and genomic DNA was extracted to analyse their CRIM1 VWFs sequences using Sanger sequencing.

None of the pterygium affected individuals from the UK carried the same H412P variant in CRIM1 and no other variants were identified either in the same protein domain (VWF2) or in any of the other VWFs domains (see Figure 2.3A in Chapter 2).

The same analysis was carried on in pterygium affected patients from Bolivia. Nine genomic DNA samples were obtained from blood coming from Bolivia; the samples are listed in Table 3.2.

Patient	Year of birth	Sex	Eye condition
B1	1965	F	pterygium
B2		M	pterygium
B3	1949	M	pterygium
B4	1957	M	pterygium
B5	1999	M	pterygium
B6	1952	M	pterygium
B7	1947	F	pterygium
B8	1941	M	pterygium
B9	1990	M	pterygium

Table 3.2 Bolivian pterygium individual patients

List of pterygium affected individuals collected in Bolivia and the relative date of birth and gender.

Blood was collected from each individual patient and genomic DNA was extracted to analyse their CRIM1 VWFs sequences using Sanger sequencing.

Patient B1 presented another mutation in a different CRIM1 VWF: a substitution of a C (cytosine) with a T (thymine) in the first position of the 745 codon corresponding to an Arginine to Cysteine (R745C) amino acid change in exon 13 (between VWF4 and VWF5) as shown in Figure 3.2A.

Conservation analysis of R745 residue across the species using UCSC revealed that the Arginine is conserved in human, rhesus and elephant while it is lost in mouse, dog and chicken (Figure 3.2B). The R745 and the flanking amino acidic residues are not highly conserved throughout the species. The sequence position R745 was identified as rs145721446 according to dbSNP.

No additional mutations have been found in the other pterygium affected patients from Bolivia.

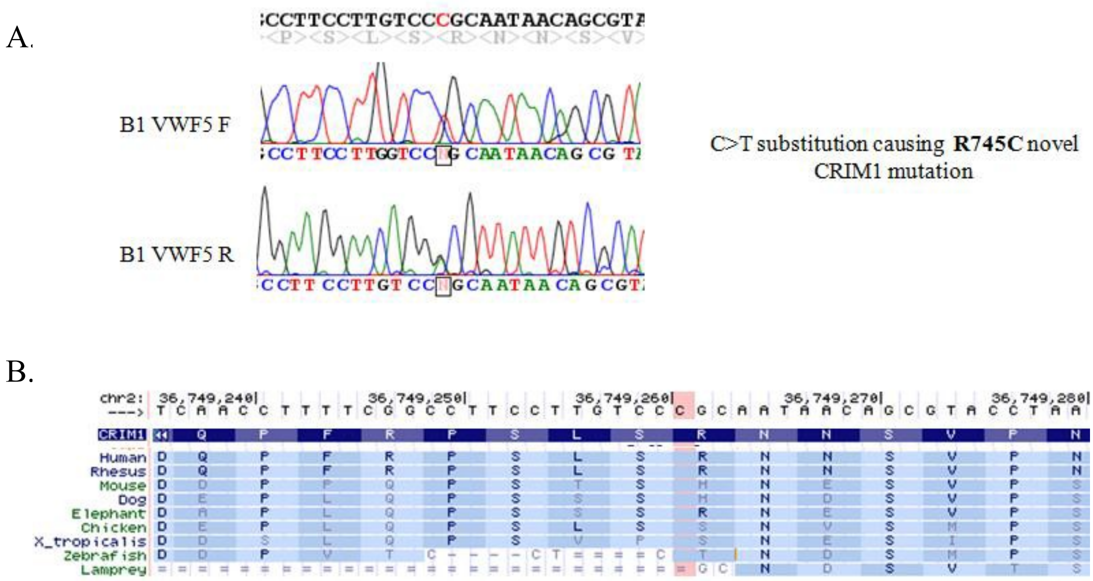

Figure 3.2 Novel CRIM1 R745C mutation in a pterygium affected individual

Panel A. Sequencing results from Patient B1, Bolivian cohort, visualized with DNA Dynamo are shown. Both forward (F) and reverse primers (R) confirmed a C>T substitution in exon 13 of the CRIM1 gene corresponding to an Arg745Cys amino acid change.

The top part of the figure shows the *CRIM1* nucleotide sequence with the corresponding amino acid sequence below in grey; the base change is highlighted in red.

Panel B. UCSC browser allows visualization of the R745 residue conservation through the species performing a multiple alignment of 100 vertebrates.

3.3.2 Pterygium affected individuals have increased CRIM1 expression

CRIM1 expression was subsequently investigated using qRT-PCR and compared a Northern European and a South American population (Figure 3.3).

RNA was obtained from impression cytology samples both from South America and Northern Europe (17 Bolivian controls, 12 Bolivian pterygium, 4 Northern Irish controls, 4 Northern Irish pterygium affected unrelated individuals and the II.2 pterygium affected member of the Northern Irish family studied in Chapter 2).

13 additional excised pterygium tissues from the Bolivian population were also included in this comparison.

Data obtained showed a slightly increased level of CRIM1 expression comparing impression cytology samples of pterygium and unaffected conjunctival controls from Bolivia ($2^{-\Delta Ct}$ mean values are respectively 1.22 ± 0.22 and 0.92 ± 0.12 while median values visible in the figures are 1.03 and 0.84, p value n.s.).

However, a significant difference in CRIM1 expression was observed in the Northern Irish population, comparing the pterygium affected with the unaffected controls ($2^{-\Delta Ct}$ mean values are respectively 4.22 ± 0.76 and 1.28 ± 0.122, while median values visible in the figures are 3.4 and 1.3, $p = 0.028$).

A direct comparison between the IC samples from the two populations shows a significant increase of CRIM1 expression in pterygium affected participants from Northern Ireland with respect to those from Bolivia ($p \leq 0.01$).

Analysing CRIM1 expression in the whole pterygium tissue of Bolivian patients, I obtained a ~three times higher CRIM1 expression from pterygium tissue ($2^{-\Delta Ct}$ mean value of 3.13 ± 0.34 and median value of 2.9) compared to the impression cytology samples of the Bolivian affected individuals (p value ≤ 0.001).

The impression cytology of the individual pterygium affected family member II.2 showed a very low CRIM1 expression, lower than that of the unaffected controls ($2^{-\Delta Ct}$ value of 0.32 compared to average 1.28 ± 0.12 of NI controls and 4.22 ± 0.76 of NI pterygium individuals).

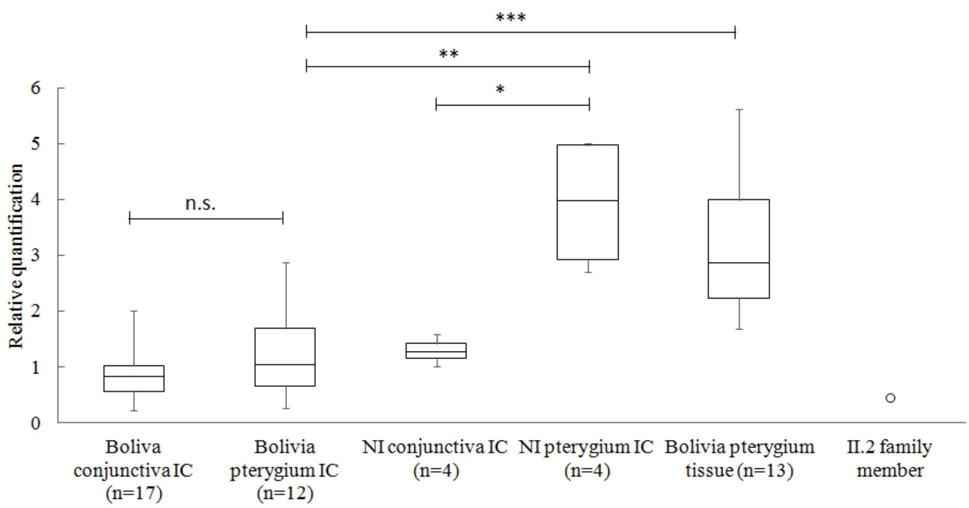

Figure 3.3 CRIM1 expression varies comparing high and low UV exposed populations

qRT-PCR analysis was carried out in cDNA obtained from two ethnically different populations originating from Northern Ireland and Bolivia.

RNA was extracted from different groups of samples: impression cytologies (IC) of conjunctival controls and pterygium individuals from Bolivia and Northern Ireland, one IC of the Northern Irish family member affected by pterygium (II.2) and whole pterygium tissues from Bolivia.

A Box plot (or Box-and-Whisker plot) was used to illustrate the data, expressed as median of the $2^{-\Delta Ct}$ value (central horizontal line) with the first and third quartile as the upper and lower box horizontal lines and whiskers delineating the minimum and maximum values. Significance was obtained with Mann-Whitney U test using GraphPad Prism 5 software. n=2 with three technical replicates each.

3.4 DISCUSSION

This chapter focuses on CRIM1 analysis both at its sequence level and at the expression level across two different populations from UK and Bolivia.

Analysing genomic DNA of two members of the pterygium family described in Chapter 2 but not included in the WES because they were not affected by pterygium symptoms I observed that they present the same H412P mutation in CRIM1 as well as the affected members (Figure 3.1).

First of all, even if not highlighted through the questionnaire, there might be other environmental triggers that have caused pterygium in some family members which have not been experienced by those two unaffected members. Moreover, the two unaffected family members carrying H412P mutation are younger than the other affected member of the family, especially patient III.3 who is only 34 years old and may not have developed pterygium yet, considering that the average onset of the family is 48 years old.

Multiple endocrine neoplasia type 1 (MEN1) is determined by the combined occurrence of tumours affecting three endocrine glands: parathyroid, pancreatic islet and anterior pituitary gland. This syndrome is caused by mutations in the *MEN1* gene which encodes for the nuclear transcription factor menin. People carrying a mutation in the *MEN1* gene develop a particular endocrine tumour more frequently as their age increases (Trump et al., 1996).

The MEN1 penetrance is highly heterogeneous, increasing gradually from the age of five years old (before is nonpenetrant) and reaching 100% only at sixty years of age (Machens et al., 2007, Bassett et al., 1998) and therefore some individuals may never develop a tumour during their lifetime even if diagnosed as a carrier of a *MEN1* mutation.

Similarly to the age-related penetrance described for the MEN-1 syndrome, it is possible that family members carrying the same H412P mutation in CRIM1 may never develop pterygium or will do very late during their lifetime.

A mechanism of incomplete penetrance, which implies that the person carrying a certain genotype may or may not manifest a clinical phenotype (Zlotogora, 2003), has been previously described in pterygium (Islam and Wagoner, 2001a, Chui et al., 2008, Bradley et al., 2010, Chen et al., 2013). In certain families hereditary factors play a pivotal role in pterygium development. However, the majority of pterygium patients show no evidence of inheritance: this can be due to a mechanism of incomplete penetrance where the external influence is just an adjuvant or alternatively the environmental stimuli represents the main etiologic factor where the genetic component is only a predisposing factor (Zhang, 1987a). Other ocular diseases which present with incomplete penetrance include retinitis pigmentosa (McGee et al., 1997) and glaucoma (Morissette et al., 1998) or corneal diseases including keratoconus (Nowak and Gajecka, 2011) and Fuchs' dystrophy (Sundin et al., 2006) or UV related diseases like melanoma (Bale et al., 1986).

With all the evidence taken into consideration, individuals III.2 and III.3 of the Northern Irish pterygium family should be monitored closely for development of pterygium in the future.

The CRIM1 H412P mutation was not found in other affected unrelated individuals from Northern Ireland and Bolivia. This is consistent with the MAF for the H412P variation in *CRIM1* gene, found to be 0.0019 according to ExAC (Exome Aggregation Consortium), an online available browser which attempts to gather together data produced by large scale exome sequencing projects.

The H412P mutation could be restricted to this Northern Irish family. Its MAF is so low (2 in 1000 individuals) that even compared to pterygium incidence in Northern Ireland (around 1-2%), it would not be unusual to not find it in other individuals.

Moreover, the 12 Northern Irish pterygium affected patients examined did not show any other mutation in the six VWFs sequenced.

Pterygium prevalence outside the equatorial zone (40^0 north and south of the equator) barely reaches 2% compared to the 22% prevalence of the equatorial area (Detorakis and Spandidos, 2009a), therefore mostly affecting people with an increased exposure to UV light. Considering the fact that the samples were collected in Northern Ireland, which is located at around 55^0 north of latitude, it was only possible to collect a limited number of samples for the study.

The UV index is a universal measurement of the amount of UV sunlight responsible for erythema, being directly proportional to the intensity of sunburn produced at the earth surface (Allaart et al., 2004). This standard indicator is used worldwide for weather reports, forecasts and to warn the population to wear protection against the damaging effects of UV by many international institutions including the World Health Organization (WHO) (Vanicek et al., 2000).

WHO information and UV index values at different geographical latitudes are available at the following link: http://www.who.int/uv/intersunprogramme/activities/uv_index/en/. Considering the latitude of Northern Ireland being 55°N and of Bolivia being 16°S we can see in Table 3.3 how the mean UV index changes between the latitudes. The UV index of Bolivia would be close to that of Darwin (13°S) and therefore it does not go below 7 even in the coldest months. This can be compared to the UV index of Northern Ireland which, being 55°N latitude, is between the one in Berlin and St Petersburg, meaning that it would not reach 7 even in the warmest months of the year.

Country (City)	.	J	F	M	A	M	J	J	A	S	O	N	D
Argentine (Buenos Aires)	35°S	9	9	7	4	3	2	2	4	5	7	9	10
Australia (Darwin)	13°S	12	13	12	10	8	8	8	10	11	13	12	12
Brazil (Rio de Janeiro)	23°S	12	11	9	7	5	5	5	7	9	10	12	12
France (Paris)	49°N	1	1	3	4	6	7	7	6	4	2	1	0
Germany (Berlin)	52°N	1	1	2	4	5	7	7	5	3	1	1	0
Russia (St Petersburg)	60°N	0	0	1	3	4	5	5	4	2	1	0	0

Table 3.3 UV index at different geographical latitudes and months of the year The table is part of a more complete list of worldwide cities available at: http://www.who.int/uv/intersunprogramme/activities/uv_index/en/index3.html

Another important factor influencing pterygium prevalence is the altitude (Roy, 2004). A study conducted in Nepal showed a stronger pterygium prevalence in the Tibetan and Thakali population living in the high altitude of Mustang when compared to the ones living in the Kathmandu valley (Shrestha and Shrestha, 2014). The Southern Harbin population, living at low altitude in a cold climate, registered instead a lower prevalence than other regions in the world (Li and Cui, 2013) .

Even if a mutation was not found in CRIM1 VWFs for the Northern Irish pterygium samples in this study, this does not exclude the occurrence of a mutation within another CRIM1 functional domain like the IGFBP or one of the four antistasin domains. Another possibility is that the interaction of the VWFs domains is impaired not because of a mutation in one of the VWF itself but rather in one of the CRIM1 interactors like VEGFA or BMPs.

The Northern Irish family may represent a rare case of a *CRIM1* germline mutation leading to pterygium.

In 1990 germline mutations in *p53* tumor suppressor gene were found to be responsible for the autosomal dominant Li-Fraumeni syndrome (LFS) (Malkin et al., 1990) which predisposes to early-onset familial syndrome of breast cancer, soft-tissue sarcomas and other neoplasms (Li and Fraumeni, 1969). Following this discovery many cancer studies looked for p53 inherited mutations, the majority of which were found in breast carcinoma (24%), bone sarcomas (12.6%), brain tumors (12%) and soft tissue sarcomas (11.6%); with half of the families diagnosed with LFS (Kleihues et al., 1997).

Somatic mutations in the same *p53* gene were found in more than half of all cancer genomes (Kandoth et al., 2013). Those somatic mutations in *p53*, despite showing heterogenous frequency in comparison to germline mutations of the same tissue, present a similar distribution within the *p53* gene in highly conserved regions of exon 5 to 8 (Kleihues et al., 1997).

The average age of onset of pterygium in the Northern Irish individuals affected by pterygium is 57 years old, higher in comparison to the 48 onset average of the Northern Irish family studied in Chapter 2 suggesting that the genetic component shared by the affected family members lowers the onset age and increases the predisposition of the individuals in developing pterygium.

Other cases of familial early onset were previously studied: a Saudi Arabian family was found with three members affected by an aggressive and early onset form of pterygium at age four, six and early 20s although no genetic study has been conducted in these patients (Islam and Wagoner, 2001a).

A study conducted using genomic DNA from 127 pterygium patients and 109 controls highlighted how younger patients enrolled in the analysis presented with a significantly higher frequency of the *GSTM1* null genotype (Tsai et al., 2004a). Another group showed that in the *hOGG1* gene involved in oxidative stress, the homozygous mutant Cys/Cys genotype substituting Ser326 was significantly more prevalent in pterygium patients than controls and in pterygium patients the mean age of individuals carrying the Cys/Cys genotype was younger than those with Ser/Ser or Ser/Cys genotypes. Finally, analysis of 50 pterygium affected genomic DNA samples revealed germline mutations in *Ki-ras* in 10% of the samples and this occurrence was positively correlated with young age of the patients (Detorakis et al., 2005a). The WES data obtained in this study did not show any mutation in these genes and therefore they were excluded from further investigation.

Analysis of VWFs in patients from Bolivia identified one patient (B1) carrying another missense mutation in exon13, R745C, identified as rs145721446 (Figure 3.2A).

According to ExAC, the MAF of R745C mutation is 0.000008237, even lower than H412P and quite rare in the general population. Moreover this mutation was considered possibly damaging by PolyPhen and deleterious by SIFT software, all information suggesting that this amino acid change may have an important role in the protein function.

The R745 residue is conserved only in human, rhesus and elephant (Figure 3.2B). Arginine amino acid substitution with Histidine, carrying similar cationic properties was found in mouse and dog. In chicken and X. tropicalis (western frog) the Arginine changes instead in Serine, a more different amino acid. However, because the eye structure in those animals is also particularly diverse from the human one, this can explain the higher amino acid variability within this CRIM1 region.

Other mutations were not found in any of the other Bolivian individual patients analysed.

CRIM1 expression level was also analysed and compared between samples coming from low and high sun exposure: Northern Ireland and Bolivia, respectively.

IC samples for the Bolivian cohort were analysed for expression of CRIM1: a difference between expression levels in the pterygium and conjunctival controls was not detected. However, a clear increase in CRIM1 expression was observed in pterygium patients from Northern Ireland compared with the relevant conjunctival controls.

According to direct clinical experience, in South America people are naturally exposed to higher doses of UV rays and culturally but also economically less used to wearing sunglasses to protect their eyes.

Moreover, in Northern Europe pterygium generally is diagnosed earlier and often treated for aesthetic reasons before vision impairment occurs while in South America the tissue is removed only once it impairs vision by which time it is completely fibrotic and highly vascularised.

The fact that pterygium is diagnosed earlier in Northern Irish population, where we observed an higher CRIM1 expression, suggests that CRIM1 may act as an early effector of a defensive mechanism to UV light: CRIM1 expression might increase as part of the eye’s attempt to counteract the damaging effects of UV radiation. This mechanism could then be lost at a later stage of the UV mediated corneal damage, when pterygium is already grown towards the central cornea, as observed in the Bolivian population.

A similar protective role has been described for transglutaminase 2 (TG2), which is overexpressed up to 15-fold in the early stages of liver fibrosis to counteract the inflammatory response and decreases in the advanced stages of the disease (Nardacci et al., 2003).

A low CRIM1 expression level in the family member analysed reinforces the idea of CRIM1 overexpression as a defensive mechanism, which is impaired in the case of the H412P mutation and therefore of the II.2 family member analysed.

The increased CRIM1 expression observed in the whole pterygium tissues compared with the IC samples from Bolivia can be explained by the different sampling procedures: ICs are taken from the superficial conjunctival epithelium, thus not including internal vessels around which CRIM1 is highly expressed (Figure 4.1 shown in the following Chapter 4).

A deeper analysis of CRIM1 as described in this chapter provides the first evidence of CRIM1 as a good candidate for pterygium development in the affected Northern Irish family.

The missense mutation identified in CRIM1 in a pterygium affected individual from Bolivia might be relevant for pathogenesis of pterygium.

Moreover, the increased CRIM1 expression observed, especially in Northern Irish pterygium patients, reveal its active function in the disease and suggests that it may act as an early response to a triggering agent of the pterygium.

CHAPTER 4

Investigation into the effect of the H412P mutation on CRIM1 function

Contribution

Eleonora Maurizi carried out all research unless otherwise stated

Dr Sarah Atkinson – supervised research, proofread

Laura Mairs – assistance with IHC showing CRIM1 expression

Prof Tara Moore - experimental design, supervised research, proofread

Dr Andrew Nesbit – experimental design, supervised research, proofread

Dr Davide Schiroli – experimental design, helped with qRT-PCR and figures design

4.1 INTRODUCTION

WES approaches have emerged as a powerful new tool to associate genes to a specific disease. Many WES studies were successful in identifying mutations in genetic disorders, achieving a molecular diagnostic rate of 25% (success rate) (Yang et al., 2013, Taylor et al., 2015), higher than all the previously used methods to determine an association between a gene variation and the corresponding phenotype.

However, the data obtained from WES and the subsequent *in silico* analysis are not always sufficient to interpret the disease relevance of single variants in different genes. Many of the identified genes and the corresponding proteins are in fact usually not completely characterised in their structure, function and disease association.

As previously discussed in Chapter 2, traditional candidate gene identification relies on large multigenerational families in which, by linkage and recombination analysis, the candidate region including a small number of genes is defined. Sequencing each gene within that region in turn should identify a mutation in only one of them.

While Linkage Analysis is generally performed in large families and is therefore quite solid in stating the region in which the altered gene is located, the outcome of WES is a list of multiple genes dispersed in all the chromosomes. Therefore, even though it is always necessary to demonstrate that the identified mutation has a functional effect, this usually becomes even more important with WES than with the traditional approach to give more strength to the association between the gene and the pathology.

It is also possible to use a combined approach of WES after linkage/recombination analysis if the number of genes is still too large to easily sequence them all. This has been done for a few genetic eye diseases such as the autosomal dominant late-onset corneal endothelial dystrophy (FCD2), associated with a missense mutation in the *LOXHD1* gene (Riazuddin et al., 2012) and the autosomal recessive retinitis pigmentosa where a mutation in the *USH1C* gene has been detected (Khateb et al., 2012).

In the first case, three large families affected by FCD2 were initially investigated and mapped in chromosome 18q. WES was then performed in one affected and one unaffected member of each family and allowed identification of a missense mutation in the *LOXHD1* gene in one family. Expression of *LOXHD1* in corneal endothelium, together with the discovery of other missense mutations in 7.5% of sporadic cases analysed and the observation of cytoplasmic aggregates in concomitance with some identified *LOXHD1* mutations, provided association of rare alleles of *LOXHD1* with FCD pathogenesis.

In the second case homozygosity mapping was performed in six members of two Yemenite Jewish families affected by retinitis pigmentosa, identifying a few regions of homozygosity. WES was then performed to provide deeper analysis of those regions, allowing detection of a novel frameshift mutation in the *USH1C* gene.

High throughput sequencing approaches alone can in fact present the substantial issue of generating false positive association of variants with the disease (MacArthur et al., 2014). This would have severe consequences if we consider the translation of genomic research discoveries into the clinical diagnostic or therapeutic setting.

It has been estimated that for 27% of the published mutations associated with severe diseases there was not any direct evidence for pathogenicity or they were shown to be common polymorphisms (Bell et al., 2011), considering that many false positive associations probably remains undetected.

Even though an unambiguous assignment of causality between variant and pathology may not always be possible, a supportive functional study would be fundamental, not only to give additional evidence for the gene variation as the cause of the disease, but also to understand the role of the gene in the aetiology of the pathology.

4.1.1 Aims of Chapter 4

CRIM1 was selected from the list of genes obtained through WES performed in the Northern Irish family affected by pterygium (Chapter 2) and was found to be highly expressed in individual pterygium samples (Chapter 3).

CRIM1 expression has been shown to play a key role in murine eye development, including lens fibre cells as well as corneal and conjunctival epithelium, corneal endothelium and retina (Lovicu et al., 2000). Its importance in eye development and association with Colobomatous macrophthalmia with microcornea syndrome (MACOM) has been demonstrated (Beleggia et al., 2015) together with its association with the reduced susceptibility of ACOP cattle in developing BOSCC under elevated solar radiation exposure (Pausch et al., 2012).

However, *CRIM1* has not been previously associated with any corneal or conjunctival abnormality in humans; therefore a functional analysis was performed to determine whether the H412P mutation found within the Northern Irish family interferes with the normal function of the protein.

Once CRIM1 expression in pterygium and conjunctiva was assessed using immunohistochemistry (IHC), I then performed a series of *in vitro* functional assays to validate the role of CRIM1 in pterygium pathogenesis and discriminate between the wild type and H412P mutant forms of CRIM1. This was achieved with a series of assays chosen for their link with pterygium features or pterygium previously associated pathways: MTT proliferation assay, ERK phosphorylation using Western Blot, Bcl-2 antiapoptotic expression levels through qRT-PCR and apoptosis analysis using the TUNEL assay.

4.2 METHODS

4.2.1 Patient recruitment

Clinical examinations were performed at Cathedral Eye Clinic, Belfast, UK and in Facultad de Medicina, Santa Cruz, Bolivia.

Pterygium and control tissues, consent forms and completed questionnaires were obtained from each individual examined under national ethical approval (see Chapter 2 and 3).

4.2.2 Cell culture

HCE-S cells were cultured as previously described (Chapter 2).

IOBA-NHC, a cell line spontaneously immortalized from human conjunctiva (a kind gift from Prof. Yolanda Diebold), was cultured as previously described (Diebold et al., 2003).

4.2.3 PCR

CRIM1 expression was determined in parallel in pterygium as well as in corneal epithelial cells scraped from a healthy cornea, corneal cell lines HCE-S and IOBA-NHC using the following exonic primers: F: 5'-CTCCCTCACCGAGTACGAAG-3' and R: 5'-GGCCTTGGAGCAATCTGG-3'. PCR was performed as following: initial denaturation at 95°C for 3 minutes, then 35 cycles of: denaturation at 95°C for 30 seconds, annealing at 60°C for 30 seconds, elongation at 72°C for 1 minute and final elongation at 72°C for 5 minutes.

VEGFA expression was evaluated in a $VEGFA_{121}$ plasmid, HCE-S cells, IOBA-NHC cells and corneal epithelial cells using the following primers: F: 5'-ATGGATCCATGAACTTTCTGCT-3' and R: 5'-TGAATTCACCGCCTCGGCTTGTC-3'. These primers amplify both $VEGF_{165}$ and $VEGF_{121}$ isoforms, which could then be discriminated on an agarose gel: $VEGF_{165}$ isoform produce an amplicon of 750bp while $VEGF_{121}$ one of 610bp.

$VEGFA_{121}$ plasmid (Cat. n. MHS6278-202759193 in pCMV SPORT6) was purchased from Dharmacon, Lafayette, US.

PCR was performed as following: initial denaturation at 95°C for 3 minutes, then 35 cycles of: denaturation at 95°C for 30 seconds, annealing at 57°C for 30 seconds, elongation at 72°C for 1 minute and final elongation at 72°C for 5 minutes.

4.2.4 Immunohistochemistry (IHC)

Pterygium and conjunctival tissues were formalin fixed and paraffin embedded. 7µm thick sections were cut and affixed to 1:50 (3-Aminopropyl) triethoxysilane (APES): acetone (both from Sigma, UK)-treated slides. The slides were left to dry overnight at 65ºC and then dewaxed using xylene and rehydrated through a graded series of ethanol solutions. After washing in PBS, the tissues were permeabilised using 0.5% Triton X-100 to allow the primary antibody access to the intracellular C-terminal domain of the CRIM1 protein. The sections were incubated in a Proteinase K solution (Fisher Bioreagents, BP1700-50, 10ug/ml in PBS) for 45 minutes at 37ºC for antigen retrieval. Specific binding sites were blocked using 5% goat serum in PBS for 30 minutes at room temperature (RT); goat serum was chosen because the secondary antibody is made in goat. After that tissue sections were incubated with a rabbit polyclonal CRIM1 antibody (Abcam-ab189203) at 1:100 in 5% goat serum in PBS for 1h at RT; rabbit IgG was used as an isotype control. After three quick slide immersions in PBS at room temperature, secondary antibody fluorescein isothiocyanate (FITC)-conjugated goat anti-rabbit IgG (Santa Cruz, USA) was used at 1:100 dilution, the sections were incubated with the antibody for 40 minutes at RT. After three final washes in PBS (1 minute each at room temperature) each section was mounted with DAPI fluorescence mounting medium (DAKO, Denmark). Images were obtained using a 20× N Archoplan lens on an AxioScope.A1 microscope equipped with an AxioCam MRc camera (Carl Zeiss, Germany).

4.2.5 Impression cytology samples

Impression cytology samples obtained from conjunctival and pterygium superficial epithelial were harvested as described in Chapter 3. Impression cytology samples were subsequently fixed in 95% ethanol for 20 minutes at room temperature and stained for CRIM1 as described in IHC methods.

4.2.6 Site Directed Mutagenesis

Human CRIM1 cloned in a pcDNA3.1 plasmid was a kind gift from Dr. L Wilkinson, Institute for Molecular Bioscience, University of Queensland, Brisbane, Australia (Wilkinson et al., 2003). Site directed mutagenesis was performed to obtain the H412P mutated CRIM1 clone, using the Quick Change II kit (Agilent Technologies), following the manufacturer's instructions. The entire *CRIM1* sequence was checked by Sanger Sequencing (Department of Zoology, University of Oxford), using the following primers (amplicon length is shown after every primer couples):

T7_F 5'TAATACGACTCACTATAGGG 3',
Seq1_R 5'GCAGAATGTGCAGTCGTCTT 3' (1.2 Kb amplicon),
Seq1_F 5' TGATCGAGGGTTATGCTCCT 3',
Seq1_R 5' GCAGAATGTGCAGTCGTCTT 3' (560bp amplicon),
Seq2_F 5' TACTACGTGCCCGAAGGAGA 3',
Seq2_R 5' GGCACTTTCACAGGGTTTGT 3' (212bp amplicon),
Seq3_F 5' TGCCGGGAATGCTACTGT 3',
Seq3_R 5' ACAGAAGGGCAGGACTCAGA 3' (420bp amplicon),
Seq4_F 5' CTGAGTCCTGGAAGCCTGAC 3',
Seq4_R 5' CCTGGAGGTGACCCATATCT 3' (420bp amplicon),
Seq5_F 5' AACCATCGAGGAGAGGTTGA 3',
Seq5_R 5' TCGTCTTCCGTCTTTTGAAAC 3' (400bp amplicon)

4.2.7 MTT assay

Reverse transfection was performed in HCE-S cells with either negative control plasmid, pCas9D10A_GFP (Addgene/Zhang lab), wild-type or H412P mutant CRIM1 plasmid using Lipofectamine 2000, according to the manufacturer's instructions, and seeded in a 12 well plate (Falcon #353043, BD Corning Life Sciences, MA, USA) at 1.5×10^5 cells/well. Eighteen hours later, cells were trypsinised, counted and seeded onto a 96 well plate (Falcon #351172 BD Corning Life Sciences, MA, USA), at 6.5×10^3 cells/well, allowing them to adhere for 2-3 hours. 3-(4,5-dimethylthiazol-2-yl)-2,5-diphenyltetrazolium bromide (MTT) solution in PBS was then added to cultures at a concentration of

0.5 mg/ml in 100ul of culture medium. Following 2h of incubation, the medium was removed and the formazan crystals which precipitated inside the cells were resuspended in DMSO. Absorbance was then measured at 570 nm using a filter-based multi-mode microplate reader, FLUOstar Omega (BMG Labtech, Aylesbury, UK) and quantified as relative percentages compared to control conditions. The MTT reading for each condition and each experiment was repeated at 24, 48, 72 and 96 hours post transfection.

4.2.8 Western Blotting

HCE-S cells were reverse transfected with negative control plasmid pCas9D10A_GFP (Addgene/Zhang lab), CRIM1 wild type and mutant plasmid, using Lipofectamine 2000 as described above.

Transfected cells were incubated for 24, 48 and 72 hours at 37°C with 5% CO_2. Lower cell seeding densities were used for the 72 and 96 hour timepoint to avoid cells becoming too confluent as this causes a decrease in ERK phosphorylation independent of the effect of CRIM1 (Vinals and Pouyssegur, 1999, Kaya et al., 2012).

Proteins were extracted using Complete Lysis-M (Roche Diagnostics) and proteinase inhibitor for mammalian cells and tissues (Sigma-Aldrich P8340) following the manufacturer's instruction.

Protein quantification was performed using the Bradford assay (BioRad) in a 96 well plate, and absorbance was determined by FLUOstar Omega Microplate Reader (BMG Labtech, Aylesbury, UK).

Absorbance values were normalised for each sample with bovine serum albumin (BSA) standard curve and 25μg of the extracted proteins were loaded in a 4-12% NuPAGE® Bis-Tris Precast Gels (Thermo Fisher Scientific UK).

Proteins were resolved within the gel using NuPAGE® MOPS SDS Running Buffer at 150V and transferred onto the Amersham TM Hybond ECL (GE Healthcare Life Sciences) nitrocellulose membrane with 10% methanol transfer buffer at 25 V. The membrane containing the proteins was then left for 1hour at room temperature submerged in 5% non-fat dry milk in TBS-Tween to prevent subsequent non-specific antibody binding.

A custom made 6% polyacrilammide gel was prepared to allow the high molecular weight CRIM1 protein to enter the gel. A custom prepared RIPA buffer was used as a more efficient method for cell lysis to obtain membrane proteins. A range of different temperatures were used for protein denaturation. CRIM1 antibody (ab189203) purchased from abcam was used at different dilutions to detect CRIM1 protein of 114kDa size. An HA tag was introduced after amino acid 73 (Phenylalanine) of CRIM1 sequence, as previously described (Wilkinson et al., 2003) using a two-stage PCR (Wang and Malcolm, 2002). HA-tag insertion was sequence verified by Sanger sequencing. An anti-HA antibody (ab9110) purchased from abcam was then used at different dilutions to recognise the HA tag introduced in CRIM1.

Phospho-ERK (#9101) and ERK (#9102) antibodies (Cell Signalling) were diluted 1:100 and 1:500 respectively in 5% milk in TBS-Tween and left to incubate overnight at 4ºC. After three washes of 10 minutes in TBS-Tween a secondary horseradish peroxide-conjugated polyclonal swine anti-rabbit antibody (DakoCytomation, Ely, UK) was used at a 1:2000 dilution in 5% milk in TBS-

Tween for 1 hour at room temperature. Protein binding was detected by standard chemiluminescence: SuperSignal™ West Pico Chemiluminescent Substrate (Thermo Fisher Scientific UK) and imaged using the G:BOX transilluminator (Syngene). Quantification was performed using GeneTools image analysis software: average peak values of phospho ERK were normalised against the average ERK values. All the obtained results were then normalised to the transfection control.

4.2.9 RNA extraction and reverse transcription from cells

RNA was extracted from corneal epithelial cells, pterygium cells, HCE-S and IOBA-NHC cells and reverse transcribed into cDNA as previously described in Chapter 3.

4.2.10 Quantitative real-time PCR

The qRT-PCR assays were performed using a Lightcycler 480 II (Roche, West Sussex UK) on cDNA which was reverse transcribed from the RNA extracted from the cells.

Real Time Ready Assays for CRIM1 (assay id. 112278), VEGFA (assay id. 140396), SRCAP (assay id. 126413), TGFβ (assay id. 104720), GAPDH (assay id. 141139) and HPRT (assay id. 102079) were purchased from Roche, West Sussex, UK.; qRT-PCR conditions used as described in Chapter 3.

SYBR green (Fermentas, Cambridge, UK) technology qRT-PCR was performed using Bcl-2 primers (For AGCATGGGAGCCACGACCCT, Rev GGCCAAGGCCACACAGCCAA) and HPRT primers (For

AGCTTGCGACCTTGACCAT, Rev GACCACTCAACAGGGGACAT), a kind gift from H. Nesbitt (Nesbitt et al., 2016). For the SYBR green qRT-PCR the cDNA was diluted 1:40. 4µl of this solution were then used for the qRT-PCR in a final volume of 10µl. qRT-PCR was set up as follows: Preincubation at 95°C for 5 minutes and then 50 cycles of 1) Denaturation at 95 °C for 10 seconds, 2) Annealing at 53°C for 10 seconds and 3) Extension at 72°C for 10 seconds. A final Melting Curve was performed after the amplification program as an indicator of a single specific PCR product under the following conditions: 95°C for 5 seconds, 65°C for 1 minute and then 64 cycles of 0.5°C increment (10 seconds each) reaching 97 °C.

4.2.11 TUNEL assay

The terminal deoxynucleotidyl transferase dUTP nick end labelling (TUNEL) assay was performed on HCE-S cells, reverse transfected with Lipofectamine 2000 using a Mock transfection with a plasmid of no relevant function: pGL4.17 [luc2/Neo] plasmid (Promega Madison, WI USA), CRIM1 wild type and CRIM1 H412P plasmids and plated in a 24 well plate (Falcon 353047, Corning Life Sciences UK) containing previously UV sterilised coverslips. After 72 hours cells were fixed with 4% PFA and stained using the In Situ Cell Death Detection kit (Fluorescein; Roche, Burgess Hill, Surrey, UK) following the manufacturer's instructions. Coverslips were mounted with Fluorescence mounting medium (DAKO, Denmark) and imaged using a fluorescent AxioScope A1 microscope equipped with an AxioCam MRc camera (Carl Zeiss, Germany), 10x objective. Twelve images for each condition and for the two experimental replicates were further quantified: total DAPI cells were normalised dividing by the higher number of total cells in each field using ImageJ software (US National Institutes of Health).

4.2.12 Statistical Analysis

Statistical analysis was performed using Student's t-test as previously described in Chapter 3.

4.3 RESULTS

4.3.1 CRIM1 is highly expressed in pterygium and conjunctiva

Given the previous experiments performed in this study (Figure 2.2 in Chapter 2) showing CRIM1 expressed in HCE-S cells, specific sites and levels of its expression in pterygium affected and unaffected conjunctival tissue were assessed.

The online TiGER gene expression database showed CRIM1 to be expressed in the whole eye, without differentiating between the specific tissues composing it. To assess CRIM1 expression in pterygium, constituted by a conjunctival epithelial layer overlying an internal fibrotic connective tissue (Kim et al., 2016), CRIM1 expression was analysed both in pterygium tissues and unaffected conjunctiva by PCR and immunostaining (Figure 4.1).

A preliminary PCR performed in different tissues of the anterior eye confirmed CRIM1 expression in normal corneal epithelium, pterygium and also in HCE-S and IOBA-NHC cell line cDNA, the latter two both endogenously expressing CRIM1 protein (Figure 4.1 A).

Immunohistochemical analysis showed that CRIM1 was present across the whole pterygium tissue section: from the anterior head (Figure 4.1 B1) to the posterior tail (Figure 4.1 B2). Moreover, CRIM1 was observed both in the external and more organised hypertrophic conjunctival epithelium and also in the internal fibroblasts immersed in the elastic and collagenous connective tissue characterising pterygium structure. CRIM1 was also detected in the vascular endothelial cells surrounding the vessels (Figure 4.1 B2 arrows).

CRIM1 was detected in conjunctiva from an unaffected individual (Figure 4.1 B3) and in impression cytology samples obtained from the superficial conjunctiva of unaffected individuals (Figure 4.1 B4).

Characteristic structures of other tissues were found inside the pterygium stroma were positive for CRIM1: staining was shown surrounding a hair follicle structure and inside a sebaceous gland (Figure 4.1 C).

A.

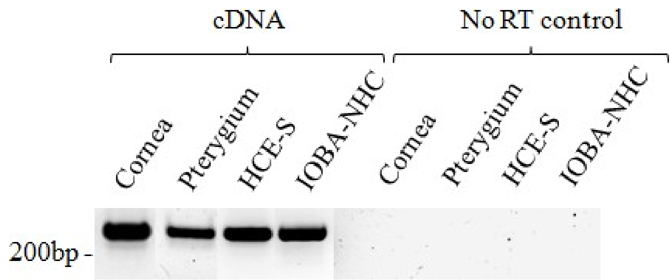

B.

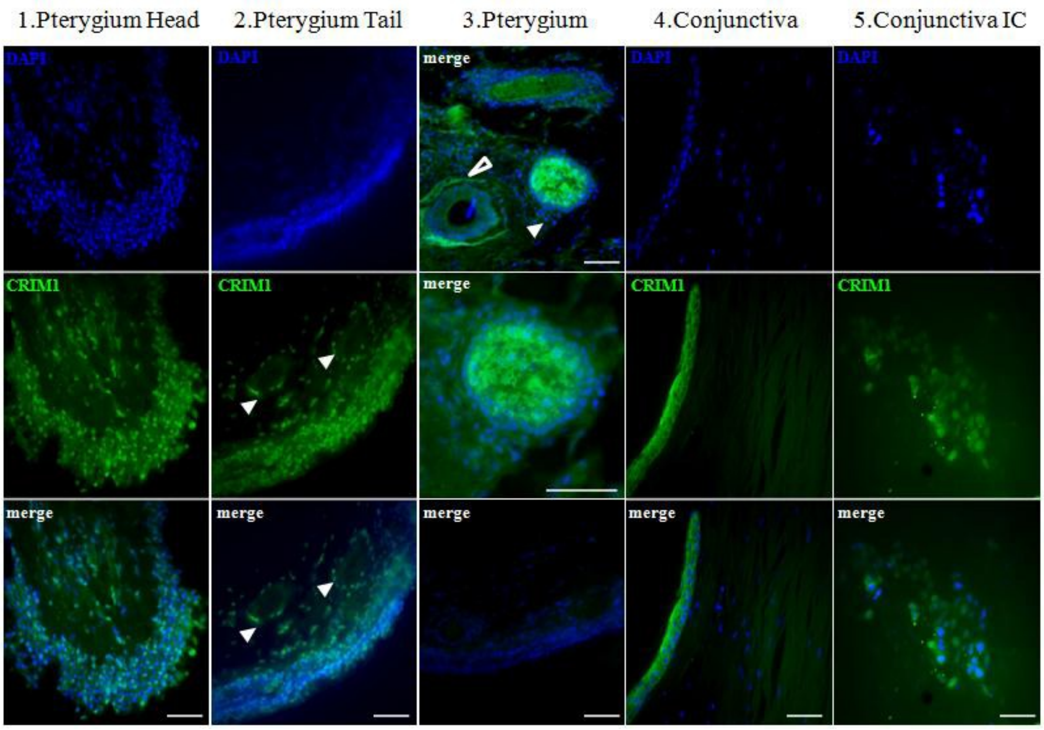

Figure 4.1 CRIM1 is expressed in pterygium, conjunctiva and cornea

Panel A. A PCR (35 cycles) showed expression of CRIM1 in different corneal tissues: corneal epithelium, pterygium, HCE-S (corneal epithelium) and IOBA-NHC (conjunctival epithelium) cell lines. A negative control, where no reverse transcripase (RT) was added when converting RNA to cDNA, is shown for each sample on the right.

Panel B. IHC showing CRIM1 (green) compared to cell nuclei (blue) on 1) pterygium head 2) pterygium tail, the plain arrows indicate vessels and 3) peculiar structures identified in pterygium stroma: an hair follicle (empty arrow) and a sebaceous gland (plain arrow, enlarged in the image below). The bottom image of column 3 identifies an IgG control in pterygium tissue. CRIM1 expression was also detected in 4) an unaffected conjunctiva and 5) an Impression cytology sample of superficial unaffected epithelial conjunctival cells. Scale bars on merge images 50μm.

4.3.2 CRIM1wt, but not H412P, is anti-proliferative if overexpressed

The high CRIM1 expression level found in conjunctiva and pterygium tissue supports a role for this gene in the aetiology of pterygium.

At this point it becomes relevant to understand which is the more appropriate functional assay able to discriminate between the two variants (wild type and H412P), but, at the same time, relate this to pterygium pathogenesis. Therefore I sought to develop assays to investigate the functional consequences of the H412P CRIM1 mutation. The HCE-S cell line, spontaneously formed from corneal epithelium (Notara and Daniels, 2010), was chosen for *in vitro* experiments as pterygium is thought to arise primarily from a limbal abnormality (Chui et al., 2011, Cardenas-Cantu et al., 2015, Das et al., 2015).

HCE-S cells grow in culture as an epithelial monolayer with limited multilayering, maintain the typical epithelial morphology, are responsive to EGF signalling promoting cell proliferation and express typical primary corneal epithelial markers like cytokeratin 3, PAX 6, the basal cell integrins β1 and α9 as well as ABCG2, characterising the stem cell population (Notara and Daniels, 2010).

Moreover, transfection efficiency was previously tested in our laboratory for HCE-S and IOBA-NHC cell lines. HCE-S presented a good transfection efficiency of 80% with GFP expression construct at 72 hours from transfection, while a low transfection efficiency of 23% was registered for the IOBA-NHC conjunctival cell line.

The H412P mutation was introduced into the human CRIM1 expression plasmid by site directed mutagenesis and the complete *CRIM1* sequence checked by

Sanger sequencing, confirming the presence of the nucleotide change Adenine > Cytosine, corresponding to the His > Pro mutation at position 412 and the absence of any other mutations.

HCE-S cells were transfected with an empty plasmid, wild type and the H412P mutant CRIM1 plasmids. qRT-PCR revealed a significant CRIM1 overexpression with respect to the endogenous CRIM1 both at 48 hours (CRIM1 wt 6 ± 0.82, p<0.01 and CRIM1 H412P 5.8 ± 0.97, p<0.05) and at 72 hours (CRIM1 wt 6.4 ± 1.075, p<0.01 and CRIM1 H412P 6.3 ± 1.4 p<0.01) (Figure 4.2A).

Despite knowing that CRISPR wt and H412P constructs transfection give a similar 6 fold RNA overexpression in HCE-S cells, protein overexpression might be different between the two constructs. Several attempts were made to show the CRIM1 protein expression using western blotting (see in Materials and Methods of Chapter 4) but unfortunately they all resulted ultimately unsuccessful.

Even though pterygium pathogenesis is still under investigation, it is generally considered a proliferative condition because it is mainly characterised by an over-proliferation of the cells composing it (Cardenas-Cantu et al., 2015, Detorakis and Spandidos, 2009b, Chui et al., 2011).

Moreover, a decrease in proliferation after transient CRIM1 overexpression has recently been reported in vascular endothelial cells (Nakashima et al., 2015).

An *in vitro* MTT proliferation assay was then performed to determine if either CRIM1 wild-type (wt) or H412P overexpression altered the proliferation rate of HCE-S cells (Figure 4.2B). Compared to Mock transfected HCE-S cells, CRIM1 wt overexpression had a significant anti-proliferative effect, which was most significant at 72 hours (Δabs 72-24hours 0.6 ± 0.017 OD; p<0.01). This effect was not observed in the CRIM1 H412P transfected cells (Δabs 72-24hours 0.52 ±

0.017 OD), which had a proliferation rate that was not significantly different from the Mock transfected control (Δabs 72-24hours 0.57 ± 0.012 OD).

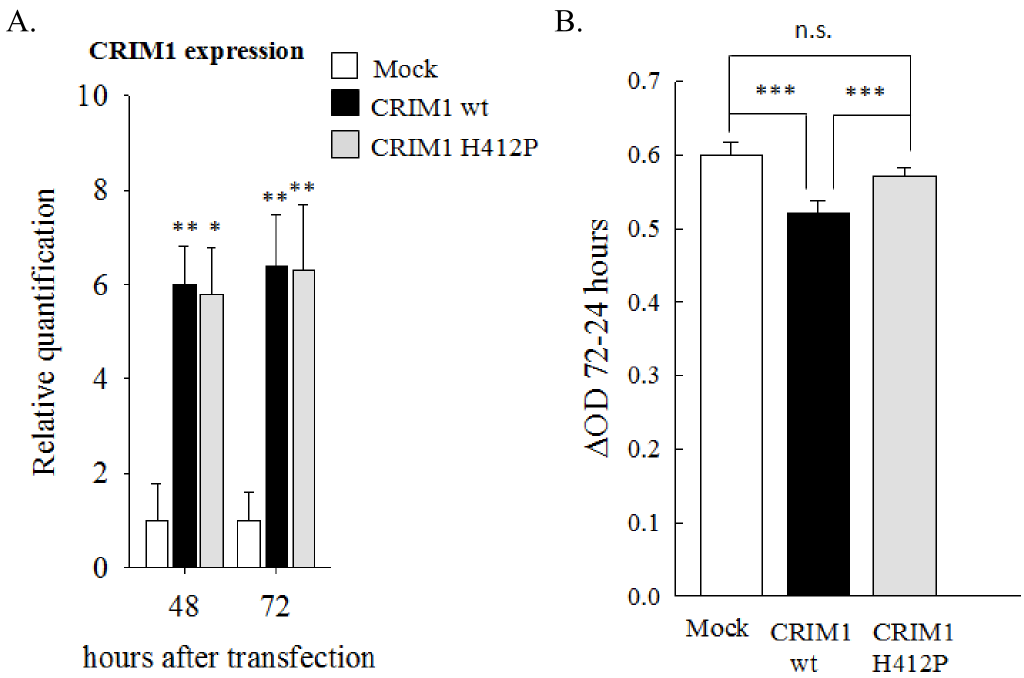

Figure 4.2 *In vitro* functional assay in HCE-S cells: decreased proliferation with CRIM1 wt overexpression

Panel A. qRT-PCR showing CRIM1 overexpression in mRNA obtained from HCE-S cells transfected with Human CRIM1 (wild type and H412P) into pcDNA3.1 plasmid. Both CRIM1 wt and H412P mutant were significantly overexpressed at 48h and 72h after transfection respect to the Mock control. Data represent fold change of the $2^{-\Delta Ct}$ mean ± SEM respect to Mock transfected HCE-S. n=3 with three technical replicates each condition.

Panel B. MTT assay showing HCE-S cell proliferation at 72h after transfection with Mock, CRIM1 wt and H412P mutant constructs. CRIM1 wt, when overexpressed, has an anti-proliferative role respect to the Mock transfected control ($p<0.001$), role which is lost overexpressing instead CRIM1 H412P. n=6 with 8 technical replicates for each condition.

MTT assay was repeated in IOBA-NHC conjunctival cells under the same conditions. However, no differences were noticed between the CRIM1 wt, H412P or mock transfected cells (data not shown). This is possibly due to the low transfection efficiency which characterize those cells as previously described and which prevented from further analysis on IOBA-NHC cells.

4.3.3 CRIM1 overexpression results in increased ERK phosphorylation

Recent literature has shown an association between the overexpression of CRIM1 and a decrease in cell proliferation in vascular endothelial cells (Nakashima et al., 2015), as mentioned in the previous paragraph. The same group also observed that, after VEGFA treatment, a parallel increase in CRIM1 expression and ERK phosphorylation occurred (Nakashima and Takahashi, 2014). This, together with other studies explaining how ERK pathway activation is involved in UV induced pterygium (Di Girolamo et al., 2003, Chao et al., 2013), directed the following research towards the analysis of ERK phosphorylation in CRIM1 wt or H412P transfected HCE-S cells.

A Western Blot assay was used to determine ERK phosphorylation levels following transfection with either CRIM1 wt or H412P. No significant differences could be detected at either 48 or 96 hours post-transfection between the groups. On the contrary, 72 hours after transfection, a significantly increased ERK phosphorylation was observed in the CRIM1 wt transfected cells compared to either the CRIM1 H412P or Mock transfected cells (Figure 4.3 A).

Densitometry quantification (GeneTool) revealed a 57 fold increase in ERK phosphorylation in CRIM1 wt transfected cells in comparison with the normal ERK phosphorylation levels of the Mock transfected control cells (value set at 1).

Only a 1.8 fold increase was observed when HCE-S cells were transfected with CRIM1 H412P mutant construct (Figure 4.3 B).

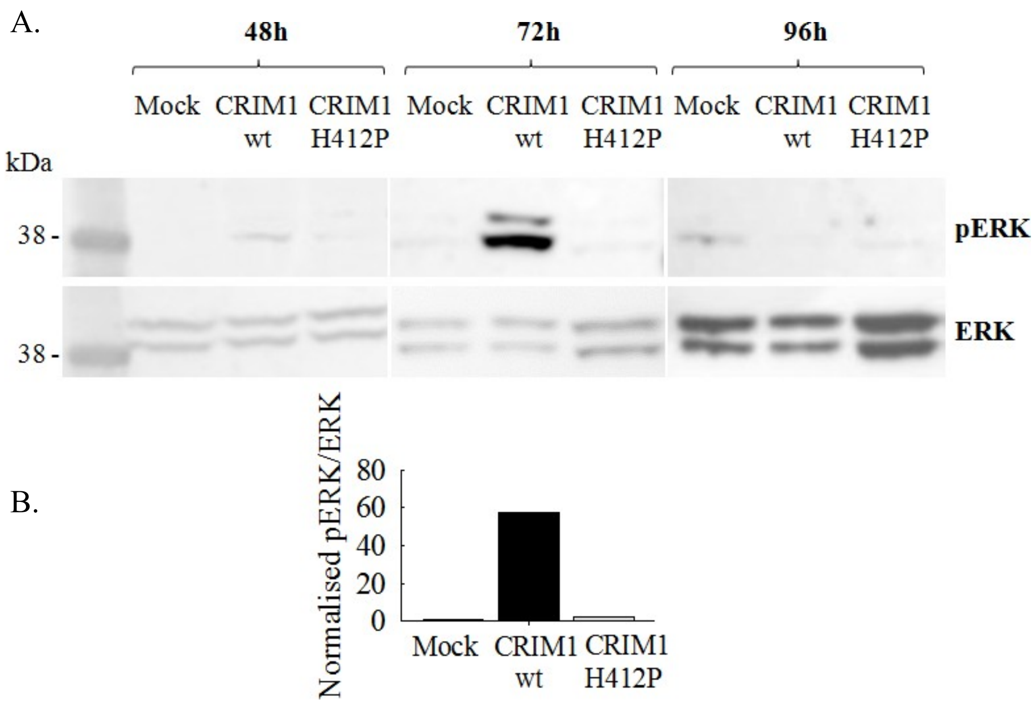

Figure 4.3 *In vitro* CRIM1 pathway analysis: ERK phosphorylation increases when overexpressing CRIM1 wt

Panel A. ERK phosphorylation (pERK) was detected by Western Blot analysis. No evident changes in pERK were appreciated overexpressing Mock, CRIM1 wt and H412P plasmids in HCE-S cells at 48 and 96 hours post transfection. On the contrary, at 72 hours post transfection ERK resulted highly phosphorylated upon CRIM1 wt overexpression when compared to CRIM1 H412P and Mock control. The figure is a representative image of two different experimental replicates.

Panel B. Western Blot results were quantified using GeneTool software (version 3, SynGene).

4.3.4 CRIM1 overexpression increases apoptosis

In parallel to ERK phosphorylation, other possible pathways predicted to be affected by CRIM1 mutation were investigated. qRT-PCR was used to determine expression of three factors implied in CRIM1 interaction and found altered in corneal diseases: VEGFA, Transforming Growth Factor beta Induced (TGFβI) and Bcl-2.

Firstly, VEGFA, which has been shown to be increased in pterygium in order to promote angiogenesis (Bianchi et al., 2012, Cardenas-Cantu et al., 2015, Detorakis and Spandidos, 2009b, Detorakis et al., 2010) was investigated. Furthermore, VEGFA described interaction with CRIM1 in kidney glomerulus (Wilkinson et al., 2007b) and their combined role in regulating retinal vasculature during development (Fan et al., 2014) suggest a synergistic activity between CRIM1 and VEGFA in vessel growth during pterygium formation.

Similarly, expression of TGFβI, found mutated in many corneal dystrophies (Kannabiran and Klintworth, 2006) was assessed. TGFβI is induced by TGFβ, which is upregulated in pterygium (Bianchi et al., 2012) and has been shown to modulate limbal cell proliferation by BMPs (Notara and Daniels, 2010), which in turn interact with CRIM1 (Wilkinson et al., 2003).

Finally levels of expression of the anti-apoptotic Bcl-2 were measured to associate apoptosis with pterygium deregulated proliferation. Bcl-2 belongs and gives the name to the wider Bcl-2 family which includes both pro-apoptotic (including Bax, Bak, BAD, BIM, BID, PUMA) and anti-apoptotic (including Bcl-2, Bcl-XL, Bcl-W, A1A, MCL1) proteins (Youle and Strasser, 2008, Adams and Cory, 1998).

A marked increase in apoptosis had previously been described in the basal epithelial layer of pterygium compared with normal conjunctival tissues, where apoptotic cells were found throughout the whole thickness of the epithelium (Tan et al., 2000).

There are at least 7 isoforms of VEGFA in human, generated by alternative splicing of the same gene; between those, $VEGFA_{165}$ is the predominant, followed by $VEGFA_{121}$ (Ferrara et al., 2003). VEGFA isoforms differ between them also by their distribution, being $VEGFA_{121}$ freely diffusible while $VEGFA_{165}$ existing in both soluble and bound status (Amadio et al., 2016). In conjunctiva, limbus and pterygium, $VEGFA_{165}$ and $VEGFA_{121}$ are the only expressed isoforms (Gebhardt et al., 2005). I therefore went to investigate $VEGFA_{165}$ and $VEGFA_{121}$ expression by PCR: they were both found endogenously expressed by HCE-S cells (Figure 4.4A), another indication suggesting HCE-S cells as a good model for the study of pterygium cellular mechanisms.

CRIM1 wt and H412P plasmids were transfected into HCE-S and gene expression assessed at 48 hours and 72 hours (Figure 4.4B). Levels of VEGFA and TGFβI expression were not significantly different between the wild type and the H412P mutant CRIM1 transfected cells (VEGFA: wt 48 hours 0.8351 ± 0.0740, H412P 48 hours 0.8966 ± 0.0630, wt 72 hours 1.1447 ± 0.0940, H412P 72 h 1.0443 ± 0.1100, TGFβ-I: wt 48h 0.7410 ± 0.0730, H412P 48h 0.8630 ± 0.0480, wt 72h 0.9428 ± 0.0650, H412P 72h 1.1810 ± 0.1080, all values are expressed in $2^{-\Delta Ct}$).

In contrast, a significant decrease in Bcl-2 expression level was observed in the CRIM1 wt with respect to H412P mutant and Mock transfected cells (p value

<0.05) both at 48 hours and 72 hours (wt 48 hours: 0.5453 ± 0.0720, H412P 48 hours: 1.1647 ± 0.1800 and wt 72 hours: 0.5977 ± 0.0240, H412P 72 hours: 1.2376 ± 0.1350, all values are expressed in $2^{-\Delta\Delta Ct}$, Figure 4.5).

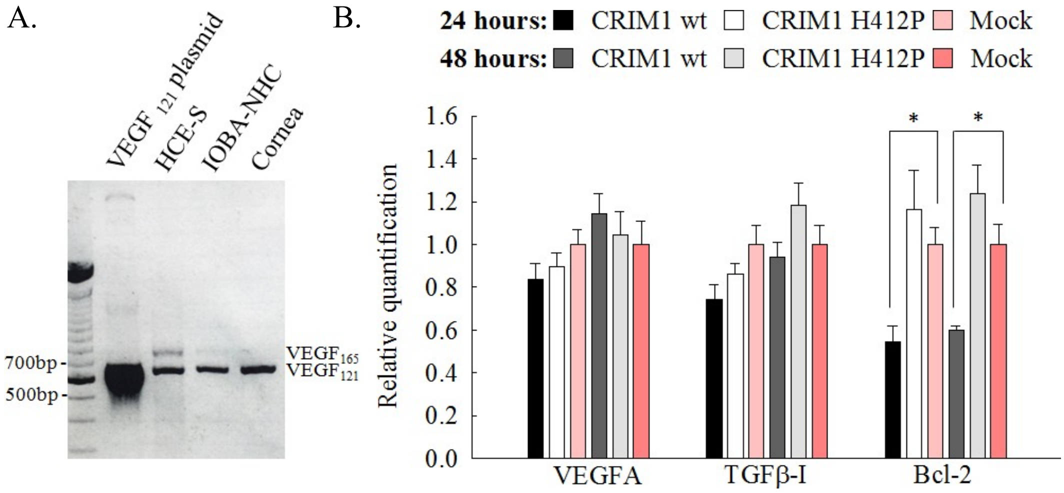

Figure 4.4 Pathway analysis: Bcl-2 expression levels decreases upon CRIM1 wt overexpression

Panel A. PCR (35 cycles) was used to evaluate VEGFA expression in HCE-S and IOBA-NHC cells, compared with the $VEGF_{121}$ plasmid and corneal epithelial cells. $VEGFA_{121}$ isoform is expressed in all the samples tested while the $VEGF_{165}$ isoform shows a lower expression, particularly visible in HCE-S cells.

Panel B. VEGFA, TGFb and Bcl-2 expression levels measured by qRT-PCR. HCE-S cells were transfected with Mock, CRIM1 wt and H412P plasmids and harvested after 48 and 72 hours. VEGFA and TGFb expression showed not significant variation between Mock, CRIM1 wt and CRIM1 H412P while Bcl-2 expression significantly decreased in CRIM1 wt compared with Mock transfected HCE-S both at 48 and 72 hours post transfection.

Data represent fold change of the $2^{-\Delta Ct}$ mean ± SEM compared to the Mock transfected HCE-S. n=3 with three technical replicates each condition.

Data obtained in Figure 4.4 suggested that CRIM1 affects the apoptotic pathway by regulating the expression of Bcl-2 and predicts that transfection with CRIM1 wt should increase the rate of apoptosis.

An increased apoptosis rate in the CRIM1wt transfected cells was confirmed by a TUNEL assay. At 72 hours the CRIM1 wt transfected HCE-S showed a significantly higher rate of apoptosis compared to the CRIM1 H412P and Mock transfected HCE-S. The number of TUNEL positive cells/relative DAPI total cells of CRIM1 wt transfected cells (25.6 ± 1.8) was significantly higher than the one of both CRIM1 H412P mutant and Mock transfected HCE-S (3.9 ± 0.4 and 2.7 ± 0.5 respectively; $p<0.001$) (Figure 4.5).

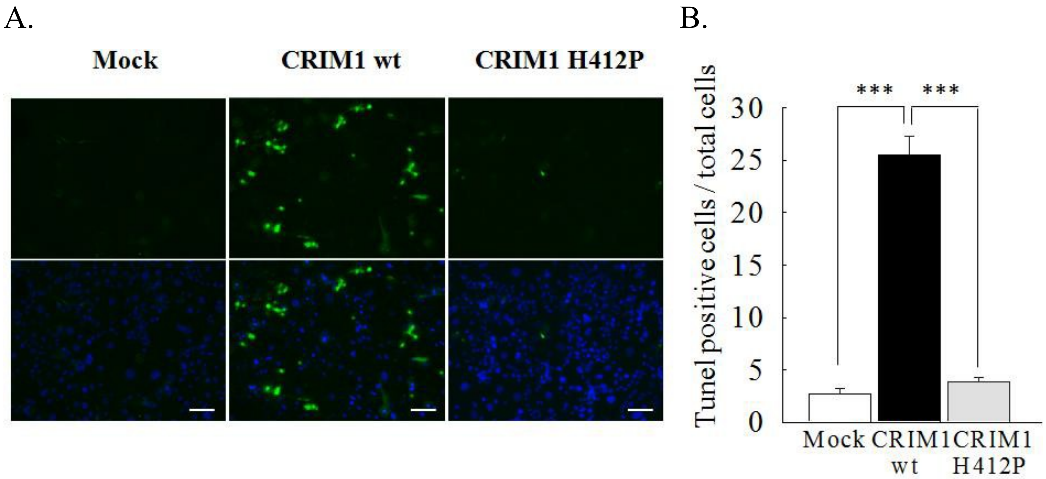

Figure 4.5 CRIM1 wt overexpression elicits apoptosis

Panel A. TUNEL assay in HCE-S cells transfected with wild type and H412P mutant CRIM1 plasmids. TUNEL-positive cells are stained in green and nuclei are stained in blue-DAPI. CRIM1 wt presents a higher apoptosis rate compared to the CRIM1 H412P transfected cells. Objective 10x; scale bar, 50μm. The figure is a representative image of twelve fields and two different experimental replicates.

Panel B. TUNEL assay quantification was performed in 12 fields for each condition using ImageJ. n=3

4.4 DISCUSSION

CRIM1 emerged from WES analysis as a candidate gene for pterygium pathogenesis in the Northern Irish family. However, the family was too small for sufficient meioses to be studied to conclude that the mutation co-segregates with, and causes, pterygium in this family.

A comprehensive functional analysis would therefore reinforce our selection of *CRIM1* as a candidate gene obtained from WES analysis and also help insert CRIM1 into a pathological context with clinical relevance.

CRIM1 expression in specific ocular tissues has not previously been described. The available online databases, such as TiGER, only show CRIM1 expression in the whole eye, without distinguishing between its different components.

Expression analysis by qRT-PCR and IHC confirmed the presence of CRIM1 in conjunctiva and in pterygium throughout its whole longitudinal section, both in the external epithelium and the internal pterygium stroma, where it could be localised in the cells surrounding the vessels.

CRIM1 expression was previously described in endothelial cells during capillary formation (Glienke et al., 2002) and an interaction between CRIM1 VWFs domains and VEGFA, the main factor promoting angiogenesis, was documented in glomerular vascular development (Wilkinson et al., 2007b). This, together with our CRIM1 observed around the vessels, suggests a possible interaction between VEGFA and CRIM1 during the critical angiogenic process of pterygium formation (Coroneo, 1993, Cardenas-Cantu et al., 2015).

CRIM1 was also detected in characteristic structures previously identified in pterygium (Chui et al., 2011): a hair follicle (Figure 4.1C, empty arrow) and a sebaceous gland (Figure 4.1C plain arrow, enlarged in the figure below).

VEGF mediated angiogenesis has an important role in mediating hair follicle growth and size (Yano et al., 2001) through ERK pathway activation (Li et al., 2012), again reinforcing the idea of an interaction between CRIM1 and VEGF, which are in turn involved in the ERK pathway.

Those cutaneous appendages have already been described during corneal epithelial transdifferentiation induced by dermal embryonic stimuli (Pearton et al., 2004), in which transient amplifying cells can be reprogrammed to the epidermal linage, demonstrating their multipotency (Ferraris et al., 2000). Therefore, during pterygium formation, the epithelium turns out to be deregulated, not only towards an epithelial-mesenchymal transition, but also initiating a transdifferentiation program toward an epidermal type tissue.

An ocular congenital benign tumor, quite similar to pterygium for its localization, symptoms and treatment, is the limbal dermoid, also presenting with those peculiar structures like sebaceous gland and hair follicles (Watson et al., 2013).

Previously, CRIM1 has been shown to have a role during eye development (Lovicu et al., 2000, Beleggia et al., 2015). However, expression of CRIM1 detected both at mRNA (qRT-PCR) and protein (IHC) level reflects its active function, even in the adult cornea even if CRIM1 function, in the eye in particular, has not yet been completely investigated.

A connection between CRIM1 and a typical feature characteristic of pterygium development: its increased cell proliferation rate was investigated. I assessed the effect of the H412P mutation upon cell proliferation using the simple and widely used MTT assay. Decreased proliferation rate in corneal cells overexpressing CRIM1 wild type was noted, which was not found in the cells transfected with mutant H412P CRIM1. A similar effect of CRIM1 upon cell proliferation has been previously described in vascular endothelial cells (Nakashima et al., 2015), This leads to the hypothesis that CRIM1 may have a role in protecting against pterygium by decreasing cell proliferation in response to mitogenic stimuli, a role which is lost in the H412P mutant protein.

An important intracellular mechanism involved in modulating cell proliferation is the ERK pathway, a subfamily of the MAPK. This pathway has been found deregulated in many tumours leading to uncontrolled growth (Johnson and Lapadat, 2002). ERK in particular has many different interactors that regulate its cascade dynamics: the resulting signal is therefore highly heterogeneous depending on the effectors and substrates, on the frequency and amplitude of the growth factor pulses and on the specific type of cell (Rauch et al., 2016).

Activation of ERK pathway through ERK phosphorylation has been described in pterygium or conjunctival cells treated with UVB (Di Girolamo et al., 2003) or with UVA (Chao et al., 2013) radiation.

Therefore, because of the proven relevance of the ERK pathway in cell proliferation and UV induced pterygium, I compared the effect of HCE-S transfection with CRIM1 wild type and H412P plasmid on ERK phosphorylation. Western blot analysis clearly showed an increase in ERK phosphorylation in the CRIM1 wt transfected cells compared to either the Mock or CRIM1 H412P transfected cells. This represents the first time an increase in CRIM1 expression has been correlated with a consequent activation of the ERK pathway in HCE-S cells and therefore suggests CRIM1 is an upstream regulator of ERK phosphorylation.

A similar concomitant elevated CRIM1 expression and ERK phosphorylation was previously described in vascular endothelial cells upon VEGFA treatment

(Nakashima and Takahashi, 2014), which has relevance to the angiogenesis observed in pterygium.

These promising results encouraged further research to investigate which are the other actors involved in CRIM1 proliferation and ERK pathway activation.

While VEGFA and TGFβI expression levels showed no variation between the three transfection conditions, the anti-apoptotic Bcl-2 was found to be significantly decreased in the CRIM1 wt transfected cells in comparison to the CRIM1 H412P and Mock transfected cells both at 48 and 72 hours (Figure 4.4). These data seem to be in accordance with the previously shown MTT proliferation results (Figure 4.2B): to a slower proliferation rate registered for the CRIM1 wt transfected HCE-S corresponds to a lower Bcl-2 expression, therefore higher apoptosis. The increase in apoptosis in the CRIM1 wt transfected HCE-S was confirmed by a TUNEL assay (Figure 4.5).

According to all the previous results obtained, several studies confirmed a decreased Bcl-2 expression upon ERK phosphorylation (Cagnol and Chambard, 2010), therefore increased apoptosis, even if ERK phosphorylation can also decrease the apoptosis depending on the tissue and conditions studied (McCubrey et al., 2007).

In conclusion, our data provide insights into the CRIM1 pathomechanism in the human cornea. A possible function of CRIM1 in the adult tissue was revealed by the expression observed both in pterygium and unaffected conjunctiva. Several experiments were then carried out to understand what this function was: overexpression of CRIM1 wt in HCE-S cells results in a decreased proliferation rate and increased apoptosis following activation of the ERK pathway. Whereas, the H412P mutation, by impairing CRIM1 function, results in a protein unable to elicit either the ERK phosphorylation or the apoptotic pathways.

CHAPTER 5

UV role in CRIM1 mediated intracellular pathway

Contribution

Eleonora Maurizi carried out all research unless otherwise stated

Dr Sarah Atkinson – supervised research, proofread

Prof Tara Moore – experimental design, supervised research, proofread

Dr Andrew Nesbit – experimental design, supervised research, proofread

Dr Davide Schiroli – experimental design, helped with qRT-PCR and figures design

5.1 INTRODUCTION

The human body, in particular the areas most frequently uncovered, like skin and the anterior eye, is exposed to UV radiation everyday. UV exposure is responsible for several beneficial effects like the induction of vitamin D production and β-endorphin release but also detrimental consequences such as photo ageing and carcinogenesis (Fell et al., 2014, Pandel et al., 2013, Holick, 2008).

UV rays can be divided into three components with differing wavelengths: UVA (320 – 400 nm), UVB (290 – 320 nm) and UVC (100 – 290 nm).

While we are shielded from UVC and 90% of UVB by absorption of the ozone layer, most of the UVA (90-99%) can penetrate the atmosphere, thus reaching the earth’s surface. Depletion of the stratospheric ozone layer intensifies the amount of UV rays reaching the earth and this has been associated with an increased eye damage rate (Štípek et al., 2004).

The human cornea also acts like a shield to protect the anterior eye from UV radiation and obstruct light transmittance. The anisotropic corneal properties ensure that UV light transmittance is reduced with the reduced wavelength: while UVB, characterized by a lower wave length, is completely arrested at the corneal epithelial layer, UVA transmittance is reduced only 20% by the corneal epithelium and can therefore penetrate the corneal stroma. The UV transmittance reduction is generally due to two different processes: absorbance and light scattering. Absorbance is mainly ascribed to the tear-film constituents, cellular components present in epithelial keratinocytes and stromal keratocytes and aromatic amino acids in stromal proteins, while light scattering is determined by the disposition of stromal collagen fibres (Lombardo et al., 2015).

UVB and UVA exert different effects once they reach the cells. While UVB with its higher incident energy induces direct damage to DNA, UVA possesses a higher wavelength and therefore less incident energy, causing mainly oxidative stress inside the cells (Rezzani et al., 2014a).

UVA, once absorbed by the cells, reacts with different chromophores like flavins and aromatic amino acids (histidine, tryptophan and tyrosine), generating reactive oxygen species (ROS) including radicals (superoxide anion $O_2\cdot^-$ and the hydroxyl radical $OH\cdot$), as well as non-radicals like hydrogen peroxide (H_2O_2 and $^1O_2$).

Mammalian cells developed two different defensive mechanisms against ROS products of oxidative stress: one involving non-enzymatic antioxidants including ascorbic acid, α-tocopherol, glutathione and β-carotenoides, while the other the enzymatic antioxidants such as superoxide dismutase (SOD), catalase, and glutathione peroxidase (GPx) (Merwald et al., 2005).

If not removed by these antioxidant systems, the ROS can damage the DNA, protein and cell membranes.

Regarding DNA damage, both UVA and UVB irradiation induces either dimerization of pyrimidines, leading to cyclobutane pyrimidine dimer (CPD) formation in DNA, or formation of oxidized DNA bases, such as 8-oxo-7,8-dihydro-2’-deoxyguanosine (8-oxo-dG).

While CPD formation, inducing C to T transitions, increases with decreasing wavelength it is therefore more frequent upon UVB irradiation; UVA mainly induces 8-oxo-dG, which is responsible for G to T transversion. The basal layer of human squamous cancer cell contains more G to T transversion than C to T transitions suggesting an more important role for UVA than UVB in human skin carcinogenesis (Agar et al., 2004).

As previously introduced in Chapter 1, 8-oxo-dG (also known as 8-OHdG) has been found to be upregulated in pterygium (Kau et al., 2006) together with its metabolising enzyme hOGG1 (Tsai et al., 2005b).

Moreover, a decrease in the antioxidant enzymes like SOD, catalase and GPx registered in pterygium in parallel to an increase in the lipid peroxidation marker MDA and NO represent other signs of a remarkable oxidative stress (Balci et al., 2011a).

The extensively documented influence of oxidative stress in pterygium implicates an important role for UVA mediated damage in its pathogenesis. UVA is also responsible for mediating gene mutation, ECM component degradation, protein kinase and phosphatase activation and inflammation (Chao et al., 2013); all key processes in pterygium formation.

Even if direct DNA damage caused by UVB rays can be more damaging in the superficial cells of the anterior eye and has been more extensively studied in pterygium, UVA rays can play a pivotal role in pterygium development because of their abundance, corneal penetration and related oxidative stress.

Other than pterygium, several other eye pathologies have been associated with a UV exposure etiology.

While for some ocular diseases the association with UV exposure is still not clear like in the case of pinguecula, nuclear and posterior subcapsular cataract, OSSN, ocular melanoma and age-related macular degeneration (AMD); for others this evidence has been more extensively proven like in the case of pterygium, photokeratitis, climatic droplet keratopathy (CDK), cortical cataract and eyelid malignancies including basal cell carcinoma (BCC) and squamous cell carcinoma (SCC) (Yam and Kwok, 2014).

The most common eye damage directly caused by UV radiation is photokeratitis, a corneal inflammation often called “snow blindness”. Photokeratitis represents the acute response to UV overexposure causing exfoliation of the superficial corneal epithelial cells through their shedding into the tear film and apoptosis. Normally, symptoms like photophobia and tearing appear up to 6 hours after sun exposure and resolves spontaneously in 24-48 hours (Cullen, 2002).

Another UV associated disease is the rarer Climatic droplet keratopathy, characterised by altered protein accumulation (droplet) in the stroma, which can lead to corneal scarring and opacification (Taylor, 1980).

A study conducted in 838 watermen from the Chesapeake Bay in Maryland revealed pterygium onset in 140 (16.7%) and climatic droplet keratopathy in 162 (19.3%) of the individuals analysed. Both the pathologies were found to be significantly associated with UV exposure following a statistical analysis considering independent contribution of UVB and UVA, age of participants and eye protection worn (Taylor et al., 1989).

UVB and UVA radiation are also responsible for altering the structure of the proteins localised in the outermost layer of the lens, the cortex, leading to its opacification and cortical cataract (DILLON et al., 1999).

More severe eye pathologies associated to UV exposure are the two kinds of carcinoma affecting the eyelid: Basal cell carcinoma (BCC) and Squamous cell carcinoma (SCC).

Even if BCC is more common, its association with UVR is more complex in comparison to SCC, for which a cumulative sun exposure as etiologic factor has been well established (Newton et al., 1996).

A similar type of eye tumour affecting cattle and responsible for substantial economic losses, the bovine ocular squamous cell carcinoma (BOSCC, eye cancer), is also etiologically associated to an extensive UV light exposure together with the lack of ambilateral circumocular pigmentation (ACOP) (Pausch et al., 2012). In this study CRIM1 was identified as a QTL for UV-protective eye area pigmentation in ACOP cattle.

This study is the first associating CRIM1 with a UV related eye disease, an association which bears directly on my investigation into pterygium.

5.1.1 Aims of Chapter 5

Based on the leading role of UV solar radiation on pterygium development, the effects UV radiation has *in vitro* were investigated in more detail.

Both UVB and UVA were initially used to irradiate HCE-S cells and measure changes in gene expression and in the intracellular signalling pathway. Because of the greater influence of UVA on pterygium-associated cellular pathways, further analyses were carried out using UVA alone. The use of qRT-PCR and western blotting helped delineating the UV triggered ERK pathway and the important involvement of CRIM1 expression regulation within it. A final confirmation of the role of CRIM1 in response to UV irradiation was sought using siRNA knocking down CRIM1 expression to the HCE-S endogenous level.

5.2 METHODS

5.2.1 Cell culture

HCE-S cells were cultured as previously described (Chapter 2).

5.2.2 UV treatment

HCE-S cells were seeded in a 24-well plate at 1×10^5 cells per well in growth medium and left to adhere overnight at 37°C and 5% CO_2. The following day they were treated using the UVA cross-linker (IROC Innocross AG, Ramsen, Switzerland) delivering a dose of 5.4 J/cm^2 as previously described (Moore et al., 2014). In parallel HCE-S cells were irradiated using the Arcadia D3 6% UVB lamp (Arcadia, UK) with an aluminium reflector at a distance of 15 cm from the cells for 34 minutes; irradiating the monolayer with a final dose of 0.5 J/cm^2 of UVB.

The same doses of UVA and UVB irradiation were used in experiments in which the ERK inhibitor (MEK inhibitor, U0126) was added to culture media an hour prior to the UV treatment as previously described (Chao et al., 2013), at a concentration of 10μM.

After irradiation, HCE-S cells were incubated in culture medium at 37°C with 5% CO_2 and harvested at 1, 6, 12, 24 and 48 hours. Every condition was repeated in two wells of a 24 well plate and the experiment was repeated three times.

5.2.3 Quantitative Real time PCR

qRT-PCR was performed as previously described (Chapter 3 and 4).

5.2.4 Western Blot

Western Blot was performed as previously described (Chapter 4).

5.2.5 siRNA transfection

Four different siRNAs targeting CRIM1 sequence (Set of 4 Upgrade: ON-TARGETplus CRIM1 siRNA, LU-008492-00-0002, 2nmol, Dharmacon) were reverse transfected in HCE-S cells using Lipofectamine RNAiMAX (Fisher Thermo Scientific), following the manufacturer's instructions. The four siRNAs were transfected singularly or as a pool at a final concentration of 10nM and normalised to the results from a non-specific siRNA control (NSC4) (Allen et al., 2013).

A titration of different concentrations (0.2-0.5-1-10nM) of the siRNA pool reverse transfected in HCE-S cells as described above was subsequently tested.

5.2.6 MTT assay

MTT proliferation assay was performed as previously described (Chapter 4)

5.3 RESULTS

5.3.1 UVA exposure increases CRIM1 expression

CRIM1 expression, previously shown to be increased in pterygium affected patients from Northern Ireland (Chapter 3), was further investigated by qRT-PCR in an *in vitro* HCE-S cell system, following UVA and UVB light exposure.

A clear estimation of the eye exposure to UV radiation has never been determined and it is very variable on the base of daylight activities which differ between individuals.

The amount of UV used for the irradiation has been estimated based on the daylight UV dose: an average dose of 60-70 J/cm^2 per day was determined in central Europe in spring, considering that UVA represents the majority of the UV irradiation reaching the earth surface (95% UVA) (Marionnet et al., 2014). The above-mentioned daily average dose can be reduced to 10% of the initial value if we consider that the effective human eye exposure in the average population is limited to a few hours daily. Based on those considerations together with the fact that UVA is 100 times more abundant than UVB, I selected a low dose of 5.4 J/cm^2 UVA and 0.5 J/cm^2 UVB for our experiments on HCE-S cells. A similar dose of UVA was also used in a previous study carried on in pterygium cells (Chao et al., 2013) and also in corneal epithelial cells demonstrating the UVA induced oxidative stress effects (Moore et al., 2014).

An increased expression of CRIM1 was observed at 3, 6 and 24 hours after UV light treatment (Figure 5.1). While UVB irradiation resulted in a significant increase in CRIM1 expression only at 24 hours after the treatment in comparison with the untreated control ($2^{-\Delta\Delta Ct}$ ± SEM values at 3, 6 and 24 hours are respectively: 1.3074 ± 0.0300, 0.9000 ± 0.0130 and 1.9509 ± 7.5147^{-3}, the latter with a $p \leq 0.05$); UVA rays elicited a significant CRIM1 increase from 6h continuing to 24h after the treatment ($2^{-\Delta\Delta Ct}$ ± SEM values at 3, 6 and 24 hours are respectively: 0.8971 ± 0.1464, 8.5940 ± 0.2158 $p \leq 0.05$ and 10.3867 ± 0.3977 $p \leq 0.01$).

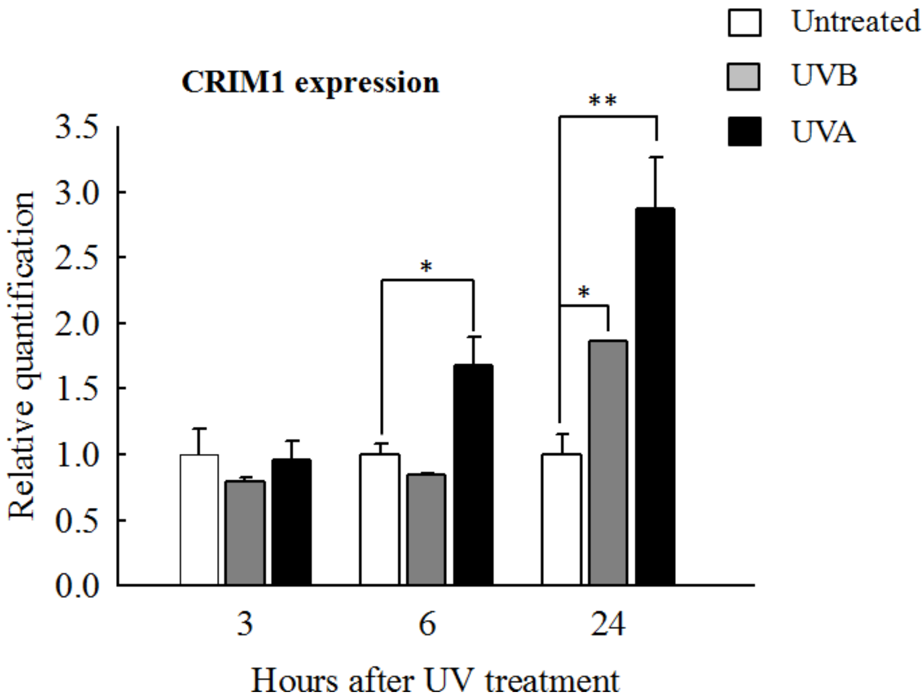

Figure 5.1 UV treatment in HCE-S increases CRIM1 expression

qRT-PCR revealed a significant increased CRIM1 expression levels in HCE-S cells at 6 ($p \leq 0.05$) and 24 hours ($p \leq 0.01$) after UVA treatment and at 24 hours ($p \leq 0.05$) after UVB treatment compared to the untreated control.

Data represent fold change of the $2^{-\Delta\Delta Ct}$ mean ± SEM respect to untreated HCE-S. n=3 with three technical replicates each condition.

After showing that a cellular response to UV involves an increase in CRIM1 expression, the other components of the previously examined pathway with and without the CRIM1 mutation were investigated (see Chapter 4).

5.3.2 UV treatment regulates ERK phosphorylation

Because CRIM1 expression was significantly elevated at 24 hours post-treatment for both UVA and UVB, the 24 hour time point was chosen to analyse the effects of an ERK phosphorylation inhibitor on CRIM1 expression following UV irradiation (Figure 5.2). Surprisingly ERK inhibitor treatment potentiated the UV-induced increase in CRIM1 expression at 24 hours after treating the HCE-S cells both with UVA and UVB light (control: 0.63 ± 0.07, inhibitor only 0.77 ± 0.02, UVA only: 1.82 ± 0.15, UVA + inhibitor: 3.75 ± 0.12, UVB: 1.26 ± 0.15 and UVB + inhibitor 3.08 ± 0.51; values were expressed as $2^{-\Delta Ct}$). CRIM1 expression levels were significantly different from the control both for UVA + inhibitor ($p \leq 0.001$) and UVB + inhibitor ($p \leq 0.05$); but also between reciprocal UV ± inhibitor values: UVA ($p \leq 0.001$) and UVB ($p \leq 0.05$).

The effect was dependent upon UV irradiation since CRIM1 expression in cells treated with the ERK phosphorylation inhibitor alone was not increased when compared with the untreated cells (Figure 5.2).

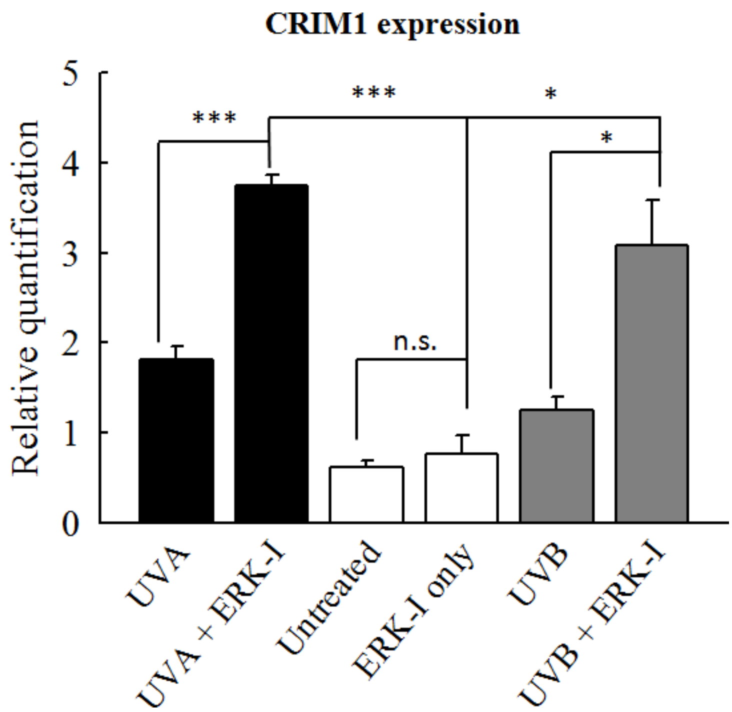

Figure 5.2 ERK-I together with UV treatment increases CRIM1 expression further

qRT-PCR evaluation of CRIM1 expression with UV treatment using ERK inhibitor (ERK-I, UO126). An additive effect in increasing CRIM1 expression was observed when treating the cells with UV irradiation (both UVA and UVB) and inhibiting ERK pathway.

Data represent fold change of the $2^{-\Delta Ct}$ mean ± SEM compared to untreated HCE-S. n=3 with three technical replicates each condition.

Since irradiation with UVA has similar, but greater effects on CRIM1 expression than UVB, subsequent experiments testing the UV effects on cellular response and gene expression were conducted using UVA irradiation alone.

ERK phosphorylation was previously shown to be increased in pterygium cells after 6 and 24 hours of UVA exposure (Chao et al., 2013). I therefore assessed levels of ERK phosphorylation in HCE-S to confirm that my model systems behave similarly.

The ERK phosphorylation I observed at 1 and 3 hours after UVA treatment was not significantly different to the untreated control but by 6 hours it was significantly elevated and remained so at 24 hours (Figure 5.3A), exactly as observed by Chao et al.

The average of the pERK/ERK bands in the membrane, normalised to each relative control, was quantified as 5.6 and 32.1 at 6 and 24 hours after UVA irradiation, respectively (Figure 5.3B).

ERK inhibitor was used in the same experiment with HCE-S harvested 24 hours after UVA treatment to confirm its inhibitory ability on ERK phosphorylation.

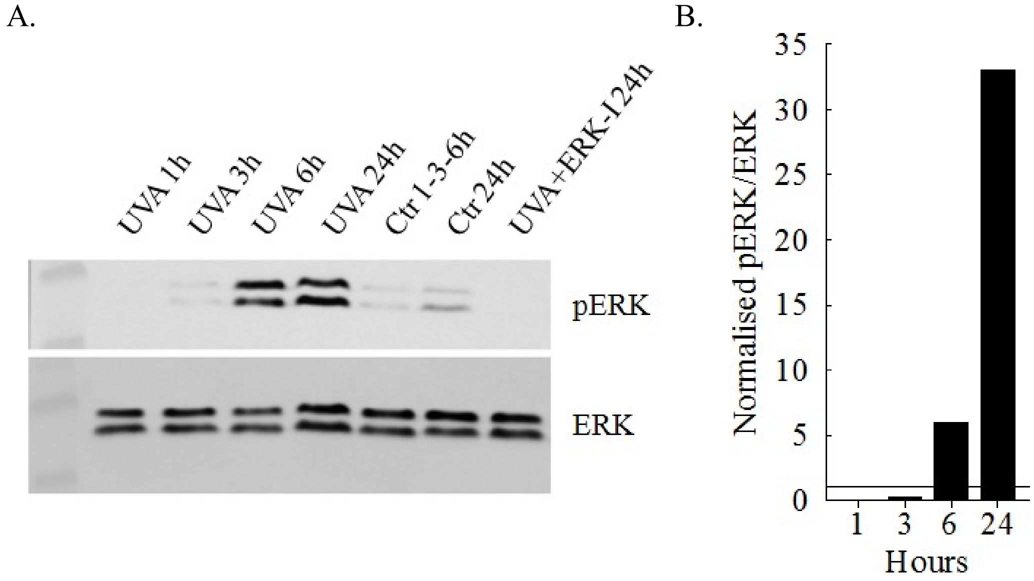

Figure 5.3 UV increases ERK phosphorylation

Panel A. Western Blot protein analysis in HCE-S cells revealed a increase in ERK phosphorylation at 6 and 24 hours after UVA irradiation.

Panel B. Western Blot quantification both at 6 hours (5 folds) and 24 hours (34 folds) respect to normal ERK phosphorylation levels of the untreated control obtained using GeneTool software.

5.3.3 UVA decreases Bcl-2 expression

Bcl-2, as discussed in Chapter 4, is an anti-apoptotic protein which, if overexpressed, inhibits cell death (Youle and Strasser, 2008).

ERK phosphorylation has been often associated with decreased Bcl-2 expression and therefore to increased apoptosis (Cagnol and Chambard, 2010), DNA damage induced in primary (MEF and IMR90), immortalized (NIH3T3) and transformed (MCF-7) cells by different treatments including ultraviolet irradiation (UV), determines ERK pathway activation and cell apoptosis, which is reduced if using U0126 (the same ERK inhibitor used here) (Tang et al., 2002). Similar experimental conditions were applied to our study, in which the rate of apoptosis was investigated following UVA treatment activating the ERK pathway in HCE-S cells (Figure 5.4).

A significantly decreased level of Bcl-2 expression was observed if compared to the control in HCE-S treated either with ERK inhibitor or UVA ($2^{-\Delta\Delta Ct} \pm$ SEM values for ERK-I: 0.53 ± 0.05 and UVA 0.48 ± 0.06; both $p \leq 0.05$ compared to the untreated control). These results imply an increased apoptosis rate in cells treated with either UVA or an inhibited ERK pathway.

However, when ERK inhibitor and UVA irradiation were used together the Bcl-2 expression increased ($2^{-\Delta\Delta Ct} \pm$ SEM of 1.45 ± 0.13) and although not significantly different from the untreated control, a significant difference was observed in comparison with solely UVA or ERK inhibitor treated HCE-S ($p \leq 0.001$).

This confirms that increased ERK phosphorylation (UVA) corresponds to decreased Bcl-2 expression, suggesting an increased apoptosis in HCE-S cells upon UV mediated ERK pathway activation, as previously shown in other cell types (Tang et al., 2002).

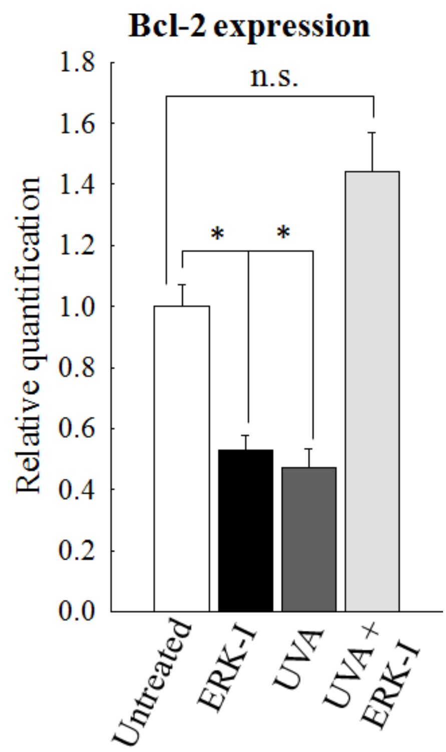

Figure 5.4 UVA decreases Bcl-2 expression, which is restored by adding ERK-I

Bcl-2 expression level was measured by qRT-PCR. HCE-S cells were UVA irradiated with and without ERK inhibitor and harvested 24hours after treatment. Data represent fold change of the $2^{-\Delta\Delta Ct}$ mean ± SEM respect to untreated HCE-S. n=3 with three technical replicates each condition.

5.3.4 UVA irradiation increases VEGFA expression but not SRCAP

The expression of two other genes, VEGFA and SRCAP, following UVA irradiation, was investigated using qRT-PCR: VEGFA, for its previously described interaction with CRIM1 (Wilkinson et al., 2007b) and its possible role in pterygium angiogenesis and SRCAP, the other variant identified by WES that is highly expressed in cornea but initially deemed less likely to be causative because the identified R968H variant in SRCAP doesn't belong to any functional domain and because of less literature association with eye or UV related diseases compared to CRIM1.

24 hours after UVA treatment, VEGFA showed a marked increase in its expression (Figure 5.5A), significantly different from the untreated control ($2^{-\Delta\Delta Ct}$ values ± SEM at 3, 6 and 24 hours respectively: 0.9600 ± 0.0300, 1.2900 ± 0.1300 and 5.8600 ± 0.9000 $p \leq 0.01$).

On the contrary, SRCAP gene expression did not show any significant variation upon UVA when compared to the untreated control (Figure 5.5B) data, which helps confirm our selection of CRIM1 as the top candidate.

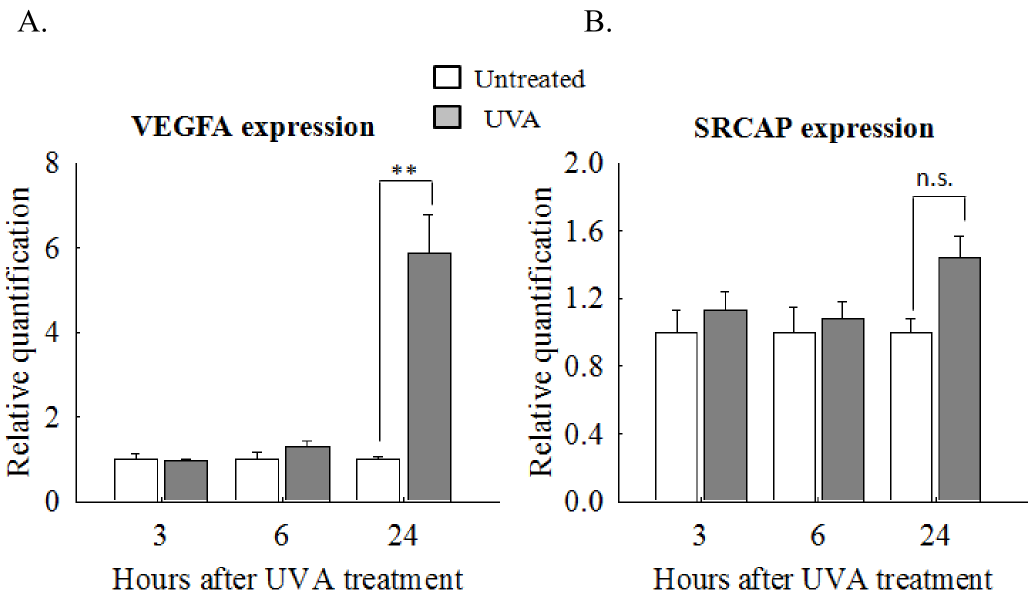

Figure 5.5 UVA increases VEGFA expression level but not SRCAP

Panel A. qRT-PCR showing a significant increased VEGF-A expression in HCE-S 24 hours after UVA treatment.

Panel B. qRT-PCR was used to evaluate SRCAP expression. No differences in SRCAP expression were observed after 3, 6 and 24 hours from UVA treatment.

Data represent fold change of the $2^{-\Delta\Delta Ct}$ mean ± SEM compared to untreated HCE-S. n=2 with three replicates each condition

5.3.5 Upon UVA exposure, 0.5nM targeted siRNA restores CRIM1 expression to basal levels in HCE-S cells

CRIM1, ERK and Bcl-2, as shown previously, are interrelated in playing a pivotal role in the intracellular pathway triggered by UV exposure. However the cause-effect or the effected-effector relationship between the actors under examination was still not completely elucidated.

Four siRNAs against CRIM1 were chosen to further analyse its effect upon the response to UV of HCE-S cells and to shed light onto the mechanism implicated in pterygium development.

All of the four siRNAs, included in the pool (the four siRNA added together reaching the same total concentration of the single siRNAs), used at a final concentration of 10nM, efficiently knocked down CRIM1 endogenous expression (Figure 5.6) at 48 hours after HCE-S transfection. I obtained the following $2^{-\Delta Ct}$ mean values ± SEM: 0.46 ± 0.07 with siRNA05, 0.4 ± 0.02 with siRNA06, 0.24 ± 0.04 with siRNA07, 0.42 ± 0.02 with siRNA08, 0.29 ± 0.04 with the pool of the four siRNAs. All of those values of CRIM1 expression were significantly ($p \leq 0.001$) different from those of the three controls used: 1.7 ± 0.03 with NSC4, 1.88 ± 0.1 in HCE-S with no siRNA (but with Lipofectamine) and 1.33 ± 0.01 with Untreated HCE-S.

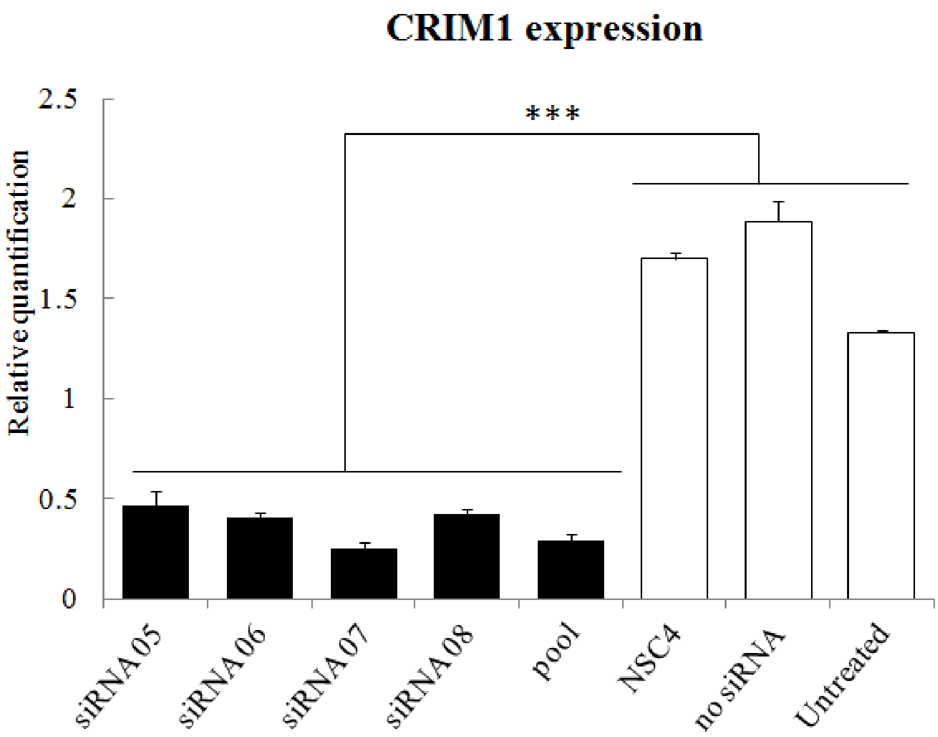

Figure 5.6 siRNAs targeting CRIM1 efficiently knocks down its expression in HCE-S cells

CRIM1 expression obtained using qRT-PCR of HCE-S cells cDNA 48 hours post transfection. All four 10 nM siRNAs tested were able to significantly knock down CRIM1 expression, including the pool of the four of them used at the same final concentration.

Data represent fold change of the $2^{-\Delta Ct}$ mean ± SEM. n=2 with three replicates each condition

The siRNA pool was used for the next experiments in which CRIM1 expression was evaluated treating HCE-S cells with UVA rays.

The HCE-S endogenous level of CRIM1 expression, which was normalised at 1 ± 0.01 $2^{-\Delta Ct}$ ± SEM for the Mock control (NSC4), increased after UVA treatment with NSC4 to 1.7 ± 0.05, $p \leq 0.05$. Because levels of CRIM1 expression appear critical and finely regulated under UV treatment, a series of siRNA concentrations were further tested (0.2nM, 0.5nM, 1nm and 10nM) in order to find the one which would bring CRIM1 expression back to the HCE-S endogenous level (Mock transfection control, NSC4).

A dose response curve of CRIM1 expression in HCE-S transfected with the siRNA pool at different concentrations was observed: $2^{-\Delta Ct}$ ± SEM values of 1.3 ± 0.13 with 0.2nM, 0.85 ± 0.1 with 0.5nM, 0.53 ± 0.08 with 1nM and 0.21 ± 0.03 with 10nM.

The concentration of 0.5nM of the siRNA pool (siCRIM1) was found to be the one able to bring the CRIM1 expression level close to the Mock (NSC4) level (Figure 5.7A).

An MTT proliferation assay was then performed in HCE-S upon UVA treatment and, through the use of the siRNA pool, confirmed the anti-proliferative effect of the CRIM1 over-expression. In fact, as shown in Figure 5.7B, exposure to UVA light significantly increased HCE-S proliferation at 72 hours (ΔOD 72-24 hours control 0.53 ± 0.02 vs UVA 0.6 ± 0.03; $p \leq 0.05$). If 0.5nM CRIM1 siRNA (siCRIM1) was added, HCE-S proliferation increased even more (ΔOD 72-24 hours: 0.7 ± 0.02, with $p \leq 0.05$ compared to UVA and $p \leq 001$ compared to the Mock NSC4 control). Those results show that using UVA irradiation and blocking CRIM1, the cells acquire an additional sprint in their proliferation.

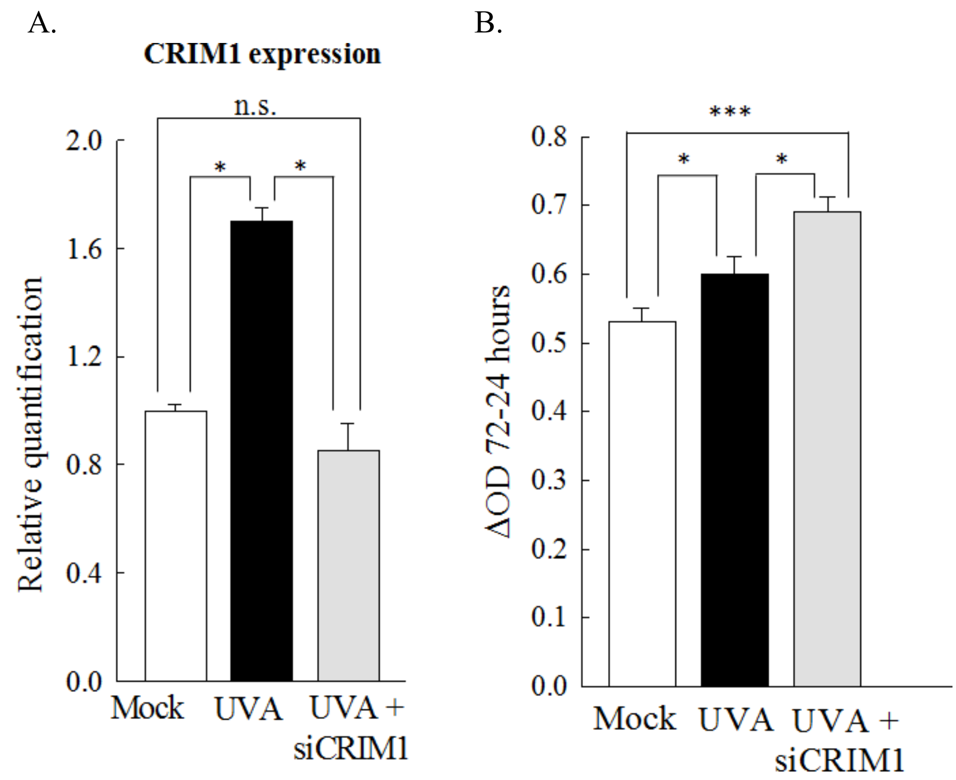

Figure 5.7 siCRIM1 0.5nM restores normal CRIM1 expression and confirms its anti-proliferative activity

Panel A. A qRT-PCR shows the amount of CRIM1 siRNA (0.5nM) able to restore the endogenous CRIM1 level in HCE-S after UVA exposure. Data represent $2^{-\Delta Ct}$ ± SEM. n=3 with three technical replicates each condition

Panel B. MTT assay demonstrating an increased proliferation upon UVA exposure which is further increased if CRIM1 is restored to endogenous levels (siRNA 0.5nM), confirming the antiproliferative effect when CRIM1 is overexpressed. n=6 with 8 technical replicates for each condition.

5.3.6 CRIM1 regulates UVA mediated ERK phosphorylation

Given the results obtained using 0.5nM of siRNA confirming the role of CRIM1 to prevent UV induced cell proliferation, the ERK phosphorylation pathway was assessed using a Western blot protein assay (Figure 5.8).

As shown previously, ERK phosphorylation was significantly increased 24 hours after UV exposure. Transfection of cells with 0.5nM CRIM1 siRNA prior to UV exposure abolished ERK phosphorylation. Quantification of western blot bands was normalised as pERK/ERK and numbered 1 for Mock control (NSC4), 13.1 for UVA (NSC4) and 1.6 for UVA + siRNA CRIM1 (0.5nM).

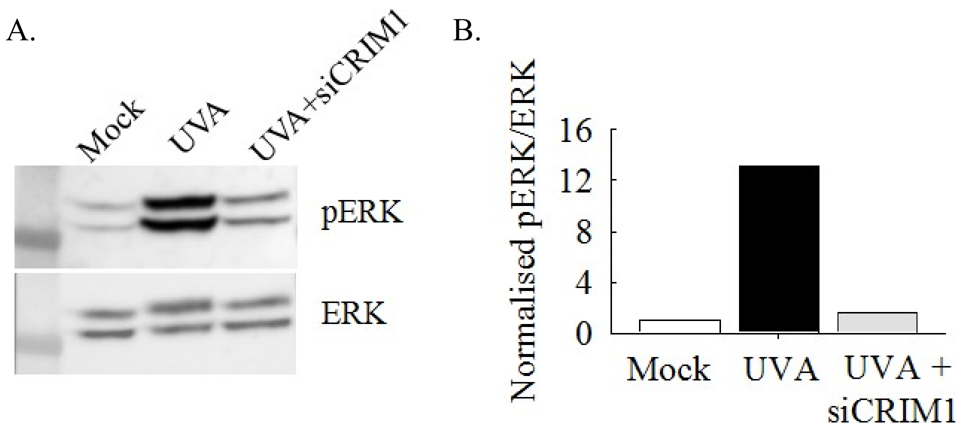

Figure 5.8 siCRIM1 0.5nM restores normal ERK phosphorylation levels

Panel A. Western Blot analysis was used to detect ERK phosphorylation at 24 hours after UVA treatment in HCE-S cells. The increased ERK phosphorylation due to UVA exposure was brought back to normal levels using 0.5nM CRIM1 siRNA. The figure is a representative image of two different experimental replicates.

Panel B. Western Blot results were quantified using GeneTool software (version 3, SynGene).

5.3.7 CRIM1 regulates UVA mediated apoptosis

Finally, to relate ERK and CRIM1 regulation with apoptosis and check the congruence with the results I obtained transfecting the HCE-S with CRIM1 wt and H412P constructs (Chapter 4), Bcl-2 expression levels were examined (Figure 5.9).

24 hours after UVA treatment of HCE-S cells, Bcl-2 expression decreased significantly compared with the untreated control ($2^{-\Delta\Delta Ct}$ values for UVA treated HCE-S: 0.61 ± 0.06, $p \leq 0.01$). However, pretreatment with 0.5nM pool siRNA prevented the decrease in Bcl-2 expression which was not significantly different from Mock NSC4 transfected cells ($2^{-\Delta\Delta Ct}$ values of siCRIM1+UVA: 0.96 ± 0.08).

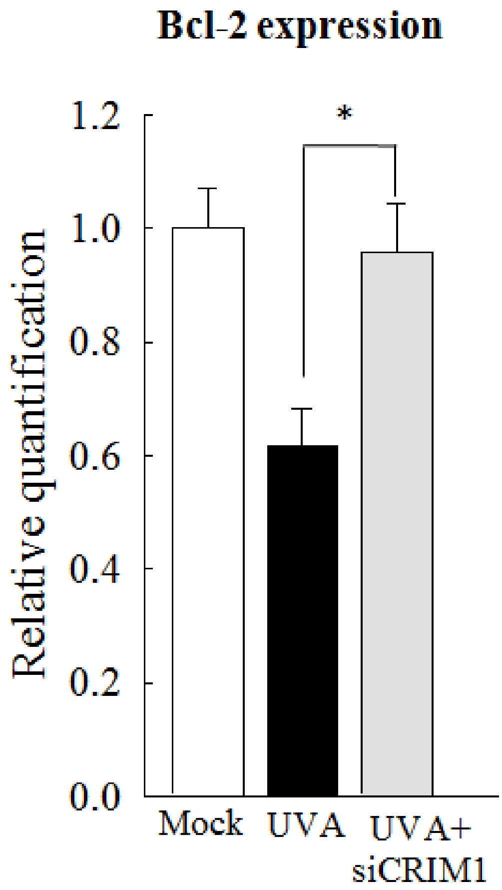

Figure 5.9 siCRIM1 0.5nM restores normal Bcl-2 expression levels

Bcl-2 expression was measured by qRT-PCR. HCE-S cells were treated with: UVA and UVA + siCRIM1 and harvested 24 hours later. Data represent $2^{-\Delta\Delta Ct}$ ± SEM with respect to Mock HCE-S. n=3 with three technical replicates.

5.4 DISCUSSION

Pterygium is considered to be one of the most common opthalmohelioses and its pathogenesis is mainly attributed to UV radiation overexposure. Studying the effects of UV irradiation on CRIM1 expression and other pathways involved in pterygium formation is fundamental to understand the function that CRIM1 exerts in cornea and how this function can be altered in pterygium.

Both UVA and UVB irradiation effects were initially investigated in HCE-S cells, testing CRIM1 expression.

Comparing the two experiments described in Figure 5.1 and Figure 5.2 is possible to see that both graphs are consistent in showing the same increase in CRIM1 expression at 24 hours post UV treatment.

UVA treatment, at the dose I used, gave both quicker and larger effects and that is why UVA only was chosen for further experiments.

This is in accordance with two observations: the vast majority of the UV radiation reaching the earth's surface is composed of UVA, 10-100 times more abundant than UVB (Moan, 2001), and the cornea transmits more UVA (80%) than UVB (60%) (Coroneo, 1993, Chao et al., 2013).

Moreover oxidative stress, mainly attributed to UVA rather than UVB rays (Rezzani et al., 2014a), has been well documented in pterygium (Balci et al., 2011a, Kau et al., 2006, Tsai et al., 2005b).

Besides the increase in CRIM1 expression as a cellular response to UV treatment, I have shown a concomitant increase in ERK phosphorylation (Figure 5.3).

Both UVA and UVB were previously shown to induce ERK phosphorylation in epidermal cells like HaCat cells (He et al., 2004) and NHEK (Normal Human

Epidermal Keratinocytes) (Syed et al., 2012) but also in pterygium fibroblasts upon UVA (Chao et al., 2013) or UVB (Di Girolamo et al., 2003) irradiation. Similar results in term of ERK phosphorylation and CRIM1 expression were obtained in Chapter 4: to a CRIM1 overexpression, induced this time by CRIM1 wt plasmid transfection, corresponds again with an increase in ERK phosphorylation (Figure 4.4).

This implies that ERK phosphorylation can be triggered either by UVA irradiation or by CRIM1 overexpression and is therefore downstream of those two factors.

However, if we block this ERK activation (using ERK inhibitor, see Figure 5.2), a feedback mechanism pushes the overexpression of CRIM1 even higher with the purpose of switching back on ERK phosphorylation and the consequent intracellular signalling.

Increased ERK phosphorylation must inhibit the increase in CRIM1 since inhibition of ERK phosphorylation potentiates the increase in CRIM1 expression. Similarly, inhibition of CRIM1 upregulation prevents an increase in ERK phosphorylation. This suggests that the two are tightly linked in a possible negative feedback loop.

Several homeostatic feedback mechanisms have been described in the ERK pathway. ERK represents the terminal kinase within the MAPK signalling pathway in several human cell lines and is phosphorylated by MEK1/2, the so-called gatekeepers of ERK activity, which is in turn phosphorylated by active RAF in a pathway triggered by growth factors receptors activation (Caunt et al., 2015).

This whole pathway can be regulated at multiple levels by feedback mechanisms which can be distinguished in post-translational and transcriptional negative feedback loop.

A post-translational feedback regulates ERK activity through direct ERK phosphorylation of inhibitory sites in upstream proteins like RAF-1 or a transcriptional negative feedback loops is able to dephosphorylate threonine and tyrosine residues through dual-specificity phosphatases (DUSPs) in turn regulated by transcription factors downstream of ERK (Fritsche-Guenther et al., 2011).

Phosphorylation of ERK is involved in different pathways with a main antiproliferative activity through apoptosis, senescence or autophagy and its regulation is fine and complex, possibly involving ROS (Cagnol and Chambard, 2010). ERK signalling pathway has been described as the most prominent in tumours because of its importance in regulating cell proliferation and survival, controlling the activity of Bcl-2 proteins and regulating the apoptosis (Caunt et al., 2015).

A dynamic balance between the growth factor induced ERK pathway and stress mediated activation of JNK-p38, other two MAPK proteins, determines cell survival fate. Induction of the apoptotic pathway in physiological condition is given by an inhibition of ERK with a concurrent activation of JNK and p38 pathway (Xia et al., 1995).

Similarly, inhibiting ERK pathway (ERK inhibitor alone), the internal HCE-S balance is disrupted and decreased Bcl-2 expression level suggests the cell are induced to apoptosis (Figure 5.4).

However, under DNA damaging agents like UV exposure, an increase in ERK phosphorylation was shown to induce apoptosis in multiple cell types (Tang et al., 2002).

Results obtained observing the expression levels of Bcl-2 seems to suggest that upon UVA treatment alone HCE-S cells tend to activate the apoptotic process (decreased Bcl-2). On the contrary, if HCE-S cells are UVA irradiated while the ERK pathway is blocked (UVA+ERK Inhibitor), Bcl-2 levels are restored to the ones of untreated cells, suggesting that the apoptotic process is reduced (Figure 5.4). ERK pathway activation is therefore essential in maintaining the activity of Bcl-2 expression upon UV irradiation.

This seems not only to confirm the data obtained in Tang et al. paper asserting that ERK activation induces apoptosis but is also in accordance with our previous results (Chapter 4) showing that an increase in ERK phosphorylation corresponds with a decreased Bcl-2 level and an increased apoptosis in HCE-S cells transfected with wild type CRIM1.

Moreover, stress induced apoptosis mediated by the ERK pathway, was shown to be downregulated by VEGFA in microvascular endothelial cells (Gupta et al., 1999). Here I have shown a VEGFA increase upon UVA treatment in HCE-S cells, highly significant after 24 hours, which, accordingly to Goupta et al. may counteract ERK pathway activation and therefore cell apoptosis. Those contrasting actions by VEGFA promoting angiogenesis in one side and ERK promoting apoptosis in the other might reach a limit beyond which pterygium can or cannot develop. Regulation of those mechanisms is delicate and therefore needs further investigation.

VEGFA, which results in an upregulation in pterygium compared to normal conjunctiva (Detorakis et al., 2010, Bianchi et al., 2012) and in pterygium fibroblasts treated with UV (Di Girolamo et al., 2006a), is well documented also in normal corneal epithelium, stroma and endothelium (Di Girolamo et al., 2004). The presence of the potent anti-angiogenetic VEGFA in the avascular cornea is counterbalanced by the expression of soluble VEGF receptor-1 (also known as sflt-1), which binds VEGFA and prevents its functionality, being in this way responsible for corneal avascularity (Ambati et al., 2006).

Finally, the observed increase in both VEGFA and CRIM1 in corneal epithelial cells at 24 hours after UVA radiation, suggest that their proven interaction (Wilkinson et al., 2007b) can have a role in UV triggered intracellular response, a role that needs further investigation to be fully elucidated.

Thus, studying the effects of UV radiation on HCE-S cells, I have demonstrated that UV rays, in particular UVA after 24 hours are able to:

- increase CRIM1 expression three fold (Figure 5.1)
- increase ERK phosphorylation roughly thirty fold (Figure 5.3)
- decrease Bcl-2 suggesting an increase in apoptosis (Figure 5.4)
- increase VEGFA expression six fold (Figure 5.5)
- activate CRIM1 - ERK pathway interaction which is regulated by a negative feedback loop mechanism (Figure 5.2)

But what would happen if, upon UVA exposure, we bring back CRIM1 levels to the normal endogenous expression level? Are we able to restore the physiological intracellular ERK pathway and apoptosis? In this case are we sure that restoring the normal conditions is good for the cell which is exposed to a damaging agent like UV?

Trying to answer all these questions is challenging; to have final proof of the cellular mechanism and to test if it was possible to restore the initial cellular physiologic conditions, CRIM1 expression was regulated using a series of concentration of the siRNA against CRIM1. Once selected the CRIM1 siRNA dose able to restore the level of CRIM1 expression similar to the endogenous HCE-S level, I analysed cell proliferation, ERK phosphorylation and apoptosis.

It is known that UVA exposure promotes cell cycle progression and cell proliferation in HaCaT keratinocytes (He et al., 2008) while UVA delivery through crosslinking causes increased apoptosis both in human (Mencucci et al., 2010) and rabbit (Wollensak et al., 2004) corneal keratinocytes.

However, not much is known about UV induced proliferation in pterygium, even though it is considered essentially to be more of a proliferative than a degenerative disease.

UV light represents a chronic stimulus in the eye surface which alters the normal processes of growth control in cornea and conjunctiva. Similar chronic inflammation processes determine tissue hyperplasia like in the case of cutaneous keloids, which shares a genetic base with pterygium, a similar ethnical prevalence (Haugen and Bertelsen, 1998) and analogue fibroblast proliferation (Cameron, 1983).

If it is true that CRIM1 has an anti-proliferative effect (as discussed in Chapter 4), bringing CRIM1 expression back to endogenous levels after UVA exposure would enhance the proliferation further because of the dearth of CRIM1 overexpression.

Irradiating HCE-S cells with UVA, I observed an increase in cell proliferation.

Using 0.5nM siRNA, the CRIM1 expression was reduced to its endogenous level in HCE-S and their proliferation increased even further compared to the UVA only treatment, as expected presuming CRIM1 preventing proliferation.

Again ERK pathway activation was investigated: besides increased ERK phosphorylation upon UVA confirming the previously obtained results (Figure 5.3), I showed a decrease of ERK phosphorylation back to normal levels when using 0.5nM siRNA against CRIM1 in addition to UVA irradiation (Figure 5.8).

As previously seen in Figure 4.4 in Chapter 4, by just modulating CRIM1 expression it is possible to influence ERK phosphorylation: an elevated CRIM1 expression corresponds in both cases to an increase in ERK phosphorylation.

Finally, a decreased Bcl-2 expression after 24 hours from UVA treatment in HCE-S cells, seems to confirm the pro-apoptotic role of UVA irradiation. Bcl-2 levels are then restored by adding 0.5nM of siCRIM1 (Figure 5.9). Therefore, the expression level of CRIM1 represents a key passage to all the downstream UV activated pathways examined: knocking down CRIM1 to return it to endogenous levels is enough to prevent ERK phosphorylation induced by UV and bring Bcl-2 levels back to the endogenous one.

The last experiments, performed modulating CRIM1 expression upon UVA treatment, confirmed all the previous results and in particular the reduced cell proliferation observed once CRIM1 is overexpressed.

CHAPTER 6

General discussion

Contribution

Eleonora Maurizi carried out all research unless otherwise stated

Dr Sarah Atkinson – proofread

Prof Tara Moore – proofread

Dr Andrew Nesbit – proofread

Dr Davide Schiroli – helped with figures design

6.1 Pterygium relevance

Pterygium, a common ocular surface tissue overgrowth, is generally associated with symptoms like tearing, dry and itchy eyes causing eye irritation and inflammation (Uy et al., 2005). In advanced cases it can invade the central cornea and reach the pupil, inducing corneal scarring and astigmatism; this impairs normal vision and requires surgical removal (Detorakis and Spandidos, 2009a).

Even if the novel methods of surgical intervention described in Chapter 1 improved the outcome from the initial bare sclera only technique, a recurrence rate of 12% still persist after the surgery (Ono et al., 2016).

Prevalence of pterygium varies highly with the latitude but can be increased by other risk factors like not wearing a hat or sunglasses, working in outdoor environments, especially in presence of dust or surfaces which reflect the solar radiation or concrete (Mackenzie et al., 1992). Also living in rural rather than urban areas represent a risk factor for pterygium development according to studies carried on in Australia and China (Ma et al., 2007, McCarty et al., 2000).

A noteworthy pterygium prevalence, averaged 10.2% worldwide (Liu et al., 2013a), correlates with an high rate of surgery which, including primary and recurrent pterygium interventions, represents the 1% of all the ocular surgeries in more developed countries and 0.5% in lower developed regions (Lucas et al., 2008).

Pterygium accounts therefore for a considerable proportion of all eye surgeries, assuming a certain weight for the National Health Service and a substantial cost to the community. If we consider Australia, a study in 2000 estimated the annual cost of pterygium surgery and health assistance to be US$ 100M, this cost might be lower in countries where pterygium is removed at a later stage but overall increased if we consider higher cases of visual loss and consequent loss of productivity (Hirst, 2000).

In order to find a specific treatment for pterygium, able to directly target the etiopathogenic factors and prevent the need for surgical intervention with the associated risk of recurrence, an understanding of the molecular basis which determines its development is required.

One path to understanding the molecular basis of pterygium is by analysing the genetic background of the affected patients.

The completion of the Human Genome Project paved the way for new perspectives in practicing medicine with the development of targeted therapies starting from each individual's molecular profile, this is the emerging area of stratified (or personalized) medicine (Ginsburg and McCarthy, 2001).

Even though this research field is in constant evolution, some successes have already been achieved in cancer (Cutter and Liu, 2012). Complex pathologies like AMD, where extensive information is already known regarding the genetic and environmental etiologic factors as well as the intracellular pathways involved, present a good model for a personalized medicine approach (Baird et al., 2009).

Several genes and mutations have also previously been associated with pterygium pathogenesis (Kau et al., 2004, Detorakis et al., 2005a, Tsai et al., 2004a, Demurtas et al., 2014), and all of those genes were mainly involved in pterygium altered cellular mechanisms: oxidative stress, proliferation and vascularisation (see Table 1.2 in Chapter1). However, there is still not a common intracellular pathway explaining pterygium etiopathogenesis.

6.2 CRIM1, selected as a candidate gene from WES analysis, revealed to be involved in UV triggered ERK pathway and apoptosis

The present study began with the identification of a Northern Irish family, rarely exposed to the sun but presenting with pterygium in three subsequent generations.

Whole exome sequencing was chosen because of the limited number of participating family members which would have made a linkage analysis approach more difficult, because of the lower costs in comparison with whole genome sequencing and because most of the disease-causing mutations occurs in the exonic portion of the genome (Rabbani et al., 2014).

Family pedigrees affected by pterygium were previously examined for their clinical relevance (Romano et al., 2016, Islam and Wagoner, 2001b, Zhang, 1987a) but their genetic background was not investigated at a deeper level. This is the first time a next generation sequencing approach has been applied to a pterygium family study.

WES data initially identified 451,153 variants in the family members participating in the study. Those variants were analyzed using Ingenuity Variant analysis software, which was able to filter the WES data through a series of filters: the first filter, Confidence, eliminated all the variants which were poorly read, the second, Common Variants excluded the ones present in more than 0.5% of the population, the third, predicted deleterious variants, selecting the ones with a possible damaging effect according to Polyphen and SIFT and finally genetic screening selected only the variants which were present in the affected and absent in the unaffected sibling.

A subsequent deeper analysis of the literature allowed the selection of five candidate genes, which were then analysed for their eye expression profile and eye disease association, directing the subsequent research on CRIM1.

CRIM1 gene screening in two additional unaffected family members revealed the same H412P mutation in CRIM1, suggesting a possible incomplete penetrance as an inheritance mechanism.

Disease penetrance can be influenced by many factors including age, for example MEN1 as described in Chapter 3, environmental factors like family history or reproductive factors which increase the risk of ovarian cancer in *BRCA1* and *BRCA2* mutant carriers (Brekelmans, 2003), by the genetic modifiers where the penetrance is given by polymorphic alleles at other gene loci or by epigenetic regulation (Cooper et al., 2013).

No other mutations in CRIM1 VWFs were identified within the 12 Northern Irish patients while a novel R745C missense mutation was found in one of the 9 Bolivian patients examined, which is possibly damaging according to Polyphen and predicted to affect protein function according to SIFT.

Given the low MAF of this mutation, its presence in one pterygium patient reinforces our hypothesis of *CRIM1* as a causative gene involved in pterygium pathogenesis but more family data and additional functional assays on R745C would be required to prove this theory.

Comparing CRIM1 expression in populations coming from a low UV exposure zone (Northern Ireland) and from a high UV exposure area (Bolivia), a higher

CRIM1 expression was found only in pterygium-affected individuals from Northern Ireland with regard to the unaffected controls.
This reinforces CRIM1's potential role in pterygium pathogenesis even if a mutation in *CRIM1* is not the direct cause of pterygium.
Given the fact that surgical excision in Northern Ireland is performed at an earlier stage of pterygium development, we can speculate here that expression of CRIM1 increases as an early response to UV damage, but is lost at a later stage of the disease, similarly to what happens in TG2 during liver fibrosis (Nardacci et al., 2003). This theory is consistent with the data of the affected family member in which CRIM1 expression was particularly low and therefore the CRIM1 protective mechanism was lost as a consequence of the H412P mutation.

Looking for the effect that the H412P mutation could have in CRIM1 function, I have shown that overexpression of CRIM1 wild-type in HCE-S cells slows down their proliferation, while no changes in proliferation were observed in cells overexpressing mutant CRIM1 H412P (Figure 4.2B in Chapter 4).
Normal levels of CRIM1, as seen in HCE-S cells (Figure 4.1 in Chapter 4), have been shown to be necessary for *in vivo* invasion of the myocardium and enhanced migration of primary epicardial cells but also for cell proliferation and apoptosis during cardiomyocyte development (Iyer et al., 2016).
This might be similar to what happens to pterygium if an individual is carrying the mutation in CRIM1: altered cell proliferation and enhanced cell migration.
Moreover, when overexpressed, CRIM1 demonstrated a decreased proliferation in vascular endothelial cells (Nakashima et al., 2015), similar to what observed in

HCE-S cells and highlights once again that normal levels of CRIM1 are necessary to maintain a regulated cell proliferation.

An abnormal proliferation is one of the main characteristics for pterygium development (Coroneo, 1993): overexpression of CRIM1 seems to counteract and contain this process, therefore slowing down pterygium formation, while this function is lost in the case of the H412P mutation.

In an attempt to determine if the effect of the mutation was due to signalling pathways I investigated other proteins involved in CRIM1 interactions: I did not find any differences in VEGFA and TGFBI gene expression between CRIM1 wt and H412P mutant transfected cells (Figure 4.5 in Chapter 4). CRIM1 overexpression, either wt or H412P, seems not to have a direct effect upon expression of these genes.

On the contrary, a decrease in anti-apoptotic Bcl-2 in CRIM1 wt overexpressing cells suggested a possible involvement of apoptosis, and this was confirmed by an increase of apoptosis in CRIM1 wild-type transfected cell using TUNEL assays (Figure 4.6 in Chapter 4). These results may explain the anti-proliferative effect I observed when overexpressing CRIM1 wt (Figure 4.2 in Chapter 4).

Basal pterygium epithelial cells were previously found to express high levels of Bcl-2 compared to the upper pterygium epithelium and normal conjunctiva and showed a higher rate of apoptosis (Tan et al., 2000). According to our results, CRIM1 overexpression increases the apoptosis but, if an H412P mutation is present, the cells seem to become unresponsive to apoptotic stimuli (Figure 4.6 in Chapter 4), showing a slower proliferation rate (Figure 4.2 in Chapter 4).

The apoptosis process induced by deregulation of the antiapoptotic Bcl-2 has also been previously shown to be mediated by ERK activity (Cagnol and Chambard, 2010). Therefore, correlation between higher apoptosis and ERK phosphorylation was investigated, demonstrating an increase in ERK phosphorylation in HCE-S cells overexpressing CRIM1 wt (Figure 4.3 in Chapter 4). Those results suggest that CRIM1, ERK and Bcl-2 are actors of the same pathway.

To understand how those factors could be related in disease pathogenesis, I focused my attention on the main pterygium triggering factor: UV light.
The role of UV in CRIM1 regulation was analysed by irradiating HCE-S cells *in vitro*: an increased expression of CRIM1 was observed at 6 and 24 hours from UV treatment (Figure 5.1 in Chapter 5), an effect which was revealed to be more marked when irradiating with UVA as compared to irradiation with UVB. As discussed in Chapter 5, this might be due to the fact that UVA induces more oxidative stress than UVB (Rezzani et al., 2014b), which is a mechanism known to play an important role during pterygium development (Balci et al., 2011b).

Upon UVA irradiation, VEGFA expression was highly increased at 24 hours (Figure 5.5A in Chapter 5), as previously observed with UVB irradiation in pterygium epithelial cells (Di Girolamo et al., 2006b). Since HCE-S cells behave similarly to pterygium cells under UVA exposure, they represent a good model for the study of pterygium.
Moreover, increased VEGFA in HCE-S cells occurs in parallel with CRIM1 overexpression under UV exposure, suggesting a possible interaction between VEGFA and CRIM1 that would benefit from further investigation.

Studying the effect of UV light upon the ERK pathway, an increased ERK phosphorylation at 6 and 24 hours following UVA irradiation was noticed (Figure 5.3 in Chapter 5), consistent with the previously reported results of studies in pterygium cells (Chao et al., 2013). The direct role of CRIM1 in this increase in ERK phosphorylation in response to UV light was demonstrated by the downregulation of ERK phosphorylation in cells by CRIM1 siRNA (Figure 5.8 in Chapter 5). Therefore, modulation of CRIM1 expression interferes with ERK phosphorylation pathway triggered by UVA exposure.
Those results imply that CRIM1, whose expression is increased by UV irradiation, is an upstream regulator of the ERK pathway leading to cell apoptosis through Bcl-2 expression modulation (Figure 5.9 in Chapter 5).

The anti-proliferative role of CRIM1 upon UVA irradiation was also confirmed: UV light, as already shown in pterygium cultured cells (Chao et al., 2013), increases cell proliferation, which was further elevated by the use of siRNA against CRIM1. In this case CRIM1 targeting siRNA prevents the increase in CRIM1 expression following UVA exposure and therefore it is unable to carry out its previously proposed protective anti-proliferative effect, explaining the increased proliferation rate with the use of CRIM1 siRNA (Figure 5.7B in Chapter 5).

Increased CRIM1 expression observed when the cells were treated with UVA and ERK inhibitor, suggests negative feedback regulation of the ERK pathway, as previously reported (Mirzoeva et al., 2009), where MEK inhibition was shown to counteract cell apoptosis in breast cancer. When ERK phosphorylation is inhibited, the cell tends to further increase CRIM1 upon UV exposure in an attempt to activate the downstream pathway. CRIM1 is not altered when the cells are treated with ERK inhibitor alone, without UV irradiation, underlying the importance of UV irradiation as an initial trigger for the whole pathway.

When studying the apoptosis involvement downstream the ERK pathway, I found that the Bcl-2 expression was decreased when HCE-S cells were treated with ERK inhibitor alone as well as with UVA alone, but the additive effect of UVA and the ERK inhibitor brought Bcl-2 levels back to normal.
Decreased Bcl-2 expression upon UVA irradiation suggested a pro-apoptotic effect of UVA (Figure 5.4 in Chapter 5). By adding ERK inhibitor alongside treatment with UVA, the pathway was blocked at the point of ERK phosphorylation and CRIM1 resulted more highly expressed than by treatment with UVA alone (Figure 5.2 in Chapter 5). The same treatment with ERK inhibitor and UVA is also able to bring Bcl-2 expression back to HCE-S endogenous levels, thus possibly inhibiting apoptosis induced by UVA alone (Figure 5.4 in Chapter 5). In this case, with the addition of ERK inhibitor, ERK phosphorylation remains blocked and is unable to reduce Bcl-2 expression. This result confirms the consequential pathway: CRIM1 expression, ERK phosphorylation, Bcl-2 expression and eventually apoptosis.

The series of cross-acting pathways analysed within this study helped delineating a cell mechanism response to UV which involves an increase in CRIM1 expression, supported by the analogous increase in CRIM1 expression within the

Northern Irish pterygium affected individuals. The increase in CRIM1 expression is therefore responsible for enabling ERK phosphorylation and decreasing Bcl-2 expression, towards an activation of the apoptosis process (Figure 6).

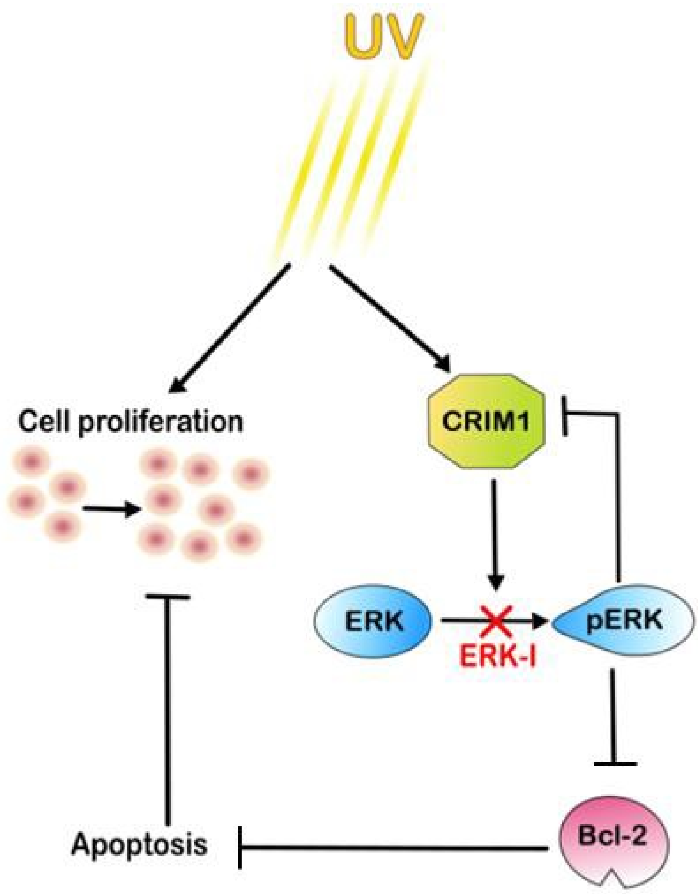

Figure 6 CRIM1 regulates pERK in a feedback loop pathway

Based on experimental evidence, this schematic image proposes the intracellular pathway triggered by UV light that may act as a protective mechanism against pterygium development.

UV irradiation results in an increase in CRIM1 cellular expression, followed by activation of the ERK pathway. In the presence of UV light, increased ERK phosphorylation down-regulates CRIM1 expression. Inhibition of the ERK phosphorylation blocks this feedback and under UV CRIM1 expression is further increased in a cellular attempt to circumvent the blocked ERK activity. Moreover, ERK phosphorylation induces a decreased expression of the anti-apoptotic Bcl-2, causing the cell to go into apoptosis. This was confirmed by adding ERK inhibitor upon UVA treatment: where CRIM1 is increased further and the downstream apoptosis is blocked.

This pathway was shown to be impaired in the case of the H412P mutation in CRIM1, found in the Northern Irish family affected by pterygium (Chapter 2).

This CRIM1 mediated protective mechanism against UV light resulted impaired in the case of the H412P mutation found in a Northern Irish family affected by pterygium.

Another protective mechanism developed against UV is observed in white-headed Fleckvieh cattle, characterised by a peculiar pigmentation surrounding the eyes (ambilateral circumocular pigmentation, ACOP). These cattle, less susceptible to development of the common UV induced bovine ocular squamous cell carcinoma (BOSCC, eye cancer), CRIM1 was identified as a quantitative trait loci (QTL) by a GWAS study together with other 11 QTLs. (Pausch et al., 2012). None of the other QTLs found in this study came up in the genes identified by our WES analysis.

Moreover, both CRIM1 and pterygium were previously associated with tissue remodelling in cancer and EMT, the molecular process in which epithelial cells acquire mesenchymal characteristics, switching on some genes like N-cadherins, integrins, MMPs and switching off others like members of the miR-200 family, E-cadherin and regulating pathways like WNT/β–catenins and TGF-β (Kalluri and Weinberg, 2009, Lamouille et al., 2014).

Pterygium pathogenesis has been associated with EMT since researchers observed a downregulation of members of the miR-200 family (Engelsvold et al., 2013) and an increased expression of β–catenin (Kato et al., 2007, Jaworski et al., 2009).

β–catenin, together with cadherins, interact with the cytosolic domain of CRIM1 to mediate cell-cell adhesion (Ponferrada et al., 2012). CRIM1 also interacts with integrins in lens surface epithelium (Zhang et al., 2015) and extracellularly as an antagonist of Bone Morphogenetic Factors (BMP) 4 and 7 (Wilkinson et al., 2003).

BMP antagonists are known to impair cancer cells migration and adhesion like for example Chordin which, antagonising BMP4, blocks migration in melanoma (Rothhammer et al., 2005) and Noggin which antagonises BMP2 and inhibit cell invasion in stomach cancer cells (Kang et al., 2010). Also the BMP antagonist CRIM1 was described as a risk factor for cancer development (Zeng and Tang, 2014), found to be upregulated in drug-resistant myeloid leukaemia HL60 cells (Prenkert et al., 2010) and to promote lung cancer cell migration and adhesion (Zeng et al., 2015). CRIM1 has been also shown to be cleaved extracellularly by MMP14, enzyme fundamental for regulation of cell invasion and tissue remodelling (Butler et al., 2008) which was found upregulated in pterygium (Bradley et al., 2010).

At the same time, as introduced in Chapter 1, also pterygium and pinguecula were described as a precursor for cancer development as squamous cell carcinoma and malignant melanoma (Chui et al., 2011).

Pterygium formation can thus be due to a disregulating mechanism triggered by UV and involving CRIM1 expression as well as EMT (Kato et al., 2007, Engelsvold et al., 2013), eventually evolving in cancer, and abnormal tissue remodelling through expression of metalloproteinases, cytokines and growth factors (Di Girolamo et al., 2004, Coroneo et al., 1999b), see Figure 1.4 in Chapter 1.

6.3 Conclusion

This research focused on the analysis of a Northern Irish family affected by pterygium but rarely exposed to its main etiogenic factor, the sun, in order to find a gene and a molecular pathway involved in its pathogenesis. The H412P mutation in CRIM1 was selected as the most likely candidate to be associated with pterygium onset in the affected members of the family.

Subsequent *CRIM1* sequence screening and expression analysis in ethnically different pterygium affected individuals suggests CRIM1 H412P as a possible founder mutation inherited within the family with reduced penetrance even if CRIM1 overexpression in some pterygium affected individuals implies CRIM1 involvement in pterygium onset.

A subsequent functional analysis demonstrated the multistep intracellular pathway triggered by CRIM1 overexpression, involving ERK phosphorylation and apoptosis; a pathway which can be induced by UV irradiation and which was blocked if the H412P mutation was introduced in CRIM1 gene.

Consequential intracellular events triggered by UV and involving the regulation of CRIM1 expression have been described within this thesis using multiple experiments which confirm the functional involvement of CRIM1 in the UV cellular response toward apoptosis.

Novel information revealed within this study leads the way for a deeper understanding of the pterygium pathomechanism and can be used as a diagnostic tool for pterygium early detection, evaluating CRIM1 mutations or levels of expression in members of families affected by pterygium or in patient individuals when they present the first pterygium symptoms.

Further studies on a higher number of patients and on CRIM1 related intracellular mechanisms hold the promise for a personalized treatment of pterygium.

6.4 Future perspectives

In order to understand which the best paths to follow from the results obtained to date are, we need to determine the remaining unsolved questions about CRIM1 and pterygium.

Firstly, are there any other mutations in other domains of the *CRIM1* gene in the individual patients investigated? Are those domains important for CRIM1 function in pterygium? Are there any other mutations in one of the CRIM1 interactors? How is CRIM1 expression regulated? Is *CRIM1* methylation involved in its expression regulation? Which are the other intracellular actors involved in the CRIM1-ERK-apoptotic pathway?

Future experiments following the results obtained within this study should therefore include both a clinical investigation and a deeper molecular study into the pathways involved in pterygium pathogenesis.

A deeper clinical investigation would start from a wider genetic screening of the population, including not only CRIM1 VWFs but also the other functional domains: IGFBP and the four antistasin-like domains.

IGFBP is part of the well characterised IGF systems composed by the type-I and type-II IGFs, type-I and type-II IGF receptors, IGFBP and IGFBP proteases. Six types of IGFBPs have been described in mammals and they bind IGF with a higher affinity than IGF receptors, modulating IGF availability and activity and prolonging their half-life. IGFBPs can bind to other molecules including insulin, all regulating important biological processes, in particular cell proliferation and differentiation (Hwa et al., 1999)

Two different microarray analyses comparing pterygium with unaffected conjunctiva have revealed differences in IGFBP expression levels: IGFBP-2 expression was found to be dramatically increased in pterygium (Solomon et al., 2003), while IGFBP-3 which was revealed to be down-regulated in pterygium (Wong et al., 2006).

In its N-terminal domain, CRIM1 contains a cluster of 10 conserved cysteines which form the IGFBP motif (GCGCCXXC) (Kim et al., 1997), similar to the 10 cysteine motif found in the N-terminal domain of IGFBP-7, also known as MAC25 (Murphy et al., 1993).

IGFBP-7 has been shown to bind IGF-I and II *in vitro* with a low affinity but also insulin (Yamanaka et al., 1997). Given the high similarity between CRIM1 and IGFBP-7, we can speculate similar interactions (Kolle et al., 2000a) responsible for cell growth regulation in pterygium together with an increased IGFBP-2 and decreased IGFBP-3 expression.

Moreover, it has been demonstrated that IGFBP-2 stimulates glioma cell proliferation and invasion though integrin β1-ERK pathway (Han et al., 2014) and IGFBP-3 activates ERK pathway and motility in HUVEC cells with a dual effect on cell survival or apoptosis depending on the experimental conditions (Granata et al., 2004).

Therefore, new mutations might be found in the N-terminal IGFBP domain of CRIM1, which has not yet been investigated.

Little information is available regarding the antistasin domain, except for the fact that it is a potent anticoagulant for its ability to inhibit factor Xa (Holstein et al., 1992) and it is also able to inhibit cell proliferation in cultured aortic smooth muscle cells (Gasic et al., 1992).

I can therefore speculate that a mutation found in one of the four CRIM1 antistasin domains could impair cell proliferation and thus be involved in pterygium pathogenesis.

A wider screen for germline *CRIM1* mutations on a higher number of patients either from low UV exposure or high UV exposure areas would then make the data more statistically significant.

However, not finding a mutation in the *CRIM1* gene does not exclude the role of CRIM1 in pterygium formation: a mutation could be found in one of many CRIM1 interactors like VEGFA, where the 936 C>T mutation has already been described in pterygium samples (Peng et al., 2014) or in another protein involved in the same cellular pathway. Alternatively the level of CRIM1 expression could be altered by epigenetic means and therefore a deeper analysis on *CRIM1* epigenetic state upon UVA treatment or in pterygium samples would be necessary.

Finding other mutations or modifications in CRIM1 or its interactors would increase the importance of CRIM1 involvement in pterygium pathogenesis, shortening the distance from a future personalized treatment and giving the patients a more solid diagnostic tool.

Additional experiments are also necessary to better understand and delineate the internal pathway which involves CRIM1 overexpression. The first CRIM1 interactor to investigate would be the pro-angiogenic VEGFA.

It is known that CRIM1 interacts with VEGFA through its VWFs in transfected fibroblastic Cos-7 cells (Wilkinson et al., 2007a) and that Crim1 is able to enhance autocrine VEGFA signalling in retinal vascular endothelial cells (Fan et al., 2014).

In order to reveal if VEGFA is involved in the same pathway and if this is due to a possible interaction with CRIM1, the first set of experiments should include *in vitro* blocking of UV induced VEGFA overexpression. This would be obtained using a VEGFA inhibitor in HCE-S treated with UV and then evaluating the effects that this would have on CRIM1 expression, ERK phosphorylation, Bcl-2 regulation and apoptosis.

A parallel experiment would include blocking CRIM1 overexpression induced by UV through 0.5nM siCRIM1 and an evaluation of VEGF expression levels that we know increased upon UV treatment (Figure 5.4).

CRIM1 has also been shown to be important for regulating the release of growth factors from the cells (Wilkinson et al., 2007a), similarly to its function in antagonizing the BMP maturation process, delivery to the cell surface and cell secretion (Wilkinson et al., 2003). This would lead to an investigation of which growth factors are involved in pterygium development and the cell proliferative activity that elicits growth towards the central cornea and how they are distributed which may give an idea on the directionality of the growth.

Candidates for growth factors involved in pterygium include, connective tissue growth factor (CTGF) for example contains a cysteine knot motif similar to CRIM1 (O'Leary et al., 2004b) and is able to regulate VEGFA induced angiogenesis (Lee et al., 2015), platelet-derived growth factor (PDGF) which can bind CRIM1 (Wilkinson et al., 2007a) and is upregulated in pterygium (Kria et al., 1996), Heparin-Binding epidermal growth factor-like growth factor (HB-EGF) (Nolan et al., 2003) or FGF-2 which are upregulated in pterygium (Detorakis et al., 2010).

Their expression could be studied by qRT-PCR and their distribution by IHC or mass spectrometry.

Evaluating the involvement of growth factors is important because the ERK pathway is generally activated by multiple cell growth factors including those involved in pterygium or CRIM1 interactions such as FGF (Lanner and Rossant, 2010, Ochi et al., 2003), PDGF (Pratsinis and Kletsas, 2007), HB-EGF (Filardo et al., 2000) and CTGF (Tan et al., 2009).

The role of CRIM1 might therefore be to interact with some of those growth factors, regulate their availability on the cell surface and thus promote the tissue overgrowth.

Finally, CRIM1 tridimensional structure has not yet been described and, as a transmembrane protein, its crystallization is not easy because of its instability and hydrophobicity (Shimamura, 2016). Novel techniques like the lipidic cubic phase crystallization was proven successful to determine membrane protein structure at high resolution (Weierstall et al., 2014) and can therefore be used with CRIM1 to elucidate domains interactors and related functional mechanisms.

Subsequent experiments could be done to validate *in vivo* the results previously obtained with the HCE-S *in vitro* model.

The UVA crosslinker lamp could be used on wild type mice eyes and CRIM1 expression evaluated comparing a UV treated mice with mice not exposed to UV light. Previous experiments were done treating the mice eyes with a UVA crosslinker once the epithelial layer was removed and this elicited an increased apoptosis in the central corneal stroma (Wang, 2008).

Cryosections and IHC staining of the mouse eyes would allow one to not only evaluate differences in CRIM1 expression between UV treated and untreated mice but also attain a better understanding of localization of CRIM1 protein in cornea and conjunctiva and therefore understanding where it exerts its major functions. ERK phosphorylation could be also analysed through anterior eye protein extraction and compared between UV irradiated and non-irradiated eyes. Within these experiments, Bcl-2 expression could be assessed within samples by extracting RNA from the anterior eye tissue and analysis by qRT-PCR.

Now that the function of CRIM1 in UV cellular response has been in part described, a deeper understanding of the role of CRIM1 and its involvement in intracellular pathways will shed light in the mechanism of pterygium pathogenesis.

At clinical level those novel information could be used to develop a non-invasive diagnostic tool which would therefore be extensively used in clinical assessments as well as a personalised treatment, beneficial to the public health system and to the general population.

REFERENCES

ABREU, J. G., COFFINIER, C., LARRAıN, J., OELGESCHLÄGER, M. & DE ROBERTIS, E. 2002. Chordin-like CR domains and the regulation of evolutionarily conserved extracellular signaling systems. *Gene,* 287**,** 39-47.

ADAMS, J. M. & CORY, S. 1998. The Bcl-2 protein family: arbiters of cell survival. *Science,* 281**,** 1322-1326.

ADZHUBEI, I. A., SCHMIDT, S., PESHKIN, L., RAMENSKY, V. E., GERASIMOVA, A., BORK, P., KONDRASHOV, A. S. & SUNYAEV, S. R. 2010. A method and server for predicting damaging missense mutations. *Nature methods,* 7**,** 248-249.

AGAR, N. S., HALLIDAY, G. M., BARNETSON, R. S., ANANTHASWAMY, H. N., WHEELER, M. & JONES, A. M. 2004. The basal layer in human squamous tumors harbors more UVA than UVB fingerprint mutations: a role for UVA in human skin carcinogenesis. *Proceedings of the National Academy of Sciences of the United States of America,* 101**,** 4954-4959.

ALLAART, M., VAN WEELE, M., FORTUIN, P. & KELDER, H. 2004. An empirical model to predict the UV-index based on solar zenith angles and total ozone. *Meteorological Applications,* 11**,** 59-65.

ALLEN, E. H., ATKINSON, S. D., LIAO, H., MOORE, J. E., PEDRIOLI, D. M. L., SMITH, F. J., MCLEAN, W. H. I. & MOORE, C. T. 2013. Allele-Specific siRNA Silencing for the Common Keratin 12 Founder Mutation in Meesmann Epithelial Corneal DystrophyAllele-Specific siRNA Silencing. *Investigative ophthalmology & visual science,* 54**,** 494-502.

AMADIO, M., GOVONI, S. & PASCALE, A. 2016. Targeting VEGF in eye neovascularization: what's new?: a comprehensive review on current therapies and oligonucleotide-based interventions under development. *Pharmacological research,* 103**,** 253-269.

AMBATI, B. K., NOZAKI, M., SINGH, N., TAKEDA, A., JANI, P. D., SUTHAR, T., ALBUQUERQUE, R. J., RICHTER, E., SAKURAI, E. & NEWCOMB, M. T. 2006. Corneal avascularity is due to soluble VEGF receptor-1. *Nature,* 443**,** 993-997.

ANDERSON, J. R. 1954. A pterygium map. *Acta Ophthalmol,* 3**,** 1631-1642.

ANGURIA, P., KITINYA, J., NTULI, S. & CARMICHAEL, T. 2014. The role of heredity in pterygium development. *Int J Ophthalmol,* 7**,** 563-73.

ASPIOTIS, M., TSANOU, E., GOREZIS, S., IOACHIM, E., SKYRLAS, A., STEFANIOTOU, M. & MALAMOU-MITSI, V. 2007. Angiogenesis in pterygium: study of microvessel density, vascular endothelial growth factor, and thrombospondin-1. *Eye,* 21**,** 1095-1101.

ASSIL, K. K., QUANTOCK, A. J., BARRETT, A. M. & SCHANZLIN, D. J. 1993. Corneal iron lines associated with the intrastromal corneal ring. *American journal of ophthalmology,* 116**,** 350-356.

AUSTIN, P., JAKOBIEC, F. A. & IWAMOTO, T. 1983. Elastodysplasia and elastodystrophy as the pathologic bases of ocular pterygia and pinguecula. *Ophthalmology,* 90**,** 96-109.

BAIRD, P. N., HAGEMAN, G. S. & GUYMER, R. H. 2009. New era for personalized medicine: the diagnosis and management of age-related macular degeneration. *Clinical & experimental ophthalmology,* 37**,** 814-821.

BALCI, M., SAHIN, S., MUTLU, F. M., YAGCI, R., KARANCI, P. & YILDIZ, M. 2011a. Investigation of oxidative stress in pterygium tissue. *Mol Vis,* 17, 443-7.

BALCI, M., ŞAHIN, Ş., MUTLU, F. M., YAĞCI, R., KARANCI, P. & YILDIZ, M. 2011b. Investigation of oxidative stress in pterygium tissue.

BALE, S. J., CHAKRAVARTI, A. & GREENE, M. 1986. Cutaneous malignant melanoma and familial dysplastic nevi: evidence for autosomal dominance and pleiotropy. *American journal of human genetics,* 38, 188.

BAMSHAD, M. J., NG, S. B., BIGHAM, A. W., TABOR, H. K., EMOND, M. J., NICKERSON, D. A. & SHENDURE, J. 2011. Exome sequencing as a tool for Mendelian disease gene discovery. *Nat Rev Genet,* 12, 745-55.

BASSETT, J., FORBES, S., PANNETT, A., LLOYD, S., CHRISTIE, P., WOODING, C., HARDING, B., BESSER, G., EDWARDS, C. & MONSON, J. 1998. Characterization of mutations in patients with multiple endocrine neoplasia type 1. *The American Journal of Human Genetics,* 62, 232-244.

BEDEN, Ü., IRKEÇ, M., ORHAN, D. & ORHAN, M. 2003. The roles of T-lymphocyte subpopulations (CD4 and CD8), intercellular adhesion molecule-1 (ICAM-1), HLA-DR receptor, and mast cells in etiopathogenesis of pterygium. *Ocular immunology and inflammation,* 11, 115-122.

BELEGGIA, F., LI, Y., FAN, J., ELCIOGLU, N. H., TOKER, E., WIELAND, T., MAUMENEE, I. H., AKARSU, N. A., MEITINGER, T., STROM, T. M., LANG, R. & WOLLNIK, B. 2015. CRIM1 haploinsufficiency causes defects in eye development in human and mouse. *Hum Mol Genet,* 24, 2267-73.

BELL, C. J., DINWIDDIE, D. L., MILLER, N. A., HATELEY, S. L., GANUSOVA, E. E., MUDGE, J., LANGLEY, R. J., ZHANG, L., LEE, C. C. & SCHILKEY, F. D. 2011. Carrier testing for severe childhood recessive diseases by next-generation sequencing. *Science translational medicine,* 3, 65ra4-65ra4.

BIANCHI, E., SCARINCI, F., GRANDE, C., PLATEROTI, R., PLATEROTI, P., PLATEROTI, A. M., FUMAGALLI, L., CAPOZZI, P., FEHER, J. & ARTICO, M. 2012. Immunohistochemical profile of VEGF, TGF-beta and PGE(2) in human pterygium and normal conjunctiva: experimental study and review of the literature. *Int J Immunopathol Pharmacol,* 25, 607-15.

BLESSING, K., SANDERS, D. & GRANT, J. 1998. Comparison of immunohistochemical staining of the novel antibody melan-A with S100 protein and HMB-45 in malignant melanoma and melanoma variants. *Histopathology,* 32, 139-146.

BLOM, N., GAMMELTOFT, S. & BRUNAK, S. 1999. Sequence and structure-based prediction of eukaryotic protein phosphorylation sites. *J Mol Biol,* 294, 1351-62.

BLOOM, A. H., PERRY, H. D., DONNENFELD, E. D., PINCHOFF, B. S. & SOLOMON, R. 2005. Childhood onset of pterygia in twins. *Eye Contact Lens,* 31, 279-80.

BOTSTEIN, D., WHITE, R. L., SKOLNICK, M. & DAVIS, R. W. 1980. Construction of a genetic linkage map in man using restriction fragment length polymorphisms. *Am J Hum Genet,* 32, 314-31.

BOYDEN, E. D., CAMPOS-XAVIER, A. B., KALAMAJSKI, S., CAMERON, T. L., SUAREZ, P., TANACKOVICH, G., ANDRIA, G., BALLHAUSEN, D., BRIGGS, M. D. & HARTLEY, C. 2011. Recurrent dominant mutations affecting two adjacent residues in the motor domain of the monomeric kinesin

KIF22 result in skeletal dysplasia and joint laxity. *The American Journal of Human Genetics,* 89, 767-772.
BRADLEY, J. C., YANG, W., BRADLEY, R. H., REID, T. W. & SCHWAB, I. R. 2010. The science of pterygia. *Br J Ophthalmol,* 94, 815-20.
BREKELMANS, C. T. 2003. Risk factors and risk reduction of breast and ovarian cancer. *Current opinion in Obstetrics and Gynecology,* 15, 63-68.
BROWN, T. A. 2006. *Genomes*, Garland science.
BUTLER, G. S., DEAN, R. A., TAM, E. M. & OVERALL, C. M. 2008. Pharmacoproteomics of a metalloproteinase hydroxamate inhibitor in breast cancer cells: dynamics of membrane type 1 matrix metalloproteinase-mediated membrane protein shedding. *Molecular and cellular biology,* 28, 4896-4914.
BUTRUS, S. I., ASHRAF, M. F., LABY, D. M., RABINOWITZ, A. I., TABBARA, S. O. & HIDAYAT, A. A. 1995. Increased numbers of mast cells in pterygia. *American journal of ophthalmology,* 119, 236-237.
CAGNOL, S. & CHAMBARD, J. C. 2010. ERK and cell death: mechanisms of ERK-induced cell death--apoptosis, autophagy and senescence. *Febs j,* 277, 2-21.
CAMERON, M. E. 1983. Histology of pterygium: an electron microscopic study. *British journal of ophthalmology,* 67, 604-608.
CAMPBELL, F. W. & MICHAELSON, I. C. 1949. Blood-vessel formation in the cornea. *Br J Ophthalmol,* 33, 248-55.
CARDENAS-CANTU, E., ZAVALA, J., VALENZUELA, J. & VALDEZ-GARCIA, J. E. 2015. Molecular Basis of Pterygium Development. *Semin Ophthalmol*, 1-17.
CAUNT, C. J., SALE, M. J., SMITH, P. D. & COOK, S. J. 2015. MEK1 and MEK2 inhibitors and cancer therapy: the long and winding road. *Nature Reviews Cancer,* 15, 577-592.
CHANDRA, A., MITRY, D., WRIGHT, A., CAMPBELL, H. & CHARTERIS, D. G. 2014. Genome-wide association studies: applications and insights gained in Ophthalmology. *Eye (Lond),* 28, 1066-79.
CHAO, S. C., HU, D. N., YANG, P. Y., LIN, C. Y., NIEN, C. W., YANG, S. F. & ROBERTS, J. E. 2013. Ultraviolet-A irradiation upregulated urokinase-type plasminogen activator in pterygium fibroblasts through ERK and JNK pathways. *Invest Ophthalmol Vis Sci,* 54, 999-1007.
CHEN, J., MAQSOOD, S., KAYE, S., TEY, A. & AHMAD, S. 2013. Pterygium: are we any closer to the cause? *British Journal of Ophthalmology*, bjophthalmol-2013-304232.
CHEN, P. L., CHENG, Y. W., CHIANG, C. C., TSENG, S. H., CHAU, P. S. & TSAI, Y. Y. 2006. Hypermethylation of the p16 gene promoter in pterygia and its association with the expression of DNA methyltransferase 3b. *Mol Vis,* 12, 1411-6.
CHIU, H. S., YORK, J. P., WILKINSON, L., ZHANG, P., LITTLE, M. H. & PENNISI, D. J. 2012. Production of a mouse line with a conditional Crim1 mutant allele. *genesis,* 50, 711-716.
CHUI, J., CORONEO, M. T., TAT, L. T., CROUCH, R., WAKEFIELD, D. & DI GIROLAMO, N. 2011. Ophthalmic pterygium: a stem cell disorder with premalignant features. *Am J Pathol,* 178, 817-27.

CHUI, J., DI GIROLAMO, N., WAKEFIELD, D. & CORONEO, M. T. 2008. The pathogenesis of pterygium: current concepts and their therapeutic implications. *Ocul Surf,* 6**,** 24-43.

CLEAR, A. S., CHIRAMBO, M. C. & HUTT, M. S. 1979. Solar keratosis, pterygium, and squamous cell carcinoma of the conjunctiva in Malawi. *Br J Ophthalmol,* 63**,** 102-9.

COLE, D. 1977. Secretion of the aqueous humour. *Experimental eye research,* 25**,** 161-176.

COLLINS, F. S. 1992. Positional cloning: let's not call it reverse anymore. *Nature genetics,* 1**,** 3-6.

CONTRUCCI FARALDI, N. & GRACIS, G. 1976. Pterygium on twins. *Ophthalmologica,* 172**,** 361-366.

COOPER, D. N., KRAWCZAK, M., POLYCHRONAKOS, C., TYLER-SMITH, C. & KEHRER-SAWATZKI, H. 2013. Where genotype is not predictive of phenotype: towards an understanding of the molecular basis of reduced penetrance in human inherited disease. *Human genetics,* 132**,** 1077-1130.

COPELAND, R. A., AFSHARI, N. A. & DOHLMAN, C. H. 2013. *Copeland and Afshari's Principles and Practice of Cornea*, JP Medical Ltd.

CORONEO, M., DI GIROLAMO, N. & WAKEFIELD, D. 1999a. The pathogenesis of pterygia. *Current opinion in ophthalmology,* 10**,** 282-288.

CORONEO, M. T. 1993. Pterygium as an early indicator of ultraviolet insolation: a hypothesis. *Br J Ophthalmol,* 77**,** 734-9.

CORONEO, M. T., DI GIROLAMO, N. & WAKEFIELD, D. 1999b. The pathogenesis of pterygia. *Curr Opin Ophthalmol,* 10**,** 282-8.

COSTER, D. 1995. Pterygium--an ophthalmic enigma. *The British journal of ophthalmology,* 79**,** 304.

CRIMELLA, C., BASCHIROTTO, C., ARNOLDI, A., TONELLI, A., TENDERINI, E., AIROLDI, G., MARTINUZZI, A., TRABACCA, A., LOSITO, L., SCARLATO, M., BENEDETTI, S., SCARPINI, E., SPINICCI, G., BRESOLIN, N. & BASSI, M. T. 2012. Mutations in the motor and stalk domains of KIF5A in spastic paraplegia type 10 and in axonal Charcot-Marie-Tooth type 2. *Clin Genet,* 82**,** 157-64.

CULLEN, A. P. 2002. Photokeratitis and other phototoxic effects on the cornea and conjunctiva. *International journal of toxicology,* 21**,** 455-464.

CUTTER, G. R. & LIU, Y. 2012. Personalized medicine The return of the house call? *Neurology: Clinical Practice,* 2**,** 343-351.

DAS, P., GOKANI, A., BAGCHI, K., BHADURI, G., CHAUDHURI, S. & LAW, S. 2015. Limbal epithelial stem-microenvironmental alteration leads to pterygium development. *Mol Cell Biochem,* 402**,** 123-39.

DAWSON, D. G., GEROSKI, D. H. & EDELHAUSER, H. F. 2009. Corneal endothelium: structure and function in health and disease. *Corneal Surgery: Theory, Technique and Tissue, ed,* 4**,** 57-70.

DE WIT, D., ATHANASIADIS, I., SHARMA, A. & MOORE, J. 2010. Sutureless and glue-free conjunctival autograft in pterygium surgery: a case series. *Eye (Lond),* 24**,** 1474-7.

DELMONTE, D. W. & KIM, T. 2011. Anatomy and physiology of the cornea. *Journal of Cataract & Refractive Surgery,* 37**,** 588-598.

DEMURTAS, P., ORRU, G., CONI, P., MINERBA, L., CORRIAS, M., SIRIGU, P., ZUCCA, I., DEMURTAS, E., MAXIA, C., PIRAS, F., MURTAS, D., LAI, S. & PERRA, M. T. 2014. Association between the ACE insertion/deletion polymorphism and pterygium in Sardinian patients: a population based case-control study. *BMJ Open,* 4**,** e005627.

DETELS, R. & DHIR, S. 1967. Pterygium: a geographical study. *Archives of Ophthalmology,* 78**,** 485-491.

DETORAKIS, E., ZAFIROPOULOS, A., ARVANITIS, D. & SPANDIDOS, D. 2005a. Detection of point mutations at codon 12 of KI-ras in ophthalmic pterygia. *Eye,* 19**,** 210-214.

DETORAKIS, E. T., SOURVINOS, G., TSAMPARLAKIS, J. & SPANDIDOS, D. A. 1998. Evaluation of loss of heterozygosity and microsatellite instability in human pterygium: clinical correlations. *Br J Ophthalmol,* 82**,** 1324-8.

DETORAKIS, E. T. & SPANDIDOS, D. A. 2009a. Pathogenetic mechanisms and treatment options for ophthalmic pterygium: trends and perspectives (Review). *International journal of molecular medicine,* 23**,** 439.

DETORAKIS, E. T. & SPANDIDOS, D. A. 2009b. Pathogenetic mechanisms and treatment options for ophthalmic pterygium: trends and perspectives (Review). *Int J Mol Med,* 23**,** 439-47.

DETORAKIS, E. T., ZAFIROPOULOS, A., ARVANITIS, D. A. & SPANDIDOS, D. A. 2005b. Detection of point mutations at codon 12 of KI-ras in ophthalmic pterygia. *Eye (Lond),* 19**,** 210-4.

DETORAKIS, E. T., ZARAVINOS, A. & SPANDIDOS, D. A. 2010. Growth factor expression in ophthalmic pterygia and normal conjunctiva. *International journal of molecular medicine,* 25**,** 513.

DHALLA, F., FOX, H., DAVENPORT, E. E., SADLER, R., ANZILOTTI, C., VAN SCHOUWENBURG, P. A., FERRY, B., CHAPEL, H., KNIGHT, J. C. & PATEL, S. Y. 2016. Chronic mucocutaneous candidiasis: characterization of a family with STAT-1 gain-of-function and development of an ex-vivo assay for Th17 deficiency of diagnostic utility. *Clin Exp Immunol,* 184**,** 216-27.

DI GIROLAMO, N., CHUI, J., CORONEO, M. T. & WAKEFIELD, D. 2004. Pathogenesis of pterygia: role of cytokines, growth factors, and matrix metalloproteinases. *Progress in retinal and eye research,* 23**,** 195-228.

DI GIROLAMO, N., CORONEO, M. T. & WAKEFIELD, D. 2003. UVB-elicited induction of MMP-1 expression in human ocular surface epithelial cells is mediated through the ERK1/2 MAPK-dependent pathway. *Invest Ophthalmol Vis Sci,* 44**,** 4705-14.

DI GIROLAMO, N., KUMAR, R. K., CORONEO, M. T. & WAKEFIELD, D. 2002. UVB-mediated induction of interleukin-6 and -8 in pterygia and cultured human pterygium epithelial cells. *Invest Ophthalmol Vis Sci,* 43**,** 3430-7.

DI GIROLAMO, N., WAKEFIELD, D. & CORONEO, M. T. 2006a. UVB-mediated induction of cytokines and growth factors in pterygium epithelial cells involves cell surface receptors and intracellular signaling. *Investigative ophthalmology & visual science,* 47**,** 2430-2437.

DI GIROLAMO, N., WAKEFIELD, D. & CORONEO, M. T. 2006b. UVB-mediated induction of cytokines and growth factors in pterygium epithelial cells involves cell surface receptors and intracellular signaling. *Invest Ophthalmol Vis Sci,* 47**,** 2430-7.

DIEBOLD, Y., CALONGE, M., DE SALAMANCA, A. E. Q., CALLEJO, S., CORRALES, R. M., SÁEZ, V., SIEMASKO, K. F. & STERN, M. E. 2003. Characterization of a spontaneously immortalized cell line (IOBA-NHC) from normal human conjunctiva. *Investigative ophthalmology & visual science,* 44**,** 4263-4274.

DILLON, J., ZHENG, L., MERRIAM, J. C. & GAILLARD, E. R. 1999. The optical properties of the anterior segment of the eye: implications for cortical cataract. *Experimental eye research,* 68**,** 785-795.

DOR, T., CINNAMON, Y., RAYMOND, L., SHAAG, A., BOUSLAM, N., BOUHOUCHE, A., GAUSSEN, M., MEYER, V., DURR, A., BRICE, A., BENOMAR, A., STEVANIN, G., SCHUELKE, M. & EDVARDSON, S. 2014. KIF1C mutations in two families with hereditary spastic paraparesis and cerebellar dysfunction. *J Med Genet,* 51**,** 137-42.

DUA, H. S., FARAJ, L. A., SAID, D. G., GRAY, T. & LOWE, J. 2013. Human corneal anatomy redefined: a novel pre-Descemet's layer (Dua's layer). *Ophthalmology,* 120**,** 1778-1785.

DUSHKU, N., JOHN, M. K., SCHULTZ, G. S. & REID, T. W. 2001. Pterygia pathogenesis: corneal invasion by matrix metalloproteinase expressing altered limbal epithelial basal cells. *Archives of Ophthalmology,* 119**,** 695-706.

DUSHKU, N. & REID, T. W. 1994. Immunohistochemical evidence that human pterygia originate from an invasion of vimentin-expressing altered limbal epithelial basal cells. *Curr Eye Res,* 13**,** 473-81.

EISSENBERG, J. C., WONG, M. & CHRIVIA, J. C. 2005. Human SRCAP and Drosophila melanogaster DOM are homologs that function in the notch signaling pathway. *Molecular and cellular biology,* 25**,** 6559-6569.

EL-HEFNAWI, H. & MORTADA, A. 1965. OCULAR MANIFESTATIONS OF XERODERMA PIGMENTOSUM. *Br J Dermatol,* 77**,** 261-76.

ELHALIS, H., AZIZI, B. & JURKUNAS, U. V. 2010. Fuchs endothelial corneal dystrophy. *The ocular surface,* 8**,** 173-184.

ENGELSVOLD, D. H., UTHEIM, T. P., OLSTAD, O. K., GONZALEZ, P., EIDET, J. R., LYBERG, T., TROSEID, A. M., DARTT, D. A. & RAEDER, S. 2013. miRNA and mRNA expression profiling identifies members of the miR-200 family as potential regulators of epithelial-mesenchymal transition in pterygium. *Exp Eye Res,* 115**,** 189-98.

ERLICH, Y., EDVARDSON, S., HODGES, E., ZENVIRT, S., THEKKAT, P., SHAAG, A., DOR, T., HANNON, G. J. & ELPELEG, O. 2011. Exome sequencing and disease-network analysis of a single family implicate a mutation in KIF1A in hereditary spastic paraparesis. *Genome research,* 21**,** 658-664.

FAN, J., PONFERRADA, V. G., SATO, T., VEMARAJU, S., FRUTTIGER, M., GERHARDT, H., FERRARA, N. & LANG, R. A. 2014. Crim1 maintains retinal vascular stability during development by regulating endothelial cell Vegfa autocrine signaling. *Development,* 141**,** 448-459.

FELL, G. L., ROBINSON, K. C., MAO, J., WOOLF, C. J. & FISHER, D. E. 2014. Skin β-endorphin mediates addiction to UV light. *Cell,* 157**,** 1527-1534.

FERRARA, N., GERBER, H.-P. & LECOUTER, J. 2003. The biology of VEGF and its receptors. *Nature medicine,* 9**,** 669-676.

FERRARIS, C., CHEVALIER, G., FAVIER, B., JAHODA, C. & DHOUAILLY, D. 2000. Adult corneal epithelium basal cells possess the capacity to activate epidermal, pilosebaceous and sweat gland genetic programs in response to embryonic dermal stimuli. *Development,* 127**,** 5487-5495.

FILARDO, E. J., QUINN, J. A., BLAND, K. I. & FRACKELTON JR, A. R. 2000. Estrogen-induced activation of Erk-1 and Erk-2 requires the G protein-coupled receptor homolog, GPR30, and occurs via trans-activation of the epidermal growth factor receptor through release of HB-EGF. *Molecular endocrinology,* 14**,** 1649-1660.

FOTOUHI, A., HASHEMI, H., KHABAZKHOOB, M. & MOHAMMAD, K. 2009. Prevalence and risk factors of pterygium and pinguecula: the Tehran Eye Study. *Eye,* 23**,** 1125-1129.

FRITSCHE-GUENTHER, R., WITZEL, F., SIEBER, A., HERR, R., SCHMIDT, N., BRAUN, S., BRUMMER, T., SERS, C. & BLÜTHGEN, N. 2011. Strong negative feedback from Erk to Raf confers robustness to MAPK signalling. *Molecular systems biology,* 7**,** 489.

FUCHS, E. 1892. Ueber das pterygium. *Albrecht von Graefes Archiv für Ophthalmologie,* 38**,** 1-90.

GABRIEL, S. B., SCHAFFNER, S. F., NGUYEN, H., MOORE, J. M., ROY, J., BLUMENSTIEL, B., HIGGINS, J., DEFELICE, M., LOCHNER, A. & FAGGART, M. 2002. The structure of haplotype blocks in the human genome. *Science,* 296**,** 2225-2229.

GARCIA-MARTIN, E., GARCIA-MENAYA, J., SANCHEZ, B., MARTINEZ, C., ROSENDO, R. & AGUNDEZ, J. A. 2007. Polymorphisms of histamine-metabolizing enzymes and clinical manifestations of asthma and allergic rhinitis. *Clin Exp Allergy,* 37**,** 1175-82.

GARCIA ABREU, J., COFFINIER, C., LARRAIN, J., OELGESCHLAGER, M. & DE ROBERTIS, E. M. 2002. Chordin-like CR domains and the regulation of evolutionarily conserved extracellular signaling systems. *Gene,* 287**,** 39-47.

GASIC, G. P., ARENAS, C. P., GASIC, T. B. & GASIC, G. J. 1992. Coagulation factors X, Xa, and protein S as potent mitogens of cultured aortic smooth muscle cells. *Proceedings of the National Academy of Sciences,* 89**,** 2317-2320.

GASS, J. D. M. 1964. The Iron Lines of the Superficial Cornea: Hudson-Stahli Line, Stocker's Line and Fleischer's Ring. *Archives of Ophthalmology,* 71**,** 348-358.

GEBHARDT, M., MENTLEIN, R., SCHAUDIG, U., PUFE, T., RECKER, K., NOLLE, B., AL-SAMIR, K., GEERLING, G. & PAULSEN, F. P. 2005. Differential expression of vascular endothelial growth factor implies the limbal origin of pterygia. *Ophthalmology,* 112**,** 1023-30.

GEORGAS, K., BOWLES, J., YAMADA, T., KOOPMAN, P. & LITTLE, M. H. 2000. Characterisation of Crim1 expression in the developing mouse urogenital tract reveals a sexually dimorphic gonadal expression pattern. *Developmental Dynamics,* 219**,** 582-587.

GINSBURG, G. S. & MCCARTHY, J. J. 2001. Personalized medicine: revolutionizing drug discovery and patient care. *TRENDS in Biotechnology,* 19**,** 491-496.

GLIENKE, J., STURZ, A., MENRAD, A. & THIERAUCH, K. H. 2002. CRIM1 is involved in endothelial cell capillary formation in vitro and is expressed in blood vessels in vivo. *Mech Dev,* 119**,** 165-75.

GORIS, A., BOONEN, S., D'HOOGHE M, B. & DUBOIS, B. 2010. Replication of KIF21B as a susceptibility locus for multiple sclerosis. *J Med Genet,* 47**,** 775-6.

GOYAL, J. L., RAO, V. A., SRINIVASAN, R. & AGRAWAL, K. 1994. Oculocutaneous manifestations in xeroderma pigmentosa. *Br J Ophthalmol,* 78**,** 295-7.

GRANATA, R., TROVATO, L., GARBARINO, G., TALIANO, M., PONTI, R., SALA, G., GHIDONI, R. & GHIGO, E. 2004. Dual effects of IGFBP-3 on endothelial cell apoptosis and survival: involvement of the sphingolipid signaling pathways. *The FASEB journal,* 18**,** 1456-1458.

GREGORY, P. A., BERT, A. G., PATERSON, E. L., BARRY, S. C., TSYKIN, A., FARSHID, G., VADAS, M. A., KHEW-GOODALL, Y. & GOODALL, G. J. 2008. The miR-200 family and miR-205 regulate epithelial to mesenchymal transition by targeting ZEB1 and SIP1. *Nature cell biology,* 10**,** 593-601.

GUPTA, K., KSHIRSAGAR, S., LI, W., GUI, L., RAMAKRISHNAN, S., GUPTA, P., LAW, P. Y. & HEBBEL, R. P. 1999. VEGF prevents apoptosis of human microvascular endothelial cells via opposing effects on MAPK/ERK and SAPK/JNK signaling. *Experimental cell research,* 247**,** 495-504.

HAN, S., LI, Z., MASTER, L., MASTER, Z. & WU, A. 2014. Exogenous IGFBP-2 promotes proliferation, invasion, and chemoresistance to temozolomide in glioma cells via the integrin β1-ERK pathway. *British journal of cancer,* 111**,** 1400-1409.

HAUGEN, O. H. & BERTELSEN, T. 1998. A new hereditary conjunctivocorneal dystrophy associated with dermal keloid formation, Report of a family. *Acta Ophthalmologica Scandinavica,* 76**,** 461-465.

HE, Y.-Y., COUNCIL, S. E., FENG, L. & CHIGNELL, C. F. 2008. UVA-induced cell cycle progression is mediated by a disintegrin and metalloprotease/epidermal growth factor receptor/AKT/Cyclin D1 pathways in keratinocytes. *Cancer Research,* 68**,** 3752-3758.

HE, Y.-Y., HUANG, J.-L. & CHIGNELL, C. F. 2004. Delayed and sustained activation of extracellular signal-regulated kinase in human keratinocytes by UVA implications in carcinogenesis. *Journal of Biological Chemistry,* 279**,** 53867-53874.

HECHT, F. & SHOPTAUGH, M. G. 1990. Winglets of the eye: dominant transmission of early adult pterygium of the conjunctiva. *J Med Genet,* 27**,** 392-4.

HILGERS, J. H. 1960. Pterygium: its incidence, heredity and etiology. *Am J Ophthalmol,* 50**,** 635-44.

HILL, J. C. & MASKE, R. 1989. Pathogenesis of pterygium. *Eye (Lond),* 3 (Pt 2)**,** 218-26.

HIRST, L. W. 2000. Distribution, risk factors, and epidemiology of pterygium. *Pterygium, Kugler Publications, The Hague, The Netherlands***,** 15-27.

HIRST, L. W., AXELSEN, R. A. & SCHWAB, I. 2009. Pterygium and associated ocular surface squamous neoplasia. *Arch Ophthalmol,* 127**,** 31-2.

HOLICK, M. F. 2008. Sunlight, UV-radiation, vitamin D and skin cancer: how much sunlight do we need? *Adv Exp Med Biol,* 624**,** 1-15.

HOLSTEIN, T. W., MALA, C., KURZ, E., BAUER, K., GREBER, M. & DAVID, C. N. 1992. The primitive metazoan Hydra expresses antistasin, a serine protease inhibitor of vertebrate blood coagulation: cDNA cloning, cellular localisation and developmental regulation. *FEBS letters,* 309**,** 288-292.

HOLZEL, M., ROHRMOSER, M., SCHLEE, M., GRIMM, T., HARASIM, T., MALAMOUSSI, A., GRUBER-EBER, A., KREMMER, E., HIDDEMANN, W., BORNKAMM, G. W. & EICK, D. 2005. Mammalian WDR12 is a novel member of the Pes1-Bop1 complex and is required for ribosome biogenesis and cell proliferation. *J Cell Biol,* 170**,** 367-78.

HOOD, R. L., LINES, M. A., NIKKEL, S. M., SCHWARTZENTRUBER, J., BEAULIEU, C., NOWACZYK, M. J., ALLANSON, J., KIM, C. A., WIECZOREK, D. & MOILANEN, J. S. 2012. Mutations in SRCAP, encoding SNF2-related CREBBP activator protein, cause Floating-Harbor syndrome. *The American Journal of Human Genetics,* 90, 308-313.

HOU, A., LAN, W., LAW, K. P., KHOO, S. C., TIN, M. Q., LIM, Y. P. & TONG, L. 2014. Evaluation of global differential gene and protein expression in primary Pterygium: S100A8 and S100A9 as possible drivers of a signaling network. *PLoS One,* 9, e97402.

HWA, V., OH, Y. & ROSENFELD, R. G. 1999. The insulin-like growth factor-binding protein (IGFBP) superfamily 1. *Endocrine reviews,* 20, 761-787.

ISHIOKA, M., SHIMMURA, S., YAGI, Y. & TSUBOTA, K. 2001. Pterygium and dry eye. *Ophthalmologica,* 215, 209-11.

ISLAM, S. I. & WAGONER, M. D. 2001a. Pterygium in young members of one family. *Cornea,* 20, 708-10.

ISLAM, S. I. & WAGONER, M. D. 2001b. Pterygium in young members of one family. *Cornea,* 20, 708-710.

IYER, S., CHOU, F. Y., WANG, R., CHIU, H. S., RAJU, V. K. S., LITTLE, M. H., THOMAS, W. G., PIPER, M. & PENNISI, D. J. 2016. Crim1 has cell-autonomous and paracrine roles during embryonic heart development. *Scientific reports,* 6.

JACKLIN, H. N. 1964. FAMILIAL PREDISPOSITION TO PTERYGIUM FORMATION; REPORT OF A FAMILY. *Am J Ophthalmol,* 57, 481-2.

JAENISCH, R. & BIRD, A. 2003. Epigenetic regulation of gene expression: how the genome integrates intrinsic and environmental signals. *Nature genetics,* 33, 245-254.

JAKOBIEC, F. A., RASHID, A., BOZORG, M. S. & DANA, R. 2014. Unusual large uniocular elastoid and collagenous pinguecula. *Graefes Arch Clin Exp Ophthalmol,* 252, 1173-5.

JAWORSKI, C., ARYANKALAYIL-JOHN, M., CAMPOS, M., FARISS, R., ROWSEY, J., AGARWALLA, N., REID, T., DUSHKU, N., COX, C. & CARPER, D. 2009. Expression analysis of human pterygium shows a predominance of conjunctival and limbal markers and genes associated with cell migration.

JOHNSON, G. L. & LAPADAT, R. 2002. Mitogen-activated protein kinase pathways mediated by ERK, JNK, and p38 protein kinases. *Science,* 298, 1911-1912.

JOHNSTON, H., KNEER, J., CHACKALAPARAMPIL, I., YACIUK, P. & CHRIVIA, J. 1999. Identification of a novel SNF2/SWI2 protein family member, SRCAP, which interacts with CREB-binding protein. *J Biol Chem,* 274, 16370-6.

JOYCE, N. C. 2012. Proliferative capacity of corneal endothelial cells. *Experimental eye research,* 95, 16-23.

KAJI, Y., OSHIKA, T., AMANO, S., OKAMOTO, F., KOITO, W. & HORIUCHI, S. 2006. Immunohistochemical localization of advanced glycation end products in pinguecula. *Graefes Arch Clin Exp Ophthalmol,* 244, 104-8.

KALLURI, R. & WEINBERG, R. A. 2009. The basics of epithelial-mesenchymal transition. *The Journal of clinical investigation,* 119, 1420-1428.

KANDOTH, C., MCLELLAN, M. D., VANDIN, F., YE, K., NIU, B., LU, C., XIE, M., ZHANG, Q., MCMICHAEL, J. F. & WYCZALKOWSKI, M. A. 2013. Mutational landscape and significance across 12 major cancer types. *Nature,* 502, 333-339.

KANG, M. H., KIM, J. S., SEO, J. E., OH, S. C. & YOO, Y. A. 2010. BMP2 accelerates the motility and invasiveness of gastric cancer cells via activation of the phosphatidylinositol 3-kinase (PI3K)/Akt pathway. *Experimental cell research,* 316**,** 24-37.

KANNABIRAN, C. & KLINTWORTH, G. K. 2006. TGFBI gene mutations in corneal dystrophies. *Human mutation,* 27**,** 615-625.

KARKI, R., PANDYA, D., ELSTON, R. C. & FERLINI, C. 2015. Defining "mutation" and "polymorphism" in the era of personal genomics. *BMC medical genomics,* 8**,** 1.

KATO, N., SHIMMURA, S., KAWAKITA, T., MIYASHITA, H., OGAWA, Y., YOSHIDA, S., HIGA, K., OKANO, H. & TSUBOTA, K. 2007. Beta-catenin activation and epithelial-mesenchymal transition in the pathogenesis of pterygium. *Invest Ophthalmol Vis Sci,* 48**,** 1511-7.

KAU, H. C., TSAI, C. C., HSU, W. M., LIU, J. H. & WEI, Y. H. 2004. Genetic polymorphism of hOGG1 and risk of pterygium in Chinese. *Eye (Lond),* 18**,** 635-9.

KAU, H. C., TSAI, C. C., LEE, C. F., KAO, S. C., HSU, W. M., LIU, J. H. & WEI, Y. H. 2006. Increased oxidative DNA damage, 8-hydroxydeoxy- guanosine, in human pterygium. *Eye (Lond),* 20**,** 826-31.

KAYA, A. I., ONARAN, H. O., OZCAN, G., AMBROSIO, C., COSTA, T., BALLI, S. & UGUR, O. 2012. Cell contact-dependent functional selectivity of beta2-adrenergic receptor ligands in stimulating cAMP accumulation and extracellular signal-regulated kinase phosphorylation. *J Biol Chem,* 287**,** 6362-74.

KHATEB, S., ZELINGER, L., BEN-YOSEF, T., MERIN, S., CRYSTAL-SHALIT, O., GROSS, M., BANIN, E. & SHARON, D. 2012. Exome sequencing identifies a founder frameshift mutation in an alternative exon of USH1C as the cause of autosomal recessive retinitis pigmentosa with late-onset hearing loss. *PloS one,* 7**,** e51566.

KIM, H.-S., NAGALLA, S. R., OH, Y., WILSON, E., ROBERTS, C. T. & ROSENFELD, R. G. 1997. Identification of a family of low-affinity insulin-like growth factor binding proteins (IGFBPs): characterization of connective tissue growth factor as a member of the IGFBP superfamily. *Proceedings of the National Academy of Sciences,* 94**,** 12981-12986.

KIM, K. W., PARK, S. H. & KIM, J. C. 2016. Fibroblast biology in pterygia. *Exp Eye Res,* 142**,** 32-9.

KINNA, G., KOLLE, G., CARTER, A., KEY, B., LIESCHKE, G. J., PERKINS, A. & LITTLE, M. H. 2006. Knockdown of zebrafish crim1 results in a bent tail phenotype with defects in somite and vascular development. *Mechanisms of development,* 123**,** 277-287.

KLEIHUES, P., SCHÄUBLE, B., ZUR HAUSEN, A., ESTEVE, J. & OHGAKI, H. 1997. Tumors associated with p53 germline mutations: a synopsis of 91 families. *The American journal of pathology,* 150**,** 1.

KLEIN, R. J., ZEISS, C., CHEW, E. Y., TSAI, J. Y., SACKLER, R. S., HAYNES, C., HENNING, A. K., SANGIOVANNI, J. P., MANE, S. M., MAYNE, S. T., BRACKEN, M. B., FERRIS, F. L., OTT, J., BARNSTABLE, C. & HOH, J. 2005. Complement factor H polymorphism in age-related macular degeneration. *Science,* 308**,** 385-9.

KNECHT, C. & KRAWCZAK, M. 2014. Molecular genetic epidemiology of human diseases: from patterns to predictions. *Human genetics,* 133**,** 425-430.

KOBAYASHI, H. & KOHSHIMA, S. 1997. Unique morphology of the human eye. *Nature,* 387**,** 767-8.

KOLLE, G., GEORGAS, K., HOLMES, G., LITTLE, M. H. & YAMADA, T. 2000a. CRIM1, a novel gene encoding a cysteine-rich repeat protein, is developmentally regulated and implicated in vertebrate CNS development and organogenesis. *Mechanisms of development,* 90**,** 181-193.

KOLLE, G., GEORGAS, K., HOLMES, G. P., LITTLE, M. H. & YAMADA, T. 2000b. CRIM1, a novel gene encoding a cysteine-rich repeat protein, is developmentally regulated and implicated in vertebrate CNS development and organogenesis. *Mech Dev,* 90**,** 181-93.

KRIA, L., OHIRA, A. & AMEMIYA, T. 1996. Immunohistochemical localization of basic fibroblast growth factor, platelet derived growth factor, transforming growth factor-β and tumor necrosis factor-α in the pterygium. *Acta histochemica,* 98**,** 195-201.

KULKARNI, B., MOHAMMED, I., HOPKINSON, A. & DUA, H. S. 2011. Validation of endogenous control genes for gene expression studies on human ocular surface epithelium. *PLoS One,* 6**,** e22301.

KUMAR, P., HENIKOFF, S. & NG, P. C. 2009. Predicting the effects of coding non-synonymous variants on protein function using the SIFT algorithm. *Nature protocols,* 4**,** 1073-1081.

KUMAR, V., ABBAS, A. K., FAUSTO, N. & ASTER, J. C. 2014. *Robbins and Cotran pathologic basis of disease*, Elsevier Health Sciences.

LAMOUILLE, S., XU, J. & DERYNCK, R. 2014. Molecular mechanisms of epithelial–mesenchymal transition. *Nature reviews. Molecular cell biology,* 15**,** 178.

LAND, M. & NILSSON, D. 2002. Animal Eyes: Oxford University Press. *New York*.

LAND, M. F. & FERNALD, R. D. 1992. The evolution of eyes. *Annu Rev Neurosci,* 15**,** 1-29.

LANNER, F. & ROSSANT, J. 2010. The role of FGF/Erk signaling in pluripotent cells. *Development,* 137**,** 3351-3360.

LEE, D. H., CHO, H. J., KIM, J. T., CHOI, J. S. & JOO, C. K. 2001. Expression of vascular endothelial growth factor and inducible nitric oxide synthase in pterygia. *Cornea,* 20**,** 738-42.

LEE, M.-S., GHIM, J., KIM, S.-J., YUN, Y. S., YOO, S.-A., SUH, P.-G., KIM, W.-U. & RYU, S. H. 2015. Functional interaction between CTGF and FPRL1 regulates VEGF-A-induced angiogenesis. *Cellular signalling,* 27**,** 1439-1448.

LEMERCIER, G., CORNAND, G. & BURCKHART, M. F. 1978. [Pinguecula and pterygium: histologic and electron microscopic study (author's transl)]. *Virchows Arch A Pathol Anat Histol,* 379**,** 321-33.

LEVINE, A. J., MOMAND, J. & FINLAY, C. A. 1991. The p53 tumour suppressor gene. *Nature,* 351**,** 453-6.

LI, F. P. & FRAUMENI, J. F., JR. 1969. Soft-tissue sarcomas, breast cancer, and other neoplasms. A familial syndrome? *Ann Intern Med,* 71**,** 747-52.

LI, W., MAN, X.-Y., LI, C.-M., CHEN, J.-Q., ZHOU, J., CAI, S.-Q., LU, Z.-F. & ZHENG, M. 2012. VEGF induces proliferation of human hair follicle dermal papilla cells through VEGFR-2-mediated activation of ERK. *Experimental cell research,* 318**,** 1633-1640.

LI, Z. & CUI, H. 2013. Prevalence and associated factors for pterygium in a rural adult population (the Southern Harbin Eye Study). *Cornea,* 32**,** 806-9.

LIANG, Q.-F., XU, L., JIN, X.-Y., YOU, Q.-S., YANG, X.-H. & CUI, T.-T. 2010. Epidemiology of pterygium in aged rural population of Beijing, China. *Chinese medical journal,* 123**,** 1699-1701.

LIN, A. D., MILES, K. U. & BRINKS, M. V. 2016. Prevalence of Pterygia in Hawaii: Examining Cumulative Surfing Hours as a Risk Factor. *Ophthalmic epidemiology***,** 1-5.

LIU, L., WU, J., GENG, J., YUAN, Z. & HUANG, D. 2013a. Geographical prevalence and risk factors for pterygium: a systematic review and meta-analysis. *BMJ open,* 3**,** e003787.

LIU, Y., ZHANG, H., LI, J., ZHAO, H., XIN, Q., SHAN, S., DANG, J., BIAN, X. & LIU, Q. 2013b. Association of common variants in KIF21B and ankylosing spondylitis in a Chinese Han population: a replication study. *Immunogenetics,* 65**,** 835-9.

LOH, A., HADZIAHMETOVIC, M. & DUNAIEF, J. L. 2009. Iron homeostasis and eye disease. *Biochimica et Biophysica Acta (BBA)-General Subjects,* 1790**,** 637-649.

LOMBARDO, M., PUCCI, G., BARBERI, R. & LOMBARDO, G. 2015. Interaction of ultraviolet light with the cornea: clinical implications for corneal crosslinking. *Journal of Cataract & Refractive Surgery,* 41**,** 446-459.

LOVICU, F., KOLLE, G., YAMADA, T., LITTLE, M. & MCAVOY, J. 2000. Expression of Crim1 during murine ocular development. *Mechanisms of development,* 94**,** 261-265.

LUCAS, R. M., MCMICHAEL, A. J., ARMSTRONG, B. K. & SMITH, W. T. 2008. Estimating the global disease burden due to ultraviolet radiation exposure. *International journal of epidemiology,* 37**,** 654-667.

LUTHRA, R., NEMESURE, B. B., WU, S. Y., XIE, S. H. & LESKE, M. C. 2001. Frequency and risk factors for pterygium in the Barbados Eye Study. *Arch Ophthalmol,* 119**,** 1827-32.

LYNCH, M. 2010. Rate, molecular spectrum, and consequences of human mutation. *Proceedings of the National Academy of Sciences,* 107**,** 961-968.

MA, K., XU, L., JIE, Y. & JONAS, J. B. 2007. Prevalence of and factors associated with pterygium in adult Chinese: the Beijing Eye Study. *Cornea,* 26**,** 1184-1186.

MACARTHUR, D., MANOLIO, T., DIMMOCK, D., REHM, H., SHENDURE, J., ABECASIS, G., ADAMS, D., ALTMAN, R., ANTONARAKIS, S. & ASHLEY, E. 2014. Guidelines for investigating causality of sequence variants in human disease. *Nature,* 508**,** 469-476.

MACHENS, A., SCHAAF, L., KARGES, W., FRANK-RAUE, K., BARTSCH, D. K., ROTHMUND, M., SCHNEYER, U., GORETZKI, P., RAUE, F. & DRALLE, H. 2007. Age-related penetrance of endocrine tumours in multiple endocrine neoplasia type 1 (MEN1): a multicentre study of 258 gene carriers. *Clinical endocrinology,* 67**,** 613-622.

MACKENZIE, F. D., HIRST, L. W., BATTISTUTTA, D. & GREEN, A. 1992. Risk analysis in the development of pterygia. *Ophthalmology,* 99**,** 1056-1061.

MAINI, R., COLLISON, D. J., MAIDMENT, J. M., DAVIES, P. D. & WORMSTONE, I. M. 2002. Pterygial derived fibroblasts express functionally active histamine and epidermal growth factor receptors. *Experimental eye research,* 74**,** 237-244.

MALKIN, D., LI, F. P., STRONG, L. C., FRAUMENI JR, J. F., NELSON, C. E., KIM, D. H., KASSEL, J., GRYKA, M. A., BISCHOFF, F. Z. & TAINSKY,

M. A. 1990. Germ line p53 mutations in a familial syndrome of breast cancer, sarcomas, and other neoplasms. *Science,* 250, 1233-1238.

MARIONNET, C., TRICAUD, C. & BERNERD, F. 2014. Exposure to non-extreme solar UV daylight: spectral characterization, effects on skin and photoprotection. *International journal of molecular sciences,* 16, 68-90.

MARSZALEK, J. R., LIU, X., ROBERTS, E. A., CHUI, D., MARTH, J. D., WILLIAMS, D. S. & GOLDSTEIN, L. S. 2000. Genetic evidence for selective transport of opsin and arrestin by kinesin-II in mammalian photoreceptors. *Cell,* 102, 175-187.

MARTINDALE, J. L. & HOLBROOK, N. J. 2002. Cellular response to oxidative stress: signaling for suicide and survival. *Journal of cellular physiology,* 192, 1-15.

MCCARTY, C. A., FU, C. L. & TAYLOR, H. R. 2000. Epidemiology of pterygium in Victoria, Australia. *British Journal of Ophthalmology,* 84, 289-292.

MCCUBREY, J. A., STEELMAN, L. S., CHAPPELL, W. H., ABRAMS, S. L., WONG, E. W., CHANG, F., LEHMANN, B., TERRIAN, D. M., MILELLA, M. & TAFURI, A. 2007. Roles of the Raf/MEK/ERK pathway in cell growth, malignant transformation and drug resistance. *Biochimica et Biophysica Acta (BBA)-Molecular Cell Research,* 1773, 1263-1284.

MCGEE, T., DEVOTO, M., OTT, J., BERSON, E. & DRYJA, T. 1997. Evidence that the penetrance of mutations at the RP11 locus causing dominant retinitis pigmentosa is influenced by a gene linked to the homologous RP11 allele. *The American Journal of Human Genetics,* 61, 1059-1066.

MENCUCCI, R., MARINI, M., PALADINI, I., SARCHIELLI, E., SGAMBATI, E., MENCHINI, U. & VANNELLI, G. B. 2010. Effects of riboflavin/UVA corneal cross-linking on keratocytes and collagen fibres in human cornea. *Clinical & experimental ophthalmology,* 38, 49-56.

MERWALD, H., KLOSNER, G., KOKESCH, C., DER-PETROSSIAN, M., HÖNIGSMANN, H. & TRAUTINGER, F. 2005. UVA-induced oxidative damage and cytotoxicity depend on the mode of exposure. *Journal of Photochemistry and Photobiology B: Biology,* 79, 197-207.

MIN, B.-J., KIM, N., CHUNG, T., KIM, O.-H., NISHIMURA, G., CHUNG, C. Y., SONG, H. R., KIM, H. W., LEE, H. R. & KIM, J. 2011. Whole-exome sequencing identifies mutations of KIF22 in spondyloepimetaphyseal dysplasia with joint laxity, leptodactylic type. *The American Journal of Human Genetics,* 89, 760-766.

MIRZOEVA, O. K., DAS, D., HEISER, L. M., BHATTACHARYA, S., SIWAK, D., GENDELMAN, R., BAYANI, N., WANG, N. J., NEVE, R. M., GUAN, Y., HU, Z., KNIGHT, Z., FEILER, H. S., GASCARD, P., PARVIN, B., SPELLMAN, P. T., SHOKAT, K. M., WYROBEK, A. J., BISSELL, M. J., MCCORMICK, F., KUO, W. L., MILLS, G. B., GRAY, J. W. & KORN, W. M. 2009. Basal subtype and MAPK/ERK kinase (MEK)-phosphoinositide 3-kinase feedback signaling determine susceptibility of breast cancer cells to MEK inhibition. *Cancer Res,* 69, 565-72.

MITTAL, R., RATH, S. & VEMUGANTI, G. K. 2013. Ocular surface squamous neoplasia–Review of etio-pathogenesis and an update on clinico-pathological diagnosis. *Saudi Journal of Ophthalmology,* 27, 177-186.

MOAN, J. 2001. 7 Visible Light and UV Radiation. *Radiation*, 69.

MOILANEN, A. M., RYSA, J., KAIKKONEN, L., KARVONEN, T., MUSTONEN, E., SERPI, R., SZABO, Z., TENHUNEN, O., BAGYURA, Z.,

NAPANKANGAS, J., OHUKAINEN, P., TAVI, P., KERKELA, R., LEOSDOTTIR, M., WAHLSTRAND, B., HEDNER, T., MELANDER, O. & RUSKOAHO, H. 2015. WDR12, a Member of Nucleolar PeBoW-Complex, Is Up-Regulated in Failing Hearts and Causes Deterioration of Cardiac Function. *PLoS One,* 10**,** e0124907.

MONROY, M. A., RUHL, D. D., XU, X., GRANNER, D. K., YACIUK, P. & CHRIVIA, J. C. 2001. Regulation of cAMP-responsive element-binding protein-mediated transcription by the SNF2/SWI-related protein, SRCAP. *J Biol Chem,* 276**,** 40721-6.

MONROY, M. A., SCHOTT, N. M., COX, L., CHEN, J. D., RUH, M. & CHRIVIA, J. C. 2003. SNF2-related CBP activator protein (SRCAP) functions as a coactivator of steroid receptor-mediated transcription through synergistic interactions with CARM-1 and GRIP-1. *Molecular endocrinology,* 17**,** 2519-2528.

MOORE, J. E., ATKINSON, S. D., AZAR, D. T., WORTHINGTON, J., DOWNES, C. S., COURTNEY, D. G. & MOORE, C. B. 2014. Protection of corneal epithelial stem cells prevents ultraviolet A damage during corneal collagen cross-linking treatment for keratoconus. *Br J Ophthalmol,* 98**,** 270-4.

MOORE, J. E., VASEY, G. T., DARTT, D. A., MCGILLIGAN, V. E., ATKINSON, S. D., GRILLS, C., LAMEY, P. J., LECCISOTTI, A., FRAZER, D. G. & MOORE, T. C. 2011. Effect of tear hyperosmolarity and signs of clinical ocular surface pathology upon conjunctival goblet cell function in the human ocular surface. *Invest Ophthalmol Vis Sci,* 52**,** 6174-80.

MORAN, D. J. & HOLLOWS, F. C. 1984. Pterygium and ultraviolet radiation: a positive correlation. *British Journal of Ophthalmology,* 68**,** 343-346.

MORISSETTE, J., CLÉPET, C., MOISAN, S., DUBOIS, S., WINSTALL, E., VERMEEREN, D., NGUYEN, T., POLANSKY, J., CÔTÉ, G. & ANCTIL, J.-L. 1998. Homozygotes carrying an autosomal dominant TIGR mutation do not manifest glaucoma. *Nature genetics,* 19**,** 319-321.

MOVAHEDAN, A., MAJDI, M., AFSHARKHAMSEH, N., SAGHA, H. M., SAADAT, N. S., SHALILEH, K., MILANI, B. Y., YING, H. & DJALILIAN, A. R. 2012. Notch inhibition during corneal epithelial wound healing promotes migration. *Invest Ophthalmol Vis Sci,* 53**,** 7476-83.

MUNIER, F. L., FRUEH, B. E., OTHENIN-GIRARD, P., UFFER, S., COUSIN, P., WANG, M. X., HÉON, E., BLACK, G. C., BLASI, M. A. & BALESTRAZZI, E. 2002. BIGH3 mutation spectrum in corneal dystrophies. *Investigative ophthalmology & visual science,* 43**,** 949-954.

MURPHY, M., PYKETT, M. J., HARNISH, P., ZANG, K. D. & GEORGE, D. L. 1993. Identification and characterization of genes differentially expressed in meningiomas. *Cell growth and differentiation,* 4**,** 715-715.

NAJAFI, M., KORDI-TAMANDANI, D. M. & ARISH, M. 2016. Evaluation of LATS1 and LATS2 Promoter Methylation with the Risk of Pterygium Formation. *Journal of ophthalmology,* 2016.

NAKAGAMI, T., MURAKAMI, A., OKISAKA, S. & EBIHARA, N. 1999. Mast cells in pterygium: number and phenotype. *Japanese journal of ophthalmology,* 43**,** 75-79.

NAKAI, T., KITAMURA, N., HASHIMOTO, T., KAJIMOTO, Y., NISHINO, N., MITA, T. & TANAKA, C. 1991. Decreased histamine H1 receptors in the frontal cortex of brains from patients with chronic schizophrenia. *Biological psychiatry,* 30**,** 349-356.

NAKASHIMA, Y., MORIMOTO, M., TODA, K., SHINYA, T., SATO, K. & TAKAHASHI, S. 2015. Inhibition of the proliferation and acceleration of migration of vascular endothelial cells by increased cysteine-rich motor neuron 1. *Biochem Biophys Res Commun,* 462, 215-20.

NAKASHIMA, Y. & TAKAHASHI, S. 2014. Induction of cysteine-rich motor neuron 1 mRNA expression in vascular endothelial cells. *Biochem Biophys Res Commun,* 451, 235-8.

NAL, B., MOHR, E., SILVA, M. I., TAGETT, R., NAVARRO, C., CARROLL, P., DEPETRIS, D., VERTHUY, C., JORDAN, B. R. & FERRIER, P. 2002. Wdr12, a mouse gene encoding a novel WD-Repeat Protein with a notchless-like amino-terminal domain. *Genomics,* 79, 77-86.

NANGIA, V., JONAS, J. B., NAIR, D., SAINI, N., NANGIA, P. & PANDA-JONAS, S. 2013. Prevalence and associated factors for pterygium in rural agrarian central India. The central India eye and medical study. *PloS one,* 8, e82439.

NARDACCI, R., IACONO, O. L., CICCOSANTI, F., FALASCA, L., ADDESSO, M., AMENDOLA, A., ANTONUCCI, G., CRAXÌ, A., FIMIA, G. M. & IADEVAIA, V. 2003. Transglutaminase type II plays a protective role in hepatic injury. *The American journal of pathology,* 162, 1293-1303.

NESBITT, H., BROWNE, G., O'DONOVAN, K. M., BYRNE, N. M., WORTHINGTON, J., MCKEOWN, S. R. & MCKENNA, D. J. 2016. Nitric Oxide Up-Regulates RUNX2 in LNCaP Prostate Tumours: Implications for Tumour Growth In Vitro and In Vivo. *Journal of cellular physiology,* 231, 473-482.

NEWTON, R., REEVES, G., BERAL, V., FERLAY, J. & PARKIN, D. 1996. Effect of ambient solar ultraviolet radiation on incidence of squamous-cell carcinoma of the eye. *The Lancet,* 347, 1450-1451.

NG, P. C. & HENIKOFF, S. 2001. Predicting deleterious amino acid substitutions. *Genome research,* 11, 863-874.

NOLAN, T. M., DIGIROLAMO, N., SACHDEV, N. H., HAMPARTZOUMIAN, T., CORONEO, M. T. & WAKEFIELD, D. 2003. The role of ultraviolet irradiation and heparin-binding epidermal growth factor-like growth factor in the pathogenesis of pterygium. *The American journal of pathology,* 162, 567-574.

NONAKA, D., CHIRIBOGA, L. & RUBIN, B. P. 2008. Differential expression of S100 protein subtypes in malignant melanoma, and benign and malignant peripheral nerve sheath tumors. *J Cutan Pathol,* 35, 1014-9.

NOTARA, M. & DANIELS, J. T. 2010. Characterisation and functional features of a spontaneously immortalised human corneal epithelial cell line with progenitor-like characteristics. *Brain Res Bull,* 81, 279-86.

NOWAK, D. M. & GAJECKA, M. 2011. The Genetics of Keratoconus. *Middle East African Journal of Ophthalmology,* 18, 2-6.

NUBILE, M., CURCIO, C., LANZINI, M., CALIENNO, R., IEZZI, M., MASTROPASQUA, A., DI NICOLA, M. & MASTROPASQUA, L. 2013. Expression of CREB in primary pterygium and correlation with cyclin D1, ki-67, MMP7, p53, p63, Survivin and Vimentin. *Ophthalmic research,* 50, 99-107.

O'LEARY, J. M., HAMILTON, J. M., DEANE, C. M., VALEYEV, N. V., SANDELL, L. J. & DOWNING, A. K. 2004a. Solution structure and dynamics of a prototypical chordin-like cysteine-rich repeat (von Willebrand

Factor type C module) from collagen IIA. *Journal of Biological Chemistry,* 279, 53857-53866.

O'LEARY, J. M., HAMILTON, J. M., DEANE, C. M., VALEYEV, N. V., SANDELL, L. J. & DOWNING, A. K. 2004b. Solution structure and dynamics of a prototypical chordin-like cysteine-rich repeat (von Willebrand Factor type C module) from collagen IIA. *J Biol Chem,* 279, 53857-66.

OCHI, H., OGINO, H., KAGEYAMA, Y. & YASUDA, K. 2003. The stability of the lens-specific Maf protein is regulated by fibroblast growth factor (FGF)/ERK signaling in lens fiber differentiation. *Journal of Biological Chemistry,* 278, 537-544.

OELLERS, P., KARP, C. L., SHETH, A., KAO, A. A., ABDELAZIZ, A., MATTHEWS, J. L., DUBOVY, S. R. & GALOR, A. 2013. Prevalence, treatment, and outcomes of coexistent ocular surface squamous neoplasia and pterygium. *Ophthalmology,* 120, 445-50.

ONO, T., MORI, Y., NEJIMA, R., TOKUNAGA, T., MIYATA, K. & AMANO, S. 2016. Long-term follow-up of transplantation of preserved limbal allograft and amniotic membrane for recurrent pterygium. *Graefe's Archive for Clinical and Experimental Ophthalmology*, 1-6.

ORTAK, H., DEMIR, H. D., MENDIL, D., SÖĞÜT, E., ARDAGIL, A. & EĞRI, M. 2012. Evaluation of iron, zinc, and copper levels in pterygium tissue. *Japanese journal of ophthalmology,* 56, 219-223.

OTLU, B., EMRE, S., TURKCUOGLU, P., DOGANAY, S. & DURMAZ, R. 2009. Investigation of human papillomavirus and Epstein-Barr virus DNAs in pterygium tissue. *Eur J Ophthalmol,* 19, 175-9.

OZDEMIR, G., INANC, F. & KILINC, M. 2005. Investigation of nitric oxide in pterygium. *Canadian Journal of Ophthalmology/Journal Canadien d'Ophtalmologie,* 40, 743-746.

PANDEL, R., POLJŠAK, B., GODIC, A. & DAHMANE, R. 2013. Skin photoaging and the role of antioxidants in its prevention. *ISRN dermatology,* 2013.

PAUSCH, H., WANG, X., JUNG, S., KROGMEIER, D., EDEL, C., EMMERLING, R., GOTZ, K. U. & FRIES, R. 2012. Identification of QTL for UV-protective eye area pigmentation in cattle by progeny phenotyping and genome-wide association analysis. *PLoS One,* 7, e36346.

PEARTON, D. J., FERRARIS, C. & DHOUAILLY, D. 2004. Transdifferentiation of corneal epithelium: evidence for a linkage between the segregation of epidermal stem cells and the induction of hair follicles during embryogenesis. *Int J Dev Biol,* 48, 197-201.

PEIRETTI, E., DESSÌ, S., NORFO, C., MULAS, C., ABETE, C., GALANTUOMO, S., ZUCCA, I. & FOSSARELLO, M. 2006. mRNA Level Alterations of Proteins Involved in Cholesterol Esters Metabolism in Pterygium Fibroblasts. *Investigative Ophthalmology & Visual Science,* 47, 4982-4982.

PEIRETTI, E., DESSI, S., PUTZOLU, M. & FOSSARELLO, M. 2004. Hyperexpression of low-density lipoprotein receptors and hydroxy-methylglutaryl-coenzyme A-reductase in human pinguecula and primary pterygium. *Invest Ophthalmol Vis Sci,* 45, 3982-5.

PELLEGRINI, G., RAMA, P., DI ROCCO, A., PANARAS, A. & DE LUCA, M. 2014. Concise review: hurdles in a successful example of limbal stem cell-based regenerative medicine. *Stem Cells,* 32, 26-34.

PENG, M. L., TSAI, Y. Y., TUNG, J. N., CHIANG, C. C., HUANG, Y. C., LEE, H. & CHENG, Y. W. 2014. Vascular endothelial growth factor gene polymorphism and protein expression in the pathogenesis of pterygium. *Br J Ophthalmol,* 98**,** 556-61.

PENNISI, D. J., WILKINSON, L., KOLLE, G., SOHASKEY, M. L., GILLINDER, K., PIPER, M. J., MCAVOY, J. W., LOVICU, F. J. & LITTLE, M. H. 2007. Crim1KST264/KST264 mice display a disruption of the Crim1 gene resulting in perinatal lethality with defects in multiple organ systems. *Developmental Dynamics,* 236**,** 502-511.

PERRA, M. T., COLOMBARI, R., MAXIA, C., ZUCCA, I., PIRAS, F., CORBU, A., BRAVO, S., SCARPA, A. & SIRIGU, P. 2006. Finding of conjunctival melanocytic pigmented lesions within pterygium. *Histopathology,* 48**,** 387-93.

PIRAS, F., MOORE, P. S., UGALDE, J., PERRA, M. T., SCARPA, A. & SIRIGU, P. 2003. Detection of human papillomavirus DNA in pterygia from different geographical regions. *Br J Ophthalmol,* 87**,** 864-6.

PONFERRADA, V. G., FAN, J., VALLANCE, J. E., HU, S., MAMEDOVA, A., RANKIN, S. A., KOFRON, M., ZORN, A. M., HEGDE, R. S. & LANG, R. A. 2012. CRIM1 complexes with ss-catenin and cadherins, stabilizes cell-cell junctions and is critical for neural morphogenesis. *PLoS One,* 7**,** e32635.

PRATSINIS, H. & KLETSAS, D. 2007. PDGF, bFGF and IGF-I stimulate the proliferation of intervertebral disc cells in vitro via the activation of the ERK and Akt signaling pathways. *European Spine Journal,* 16**,** 1858-1866.

PRENKERT, M., UGGLA, B., TIDEFELT, U. & STRID, H. 2010. CRIM1 is expressed at higher levels in drug-resistant than in drug-sensitive myeloid leukemia HL60 cells. *Anticancer research,* 30**,** 4157-4161.

RABBANI, B., TEKIN, M. & MAHDIEH, N. 2014. The promise of whole-exome sequencing in medical genetics. *Journal of human genetics,* 59**,** 5-15.

RAMALHO, F. S., MAESTRI, C., RAMALHO, L. N., RIBEIRO-SILVA, A. & ROMAO, E. 2006. Expression of p63 and p16 in primary and recurrent pterygia. *Graefes Arch Clin Exp Ophthalmol,* 244**,** 1310-4.

RAMKUMAR, H. L., BROOKS, B. P., CAO, X., TAMURA, D., DIGIOVANNA, J. J., KRAEMER, K. H. & CHAN, C. C. 2011. Ophthalmic manifestations and histopathology of xeroderma pigmentosum: two clinicopathological cases and a review of the literature. *Surv Ophthalmol,* 56**,** 348-61.

RATNAKAR, K. S., GOSWAMY, V. & AGARWAL, L. P. 1976. Mast cells and pterygium. *Acta Ophthalmol (Copenh),* 54**,** 363-8.

RATNAPRIYA, R., ZHAN, X., FARISS, R. N., BRANHAM, K. E., ZIPPRER, D., CHAKAROVA, C. F., SERGEEV, Y. V., CAMPOS, M. M., OTHMAN, M., FRIEDMAN, J. S., MAMINISHKIS, A., WASEEM, N. H., BROOKS, M., RAJASIMHA, H. K., EDWARDS, A. O., LOTERY, A., KLEIN, B. E., TRUITT, B. J., LI, B., SCHAUMBERG, D. A., MORGAN, D. J., MORRISON, M. A., SOUIED, E., TSIRONI, E. E., GRASSMANN, F., FISHMAN, G. A., SILVESTRI, G., SCHOLL, H. P., KIM, I. K., RAMKE, J., TUO, J., MERRIAM, J. E., MERRIAM, J. C., PARK, K. H., OLSON, L. M., FARRER, L. A., JOHNSON, M. P., PEACHEY, N. S., LATHROP, M., BARON, R. V., IGO, R. P., JR., KLEIN, R., HAGSTROM, S. A., KAMATANI, Y., MARTIN, T. M., JIANG, Y., CONLEY, Y., SAHEL, J. A., ZACK, D. J., CHAN, C. C., PERICAK-VANCE, M. A., JACOBSON, S. G., GORIN, M. B., KLEIN, M. L., ALLIKMETS, R., IYENGAR, S. K., WEBER, B. H., HAINES, J. L., LEVEILLARD, T., DEANGELIS, M. M., STAMBOLIAN, D., WEEKS, D. E., BHATTACHARYA, S. S., CHEW, E. Y., HECKENLIVELY, J. R., ABECASIS, G. R. & SWAROOP, A. 2014.

Rare and common variants in extracellular matrix gene Fibrillin 2 (FBN2) are associated with macular degeneration. *Hum Mol Genet,* 23**,** 5827-37.

RAUCH, N., RUKHLENKO, O. S., KOLCH, W. & KHOLODENKO, B. N. 2016. MAPK kinase signalling dynamics regulate cell fate decisions and drug resistance. *Curr Opin Struct Biol,* 41**,** 151-158.

REISMAN, D., MCFADDEN, J. W. & LU, G. 2004. Loss of heterozygosity and p53 expression in Pterygium. *Cancer Lett,* 206**,** 77-83.

REZVAN, F., HASHEMI, H., EMAMIAN, M. H., KHEIRKHAH, A., SHARIATI, M., KHABAZKHOOB, M. & FOTOUHI, A. 2012. The prevalence and determinants of pterygium and pinguecula in an urban population in Shahroud, Iran. *Acta Med Iran,* 50**,** 689-96.

REZZANI, R., RODELLA, L., FAVERO, G., DAMIANI, G., PAGANELLI, C. & REITER, R. 2014a. Attenuation of ultraviolet A-induced alterations in NIH3T3 dermal fibroblasts by melatonin. *British Journal of Dermatology,* 170**,** 382-391.

REZZANI, R., RODELLA, L. F., FAVERO, G., DAMIANI, G., PAGANELLI, C. & REITER, R. J. 2014b. Attenuation of ultraviolet A-induced alterations in NIH3T3 dermal fibroblasts by melatonin. *Br J Dermatol,* 170**,** 382-91.

RIAU, A. K., WONG, T. T., BEUERMAN, R. W. & TONG, L. 2009. Calcium-binding S100 protein expression in pterygium. *Mol Vis,* 15**,** 335-42.

RIAU, A. K., WONG, T. T., LAN, W., FINGER, S. N., CHAURASIA, S. S., HOU, A. H., CHEN, S., YU, S. J. & TONG, L. 2011. Aberrant DNA methylation of matrix remodeling and cell adhesion related genes in pterygium. *PLoS One,* 6**,** e14687.

RIAZUDDIN, S. A., PARKER, D. S., MCGLUMPHY, E. J., OH, E. C., ILIFF, B. W., SCHMEDT, T., JURKUNAS, U., SCHLEIF, R., KATSANIS, N. & GOTTSCH, J. D. 2012. Mutations in LOXHD1, a recessive-deafness locus, cause dominant late-onset Fuchs corneal dystrophy. *The American Journal of Human Genetics,* 90**,** 533-539.

RIORDAN, J. R., ROMMENS, J. M., KEREM, B.-S., ALON, N., ROZMAHEL, R., GRZELCZAK, Z., ZIELENSKI, J., LOK, S., PLAVSIC, N. & CHOU, J.-L. 1989. Identification of the cystic fibrosis gene: cloning and characterization of complementary DNA. *Science,* 245**,** 1066-1073.

ROMANO, V., STEGER, B., KOVACOVA, A., KAYE, S. B. & WILLOUGHBY, C. E. 2016. Further evidence for heredity of pterygium. *Ophthalmic Genet***,** 1-3.

ROSE, G. E. & LAVIN, M. J. 1987. The Hudson-Stahli line. III: Observations on morphology, a critical review of aetiology and a unified theory for the formation of iron lines of the corneal epithelium. *Eye,* 1**,** 475-479.

ROSENTHAL, J. W. 1953. Chronology of pterygium therapy. *Am J Ophthalmol,* 36**,** 1601-16.

ROTHHAMMER, T., POSER, I., SONCIN, F., BATAILLE, F., MOSER, M. & BOSSERHOFF, A.-K. 2005. Bone morphogenic proteins are overexpressed in malignant melanoma and promote cell invasion and migration. *Cancer research,* 65**,** 448-456.

ROY, B. 2004. Increase in Incidence of Pterygium in High Altitude Areas. *Med J Armed Forces India,* 60**,** 318.

RÚA, O., LARRÁYOZ, I. M., BARAJAS, M. T., VELILLA, S. & MARTÍNEZ, A. 2012. Oral doxycycline reduces pterygium lesions; results from a double blind, randomized, placebo controlled clinical trial. *PloS one,* 7**,** e52696.

RUNAGER, K., BASAIAWMOIT, R. V., DEVA, T., ANDREASEN, M., VALNICKOVA, Z., SØRENSEN, C. S., KARRING, H., THØGERSEN, I. B., CHRISTIANSEN, G. & UNDERHAUG, J. 2011. Human phenotypically distinct TGFBI corneal dystrophies are linked to the stability of the fourth FAS1 domain of TGFBIp. *Journal of Biological Chemistry,* 286**,** 4951-4958.

SACHIDANANDAM, R., WEISSMAN, D., SCHMIDT, S. C., KAKOL, J. M., STEIN, L. D., MARTH, G., SHERRY, S., MULLIKIN, J. C., MORTIMORE, B. J., WILLEY, D. L., HUNT, S. E., COLE, C. G., COGGILL, P. C., RICE, C. M., NING, Z., ROGERS, J., BENTLEY, D. R., KWOK, P. Y., MARDIS, E. R., YEH, R. T., SCHULTZ, B., COOK, L., DAVENPORT, R., DANTE, M., FULTON, L., HILLIER, L., WATERSTON, R. H., MCPHERSON, J. D., GILMAN, B., SCHAFFNER, S., VAN ETTEN, W. J., REICH, D., HIGGINS, J., DALY, M. J., BLUMENSTIEL, B., BALDWIN, J., STANGE-THOMANN, N., ZODY, M. C., LINTON, L., LANDER, E. S. & ALTSHULER, D. 2001. A map of human genome sequence variation containing 1.42 million single nucleotide polymorphisms. *Nature,* 409**,** 928-33.

SASTRE, L. 2014. exome sequencing: what clinicians need to know.

SCALLY, A. & DURBIN, R. 2012. Revising the human mutation rate: implications for understanding human evolution. *Nature Reviews Genetics,* 13**,** 745-753.

SCHMITTGEN, T. D. & LIVAK, K. J. 2008. Analyzing real-time PCR data by the comparative CT method. *Nature protocols,* 3**,** 1101-1108.

SHIMAMURA, T. 2016. Overview of Membrane Protein Purification and Crystallization. *Advanced Methods in Structural Biology***,** 105-122.

SHRESTHA, S. & SHRESTHA, S. M. 2014. Comparative study of prevalence of pterygium at high altitude and Kathmandu Valley. *J Nepal Health Res Counc,* 12**,** 187-90.

SOLOMON, A., GRUETERICH, M., LI, D.-Q., MELLER, D., LEE, S.-B. & TSENG, S. C. 2003. Overexpression of Insulin-like growth factor-binding protein-2 in pterygium body fibroblasts. *Investigative ophthalmology & visual science,* 44**,** 573-580.

SPANDIDOS, D. A., SOURVINOS, G., KIARIS, H. & TSAMPARLAKIS, J. 1997. Microsatellite instability and loss of heterozygosity in human pterygia. *Br J Ophthalmol,* 81**,** 493-6.

ŠTÍPEK, S., ARDAN, T. & MIDELFART, A. 2004. UV rays, the prooxidant/antioxidant imbalance in the cornea and oxidative eye damage. *Physiol. Res,* 53**,** 1-10.

STRACHAN, T. & ANDREW, P. 1999. Read, Human molecule genetics. BIOS Scientific Publishers Ltd.

SUNDIN, O. H., BROMAN, K. W., CHANG, H. H., VITO, E. C., STARK, W. J. & GOTTSCH, J. D. 2006. A common locus for late-onset Fuchs corneal dystrophy maps to 18q21. 2-q21. 32. *Investigative ophthalmology & visual science,* 47**,** 3919-3926.

SYED, D. N., AFAQ, F. & MUKHTAR, H. 2012. Differential activation of signaling pathways by UVA and UVB radiation in normal human epidermal keratinocytes. *Photochemistry and photobiology,* 88**,** 1184-1190.

TAKAMURA, Y., KUBO, E., TSUZUKI, S. & AKAGI, Y. 2008. Detection of human papillomavirus in pterygium and conjunctival papilloma by hybrid capture II and PCR assays. *Eye (Lond),* 22**,** 1442-5.

TAN, D. T., LIM, A. S., GOH, H.-S. & SMITH, D. R. 1997. Abnormal expression of the p53 tumor suppressor gene in the conjunctiva of patients with pterygium. *American journal of ophthalmology,* 123**,** 404-405.

TAN, D. T., TANG, W. Y., LIU, Y. P., GOH, H. S. & SMITH, D. R. 2000. Apoptosis and apoptosis related gene expression in normal conjunctiva and pterygium. *Br J Ophthalmol,* 84**,** 212-6.

TAN, T. W., LAI, C. H., HUANG, C. Y., YANG, W. H., CHEN, H. T., HSU, H. C., FONG, Y. C. & TANG, C. H. 2009. CTGF enhances migration and MMP-13 up-regulation via αvβ3 integrin, FAK, ERK, and NF-κB-dependent pathway in human chondrosarcoma cells. *Journal of cellular biochemistry,* 107**,** 345-356.

TANG, D., WU, D., HIRAO, A., LAHTI, J. M., LIU, L., MAZZA, B., KIDD, V. J., MAK, T. W. & INGRAM, A. J. 2002. ERK activation mediates cell cycle arrest and apoptosis after DNA damage independently of p53. *Journal of Biological Chemistry,* 277**,** 12710-12717.

TAYLOR, H. R. 1980. Studies on the tear film in climatic droplet keratopathy and pterygium. *Archives of Ophthalmology,* 98**,** 86-88.

TAYLOR, H. R., WEST, S. K., ROSENTHAL, F. S., MUNOZ, B., NEWLAND, H. S. & EMMETT, E. A. 1989. Corneal changes associated with chronic UV irradiation. *Archives of Ophthalmology,* 107**,** 1481-1484.

TAYLOR, J. C., MARTIN, H. C., LISE, S., BROXHOLME, J., CAZIER, J. B., RIMMER, A., KANAPIN, A., LUNTER, G., FIDDY, S., ALLAN, C., ARICESCU, A. R., ATTAR, M., BABBS, C., BECQ, J., BEESON, D., BENTO, C., BIGNELL, P., BLAIR, E., BUCKLE, V. J., BULL, K., CAIS, O., CARIO, H., CHAPEL, H., COPLEY, R. R., CORNALL, R., CRAFT, J., DAHAN, K., DAVENPORT, E. E., DENDROU, C., DEVUYST, O., FENWICK, A. L., FLINT, J., FUGGER, L. & GILBERT, R. D. 2015. Factors influencing success of clinical genome sequencing across a broad spectrum of disorders. 47**,** 717-26.

THRELFALL, T. J. & ENGLISH, D. R. 1999. Sun exposure and pterygium of the eye: a dose-response curve. *American journal of ophthalmology,* 128**,** 280-287.

TONG, L., LI, J., CHEW, J., TAN, D. & BEUERMAN, R. 2008. Phospholipase D in the human ocular surface and in pterygium. *Cornea,* 27**,** 693-8.

TORRES, J., ENRÍQUEZ-DE-SALAMANCA, A., FERNÁNDEZ, I., RODRÍGUEZ-ARES, M. T., QUADRADO, M. J., MURTA, J., DEL CASTILLO, J. M. B., STERN, M. E. & CALONGE, M. 2011. Activation of MAPK signaling pathway and NF-κB activation in pterygium and ipsilateral pterygium-free conjunctival specimens. *Investigative ophthalmology & visual science,* 52**,** 5842-5852.

TRUMP, D., FARREN, B., WOODING, C., PANG, J., BESSER, G., BUCHANAN, K., EDWARDS, C., HEATH, D., JACKSON, C. & JANSEN, S. 1996. Clinical studies of multiple endocrine neoplasia type 1 (MEN1). *Qjm,* 89**,** 653-670.

TSAI, Y.-Y., LEE, H., TSENG, S.-H., CHENG, Y.-W., TSAI, C.-H., WU, Y.-H. & TSAI, F.-J. 2004a. Null type of glutathione S-transferase M1 polymorphism is associated with early onset pterygium. *Mol Vis,* 10**,** 458-61.

TSAI, Y. Y., BAU, D. T., CHIANG, C. C., CHENG, Y. W., TSENG, S. H. & TSAI, F. J. 2007. Pterygium and genetic polymorphism of DNA double strand break repair gene Ku70. *Mol Vis,* 13**,** 1436-40.

TSAI, Y. Y., CHENG, Y. W., LEE, H., TSAI, F. J., TSENG, S. H. & CHANG, K. C. 2005a. P53 gene mutation spectrum and the relationship between gene mutation and protein levels in pterygium. *Mol Vis,* 11**,** 50-5.

TSAI, Y. Y., CHENG, Y. W., LEE, H., TSAI, F. J., TSENG, S. H., LIN, C. L. & CHANG, K. C. 2005b. Oxidative DNA damage in pterygium. *Mol Vis,* 11**,** 71-5.

TSAI, Y. Y., LEE, H., TSENG, S. H., CHENG, Y. W., TSAI, C. H., WU, Y. H. & TSAI, F. J. 2004b. Null type of glutathione S-transferase M1 polymorphism is associated with early onset pterygium. *Mol Vis,* 10**,** 458-61.

UNDERHAUG, J., KOLDSØ, H., RUNAGER, K., NIELSEN, J. T., SØRENSEN, C. S., KRISTENSEN, T., OTZEN, D. E., KARRING, H., MALMENDAL, A. & SCHIØTT, B. 2013. Mutation in transforming growth factor beta induced protein associated with granular corneal dystrophy type 1 reduces the proteolytic susceptibility through local structural stabilization. *Biochimica et Biophysica Acta (BBA)-Proteins and Proteomics,* 1834**,** 2812-2822.

UY, H. S., REYES, J. M. G., FLORES, J. D. & LIM-BON-SIONG, R. 2005. Comparison of fibrin glue and sutures for attaching conjunctival autografts after pterygium excision. *Ophthalmology,* 112**,** 667-671.

VANICEK, K., FREI, T., LITYNSKA, Z. & SCHMALWIESER, A. 2000. UV-Index for the Public. *Publication of the European Communities, Brussels, Belgium*.

VAUCLAIR, S., MAJO, F., DURHAM, A. D., GHYSELINCK, N. B., BARRANDON, Y. & RADTKE, F. 2007. Corneal epithelial cell fate is maintained during repair by Notch1 signaling via the regulation of vitamin A metabolism. *Dev Cell,* 13**,** 242-53.

VELTMAN, J. A. & BRUNNER, H. G. 2012. De novo mutations in human genetic disease. *Nature Reviews Genetics,* 13**,** 565-575.

VINALS, F. & POUYSSEGUR, J. 1999. Confluence of vascular endothelial cells induces cell cycle exit by inhibiting p42/p44 mitogen-activated protein kinase activity. *Mol Cell Biol,* 19**,** 2763-72.

VISO, E., GUDE, F. & RODRIGUEZ-ARES, M. T. 2011. Prevalence of pinguecula and pterygium in a general population in Spain. *Eye (Lond),* 25**,** 350-7.

VITT, U. A., HSU, S. Y. & HSUEH, A. J. 2001. Evolution and classification of cystine knot-containing hormones and related extracellular signaling molecules. *Molecular endocrinology,* 15**,** 681-694.

WAGONER, M. D. 1997. Chemical injuries of the eye: current concepts in pathophysiology and therapy. *Surv Ophthalmol,* 41**,** 275-313.

WANG, F. 2008. UVA/riboflavin-induced apoptosis in mouse cornea. *Ophthalmologica,* 222**,** 369-372.

WANG, W. & MALCOLM, B. A. 2002. Two-stage polymerase chain reaction protocol allowing introduction of multiple mutations, deletions, and insertions, using QuikChange TM site-directed mutagenesis. *In Vitro Mutagenesis Protocols***,** 37-43.

WATSON, S., SARRIS, M., KUISHEK, M., MCKELVIE, P., FIGUERIA, E., MCCLUSKEY, P., CORONEO, M. & WAKEFIELD, D. 2013. Limbal dermoid epithelium shares phenotypic characteristics common to both hair epidermal and limbal epithelial stem cells. *Curr Eye Res,* 38**,** 835-42.

WEIERSTALL, U., JAMES, D., WANG, C., WHITE, T. A., WANG, D., LIU, W., SPENCE, J. C., DOAK, R. B., NELSON, G. & FROMME, P. 2014. Lipidic cubic phase injector facilitates membrane protein serial femtosecond crystallography. *Nature communications,* 5.

WEINSTEIN, O., ROSENTHAL, G., ZIRKIN, H., MONOS, T., LIFSHITZ, T. & ARGOV, S. 2002. Overexpression of p53 tumor suppressor gene in pterygia. *Eye,* 16**,** 619-621.

WEISS, J. S., MOLLER, H. U., ALDAVE, A. J., SEITZ, B., BREDRUP, C., KIVELA, T., MUNIER, F. L., RAPUANO, C. J., NISCHAL, K. K., KIM, E. K., SUTPHIN, J., BUSIN, M., LABBE, A., KENYON, K. R., KINOSHITA, S. & LISCH, W. 2015. IC3D classification of corneal dystrophies--edition 2. *Cornea,* 34**,** 117-59.

WILKINSON, L., GILBERT, T., KINNA, G., RUTA, L.-A., PENNISI, D., KETT, M. & LITTLE, M. H. 2007a. Crim1KST264/KST264 mice implicate Crim1 in the regulation of vascular endothelial growth factor-A activity during glomerular vascular development. *Journal of the American Society of Nephrology,* 18**,** 1697-1708.

WILKINSON, L., GILBERT, T., KINNA, G., RUTA, L. A., PENNISI, D., KETT, M. & LITTLE, M. H. 2007b. Crim1KST264/KST264 mice implicate Crim1 in the regulation of vascular endothelial growth factor-A activity during glomerular vascular development. *J Am Soc Nephrol,* 18**,** 1697-708.

WILKINSON, L., KOLLE, G., WEN, D., PIPER, M., SCOTT, J. & LITTLE, M. 2003. CRIM1 regulates the rate of processing and delivery of bone morphogenetic proteins to the cell surface. *J Biol Chem,* 278**,** 34181-8.

WOLLENSAK, G., SPOERL, E., WILSCH, M. & SEILER, T. 2004. Keratocyte apoptosis after corneal collagen cross-linking using riboflavin/UVA treatment. *Cornea,* 23**,** 43-49.

WONG, Y. W., CHEW, J., YANG, H., TAN, D. & BEUERMAN, R. 2006. Expression of insulin-like growth factor binding protein-3 in pterygium tissue. *British journal of ophthalmology,* 90**,** 769-772.

WYNN, T. A. 2007. Common and unique mechanisms regulate fibrosis in various fibroproliferative diseases. *The Journal of clinical investigation,* 117**,** 524-529.

XIA, Z., DICKENS, M., RAINGEAUD, J., DAVIS, R. J. & GREENBERG, M. E. 1995. Opposing effects of ERK and JNK-p38 MAP kinases on apoptosis. *Science,* 270**,** 1326.

YAM, J. C. & KWOK, A. K. 2014. Ultraviolet light and ocular diseases. *International ophthalmology,* 34**,** 383-400.

YAMADA, K., ANDREWS, C., CHAN, W.-M., MCKEOWN, C. A., MAGLI, A., DE BERARDINIS, T., LOEWENSTEIN, A., LAZAR, M., O'KEEFE, M. & LETSON, R. 2003. Heterozygous mutations of the kinesin KIF21A in congenital fibrosis of the extraocular muscles type 1 (CFEOM1). *Nature genetics,* 35**,** 318-321.

YAMANAKA, Y., WILSON, E. M., ROSENFELD, R. G. & OH, Y. 1997. Inhibition of insulin receptor activation by insulin-like growth factor binding proteins. *Journal of Biological Chemistry,* 272**,** 30729-30734.

YANG, Y., MUZNY, D. M., REID, J. G., BAINBRIDGE, M. N., WILLIS, A., WARD, P. A., BRAXTON, A., BEUTEN, J., XIA, F. & NIU, Z. 2013. Clinical whole-exome sequencing for the diagnosis of mendelian disorders. *New England Journal of Medicine,* 369**,** 1502-1511.

YANO, K., BROWN, L. F. & DETMAR, M. 2001. Control of hair growth and follicle size by VEGF-mediated angiogenesis. *The Journal of clinical investigation,* 107**,** 409-417.

YOULE, R. J. & STRASSER, A. 2008. The BCL-2 protein family: opposing activities that mediate cell death. *Nature reviews Molecular cell biology,* 9**,** 47-59.

YOUNG, C. H., CHIU, Y. T., SHIH, T. S., LIN, W. R., CHIANG, C. C., CHOU, Y. E., CHENG, Y. W. & TSAI, Y. Y. 2010. E-cadherin promoter hypermethylation may contribute to protein inactivation in pterygia. *Mol Vis,* 16**,** 1047-53.

ZEISBERG, M. & NEILSON, E. G. 2009. Biomarkers for epithelial-mesenchymal transitions. *The Journal of clinical investigation,* 119**,** 1429-1437.

ZENG, H. & TANG, L. 2014. CRIM1, the antagonist of BMPs, is a potential risk factor of cancer. *Curr Cancer Drug Targets,* 14**,** 652-8.

ZENG, H., ZHANG, Y., YI, Q., WU, Y., WAN, R. & TANG, L. 2015. CRIM1, a newfound cancer-related player, regulates the adhesion and migration of lung cancer cells. *Growth Factors,* 33**,** 384-92.

ZHANG, J.-L., HUANG, Y., QIU, L.-Y., NICKEL, J. & SEBALD, W. 2007. von Willebrand factor type C domain-containing proteins regulate bone morphogenetic protein signaling through different recognition mechanisms. *Journal of Biological Chemistry,* 282**,** 20002-20014.

ZHANG, J. D. 1987a. An investigation of aetiology and heredity of pterygium. *Acta ophthalmologica,* 65**,** 413-416.

ZHANG, J. D. 1987b. An investigation of aetiology and heredity of pterygium. Report of 11 cases in a family. *Acta Ophthalmol (Copenh),* 65**,** 413-6.

ZHANG, Y., FAN, J., HO, J. W., HU, T., KNEELAND, S. C., FAN, X., XI, Q., SELLAROLE, M. A., DE VRIES, W. N. & LU, W. 2016. Crim1 regulates integrin signaling in murine lens development. *Development,* 143**,** 356-366.

ZHANG, Y., FAN, J., HO, J. W., HU, T., KNEELAND, S. C., FAN, X., XI, Q., SELLAROLE, M. A., DE VRIES, W. N., LU, W., LACHKE, S. A., LANG, R. A., JOHN, S. W. & MAAS, R. L. 2015. Crim1 regulates integrin signaling in murine lens development. *Development*.

ZHOU, L., BEUERMAN, R. W., ANG, L. P., CHAN, C. M., LI, S. F., CHEW, F. T. & TAN, D. T. 2009. Elevation of human alpha-defensins and S100 calcium-binding proteins A8 and A9 in tear fluid of patients with pterygium. *Invest Ophthalmol Vis Sci,* 50**,** 2077-86.

ZLOTOGORA, J. 2003. Penetrance and expressivity in the molecular age. *Genet Med,* 5**,** 347-52.